

# NGNP Data Management and Analysis System Modeling Capabilities

C. D. Gentillon  
M. L. Abbott  
L. C. Hull  
B. T. Pham  
M. A. Plummer

September 2009



The INL is a U.S. Department of Energy National Laboratory  
operated by Battelle Energy Alliance

# **NGNP Data Management and Analysis System Modeling Capabilities**

**C. D. Gentillon  
M. L. Abbott  
L. C. Hull  
B. T. Pham  
M. A. Plummer**

**September 2009**

**Idaho National Laboratory  
Next Generation Nuclear Plant Project  
Idaho Falls, Idaho 83415**

**<http://www.inl.gov>**

**Prepared for the  
U.S. Department of Energy  
Office of Nuclear Energy  
Under DOE Idaho Operations Office  
Contract DE-AC07-05ID14517**

#### **DISCLAIMER**

This information was prepared as an account of work sponsored by an agency of the U.S. Government. Neither the U.S. Government nor any agency thereof, nor any of their employees, makes any warranty, expressed or implied, or assumes any legal liability or responsibility for the accuracy, completeness, or usefulness, of any information, apparatus, product, or process disclosed, or represents that its use would not infringe privately owned rights. References herein to any specific commercial product, process, or service by trade name, trade mark, manufacturer, or otherwise, does not necessarily constitute or imply its endorsement, recommendation, or favoring by the U.S. Government or any agency thereof. The views and opinions of authors expressed herein do not necessarily state or reflect those of the U.S. Government or any agency thereof.



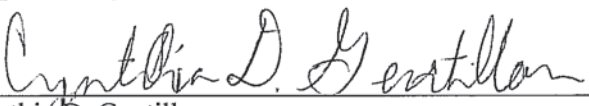
## Next Generation Nuclear Plant Project

# NGNP Data Management and Analysis System Modeling Capabilities


INL/EXT-09-16327

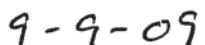
September 2009

Approved by:

  
Cynthia D. Gentillon  
NDMAS Modeling and Analysis Lead

  
Date

  
Jeffrey J. Einerson  
VHTR NDMAS Lead

  
Date

  
John R. Cox  
VHTR TDO Deputy Director

  
Date



## **ABSTRACT**

Projects for the very high temperature reactor (VHTR) Technology Development Office provide data in support of Nuclear Regulatory Commission licensing of the VHTR. Fuel and materials to be used in the reactor are tested and characterized to quantify performance in high-temperature and high-fluence environments. In addition, thermal-hydraulic experiments are conducted to validate codes used to assess reactor safety. The VHTR Technology Development Office has established the NGNP Data Management and Analysis System (NDMAS) at the Idaho National Laboratory to ensure that VHTR data are (1) qualified for use, (2) stored in a readily accessible electronic form, and (3) analyzed to extract useful results.

This document focuses on the third NDMAS objective. It describes capabilities for displaying the data in meaningful ways and identifying relationships among the measured quantities that contribute to their understanding. The capabilities are described from the perspective of NDMAS users, starting with those who just view experimental data and analytical results on the Idaho National Laboratory NDMAS web portal. The web modeling examples and user capabilities are described in detail. Capabilities available to NDMAS developers are more extensive, and are described using a series of examples. Most of the modeling efforts performed thus far focus on understanding how the initial Advanced Gas Reactor (AGR-1) fuel irradiation experiment temperature measurements relate to each other and to other experimental parameters. Future modeling developments and enhanced capabilities are described, such as the possible role of the temperature models in monitoring the accuracy of thermocouple measurements in ongoing VHTR irradiation experiments. Modeling capabilities available to users who download and analyze data using the software of their choice are virtually unlimited.

Overall, the NDMAS provides convenient modeling capabilities for studying a very large and rapidly increasing database of well-documented, pedigreed data via the Idaho National Laboratory NDMAS web portal, the NDMAS developers team, and direct use of downloaded data.





## EXECUTIVE SUMMARY

Projects for the very-high-temperature reactor (VHTR) Technology Development Office (TDO) provide data in support of Nuclear Regulatory Commission licensing of the VHTR. Fuel and materials to be used in the reactor are tested and characterized to quantify performance in high-temperature and high-fluence environments. In addition, thermal-hydraulic experiments are conducted to validate codes used to assess reactor safety. The VHTR Program has established the NGNP Data Management and Analysis System (NDMAS) to ensure that VHTR data are (1) qualified for use, (2) stored in a readily accessible electronic form, and (3) analyzed to extract useful results.

This document focuses on the third NDMAS objective. It describes capabilities for displaying the data in meaningful ways and identifying relationships among the measured quantities that contribute to their understanding. The capabilities are described from the perspective of NDMAS users, starting with those who just view experimental data and analytical results on the INL NDMAS web portal. Table S-1 provides an overview of the webpage modeling capabilities.

Table S-1. Modeling capabilities in the NDMAS webpages.

Webpage <sup>a</sup>	Modeling Capabilities							
	Graphs	Lattice graphs	Tabular drill-down	Data Exploration	Stored processes	Box plots, histograms	ActiveX graphs	Data downloads
Fuel graphical summary	X	X	—	—	—	—	—	—
Fuel tabular drilldown	X	—	X	—	—	—	—	X
FPMS gross gamma data	X	—	—	—	X	—	X	—
FPMS release and R/B data	X	X	—	X	—	X	—	X
Fuel thermocouple analysis	X	X	—	—	—	—	—	—
Fuel data cycle summary	X	X	—	—	—	—	—	X
Graphite characterization data	X	—	—	X	—	X	X	X
Live JMP reports	X	X	—	—	—	—	—	X

a. Acronyms: FPMS, Fission Product Monitoring System; R/B, Release/Birth; JMP, software from SAS Institute, Inc.

In Table S-1, most of the modeling capabilities are self-explanatory. Lattice graphs are graphs with panels that show the data for different groupings, such as different Advanced Gas Reactor 1 (AGR-1) fuel irradiation experiment capsules. Tabular drilldowns allow the data to be expanded or contracted for different levels of detail in the data display, with all graphs and tables in that display linked to respond accordingly. The NDMAS applications particularly allow the user to view the data in different time spans. Data Exploration tools allow the user to create aggregations and plots of data on the fly. Stored processes perform calculations and access data on a real-time basis, so that the information is always current. Boxplots and histograms are forms of graphs that show the distributions of data. ActiveX graphs are dynamic, high-resolution, web figures that allow on-the-fly alteration, such as rescaling of axes, subsetting of data, and viewing data values associated with each point. Data downloads are self-explanatory. Together, these capabilities allow the user to view the data and think about possible inter-relationships.

The report provides a detailed description of each content item in the webpages listed in Table S-1, with references to the modeling capabilities that they provide. The descriptions apply for the webpages as of August, 2009.

Capabilities available to NDMAS developers are more extensive, since the full power of the SAS Institute, Inc. statistical and analysis software that supports much of the system is available. An appendix describes some of the modeling tools. The current capabilities are described through a series of examples.

Most of the modeling efforts performed thus far have focused on understanding the AGR-1 fuel irradiation experiment temperature measurements. The temperatures are driven by Advanced Test Reactor (ATR) operating conditions such as control cylinder and regulating rod positions that modulate the neutron flux to the fuel compacts in the experiment test train. The AGR-1 control system adjusts the mixture and flow of Ne and He for each capsule in the experiment test train in order to maintain capsule temperatures in a predefined target range. The gas flow adjustments provide a temperature control function because He conducts heat away from the fuel capsules at a much faster rate than does Ne. The control gas system needs accurate temperature feedback in order to stabilize the temperatures at desired levels.

Nine of eighteen thermocouples (TCs) installed in the AGR-1 fuel irradiation test train to monitor the temperatures have failed since the experiment began in late 2006. Two were failed from the start of the experiment (in fabrication or installation). Three failure modes occur: (1) catastrophic or sudden failures that result in an immediate loss of signal, (2) drift that leads readings to be inaccurate, and (3) spurious or virtual TC junctions, which are instances of TC leads connecting in locations other than where the temperature is to be monitored. In the latter case, the readings can be a combination of the desired readings and the reading where the new junction formed. The drift and junction failures are not immediately obvious from observing the generated data streams.

Temperature analyses presented in this report include:

- Prediction of temperatures in capsules with no working TCs, using functioning TCs.
- Calculations of correlation coefficients for readings from pairs of TCs. Particularly when between-capsule correlation coefficients are higher than within-capsule correlations, a possibility of an unwanted junction exists.
- Prediction of temperatures based on functions of Ne fraction and fission power estimates. The fission power estimates were calculated outside NDMAS using 3-D finite element reactor physics models.
- Assessments of correlation coefficients for each reactor cycle between particular TC readings and a variety of ATR reactor parameters, such as control cylinder positions and lobe powers, in order to identify the reactor configuration variables that might be most helpful in predicting temperatures.
- Evaluation of regression models for temperatures using a range of ATR parameters.

Fission power has also been modeled as a function of the ATR reactor parameters.

Analyses have also been performed to identify mathematical models that can describe the relationship between radioisotope release-to-birth rates and capsule temperatures. Those models are all still under development. They show the feasibility of the methods, but they have not yet been finalized or applied across the board to all the AGR-1 capsules. They have potential for accuracy tests for the data, but limits that would trigger identification of possible off-normal behavior have not yet been derived.

One use of the models is for predictions of behavior of temperatures or other attributes for the next ATR cycle, based on the data from the most recent cycles. A moving window is recommended for fitting models, with projections going just one cycle into the future. Data for the models can be split into training

and testing intervals. Regression models or other statistical models are constructed using the training data, then evaluated with the testing data to see how well they perform. The success of these evaluations depends largely on whether the training and testing data are similar. If the range of conditions present in the testing data is also present in the training data, the models are likely to perform well.

In addition to modeling capabilities for NDMAS developers, a third set of modeling capabilities applies to researchers who download data from NDMAS. These capabilities are virtually unlimited, since users can apply their own modeling tools or software.

The modeling and analysis by NDMAS developers is an ongoing effort. Ideas for extensions of the existing models are listed. Additional data sets that will enter NDMAS in the next year will provide still more opportunities for model development. In summary, the NDMAS provides a wide array of modeling capabilities through the INL-NDMAS web portal, interaction with the NDMAS staff, and direct use of downloaded data.



## **ACKNOWLEDGEMENTS**

In addition to the authors of this report, many NDMAS team members contributed to the web pages that show many of the modeling capabilities discussed herein, including the following:

Jeffrey J. Einerson

R. Sam Alessi

Thomas L. Baldwin

Jordan H. Cox

David O. McGrath

Jodi L. Tokita

Review comments from David Petti, John Cox, Jack Simonds, Dawn Scates, Jodi Tokita, Gary Roberts, and Jeff Einerson have enhanced the content and increased the clarity of this report. Thomas Baldwin provided ideas to be implemented for identifying stable reactor operating periods. David McGrath provided details for the Enhanced Capabilities section.

Barry King's technical editing is gratefully acknowledged.



## CONTENTS

ABSTRACT.....	v
EXECUTIVE SUMMARY .....	vii
ACKNOWLEDGEMENTS.....	xi
ACRONYMS.....	xvii
1. INTRODUCTION.....	1
2. NDMAS MODELING OVERVIEW .....	2
2.1 Subjects of Modeling—Phenomena of Interest .....	2
2.2 Modeling Process for Various Groups of VHTR Researchers.....	3
2.2.1 Modeling Capabilities via the Webpages.....	3
2.2.2 Modeling Capabilities for the NDMAS Team.....	22
2.2.3 Modeling Capabilities via Analysis Requests.....	23
2.2.4 Modeling Capabilities via Downloads.....	23
2.3 Uses of the Applications .....	23
3. EXAMPLES OF CURRENT MODELING APPLICATIONS.....	24
3.1 Models Related to Fuel Irradiation .....	24
3.1.1 Capsule Temperature Models .....	24
3.1.2 Capsule R/B Ratio Models.....	41
3.2 Models related to Graphite.....	43
4. ONGOING AND PROPOSED FUTURE MODELING.....	44
4.1 Applications .....	44
4.1.1 Capsule Temperature Models .....	44
4.1.2 Capsule R/B Ratio Models.....	46
4.2 Enhanced Capabilities.....	46
5. SUMMARY AND CONCLUSIONS.....	48
6. REFERENCES.....	49
Appendix A VHTR Experiments and Associated Data Streams .....	A-1
Appendix B Use of SAS Tools For Modeling.....	B-1

## FIGURES

Figure 1. Graphical summary of Capsule 4 data for all cycles of the AGR-1 experiment to date.....	4
Figure 2. Example from Fuel Tabular Drilldown webpage. ....	5
Figure 3. Example of gross gamma count plot for Detector 4. ....	7
Figure 4. FPMS R/B data table for ATR Cycle 143A. ....	8

Figure 5. Kr 85m and Kr-88 release data (atoms/sec) from Cycle 143A plotted using JMP® software. ....	9
Figure 6. Distribution for an example FPMS R/B ratio. ....	9
Figure 7. Medians for the logarithm of the Kr-85m R/B ratio, grouped by capsule and ATR reactor cycle. ....	10
Figure 8. Kr85m R/B ratios as a function of TC #3 readings in four capsules (ATR Cycle 140A). ....	11
Figure 9. Scatterplot matrix with TC readings and Kr-85m R/B ratios for Capsule 6 in ATR Cycle 140A. ....	11
Figure 10. Three R/B ratios in time, with panels for each of the six capsules. ....	12
Figure 11. Daily correlation coefficients and temperatures for TC_1 (blue) and TC_3 (red) in Capsule 4, with purple correlation coefficients showing disqualified data for one or both TCs. ....	14
Figure 12. Daily correlation coefficients and temperatures for TC_2 in Capsule 6 (blue) and TC_3 in Capsule 5 (red). ....	14
Figure 13. Measured and predicted thermocouple readings, with thermal physics calculated temperatures. ....	15
Figure 14. Capsule 4 TC data summary for each cycle. ....	17
Figure 15. Capsule 4 data summary for Ne fraction for each cycle. ....	18
Figure 16. Box plots of piggyback graphite specimen diameters for different graphite grades. ....	19
Figure 17. Example of use of ActiveX graph toolbar to expand one box plot. ....	20
Figure 18. Graphite data exploration using Poisson's Ratio (grouped by graphite grade, specimen type, and with or against grain orientation). ....	20
Figure 19. Averages, within graphite grades for each specimen orientation, for elastic modulus measured using sonic resonance compared with elastic modulus measured using sonic velocity. ....	21
Figure 20. Four major steps in NDMAS data processing. ....	22
Figure 21. AGR-1 fuel irradiation experiment thermocouples. ....	25
Figure 22. Observed and predicted temperatures for TC_3 in Capsule 4, with 95% prediction limits. ....	29
Figure 23. Averages of daily correlation coefficients within capsules and across capsules. ....	30
Figure 24. Cycle 139 B data for regression model. ....	30
Figure 25. Thermal conductivity as a function of He fraction and temperature. ....	31
Figure 26. Predicted temperature readings for TC_3 in Capsule 4 in ATR Cycle 139B, with prediction-based confidence bounds. ....	33
Figure 27. Predicted temperature readings for TC_3 in Capsule 4 in ATR Cycle 139B, with model including TC readings from TC_1 in Capsule 4. ....	33
Figure 28. Correlations of variables with temperature, by cycle. ....	35
Figure 29. Determination of the number of terms to include in a model for readings from Capsule 4, TC_2. ....	36



Figure 30. Capsule 4 TC_2 model (gray dotted line) using all control cylinder, lobe power, and regulator rod depth variables and the measured TC_2 temperature (red line) .....	37
Figure 31. Ne fractions and control cylinder positions, with two models of Capsule 6 TC_2 readings.....	38
Figure 32. Contour plot of predicted temperature for TC_2 in Capsule 6 as a function of Ne fraction and the angular position of ATR SE control drum S1D2.....	39
Figure 33. Predicted and observed fission power in Stack 1 for Capsule 6 in Cycle 139B.....	41
Figure 34. Predicted and observed temperatures for TC_2 in Capsule 6 based on fission power and Ne fraction.....	41
Figure 35. Model from Dr. J. Kendall, showing R/B increases as EFPD increases. ....	42
Figure 36. Time profiles for failed TCs, showing periods when they reported inaccurate data. ....	46
Figure B-1. Example EG Process Flow. ....	B-4
Figure B-2. Enterprise Guide Query Builder. ....	B-5
Figure B-3. Data Task List.....	B-6
Figure B-4. Data Summary and Statistical Analysis tasks.....	B-7
Figure B-5. Graphics tasks.....	B-8
Figure B-6. New Report dialog .....	B-9
Figure B- 7. JMP analysis tools. ....	B-11

## TABLES

Table S-1. Modeling capabilities in the NDMAS webpages. ....	vii
Table 2. Failure status for AGR-1 fuel experiment thermocouples (TC) by capsule. ....	26
Table 3. Comparison of models of Capsule 6, TC_2 readings using Ne fraction and control cylinders.....	38
Table A-4. Fuel fabrication data parameters and categories.....	3
Table A-5. Reactor irradiation data parameters and attributes for the AGR (fuel) experiments. ....	3
Table A-6. Fission product monitoring data parameters and attributes. ....	3
Table A-7. ATR operating conditions data parameters and attributes. ....	4
Table A-8. NGNP neutronics and temperature analysis parameters and attributes. ....	4
Table A-9. Fuel PIE data parameters and categories (preliminary data). ....	4
Table A-10. Reactor irradiation monitoring parameters for the AGC (graphite) experiments.....	5
Table A-11. Parameters and classification for graphite specimens (characterization). ....	5



## ACRONYMS

AG	against grain
AGC	Advanced Graphite Capsule
AGR	Advanced Gas Reactor
AGR-1	Advanced Gas Reactor fuel experiment 1
ATR	Advanced Test Reactor
CV	coefficient of variation
DOE	Department of Energy
EBI	Enterprise Business Intelligence
EFPDs	effective full power days
EG	Enterprise Guide
FPMS	Fission Product Monitoring System
GLM	General Linear Model (a SAS Procedure)
INL	Idaho National Laboratory
JMP	JMP Statistical Discovery from SAS (software from SAS, Inc.)
MFC	Materials and Fuels Complex
MW	Megawatts
NDMAS	NGNP Data Management and Analysis System
NGNP	Next Generation Nuclear Plant
PIE	postirradiation examination
Q	gas flow rate (more generally, a heat transfer quantity)
QA	quality assurance
QAPP	Quality Assurance Program Plan
OLAP	online analytical processing
R&D	research and development
R/B	release to birth rate
$R^2$	coefficient of determination for a regression (correlation coefficient for predicted values and observed values)
RMSE	root mean square error (square root of sum of squares of residuals, divided by degrees of freedom)
SAS	software from SAS Institute, Cary, NC
SPC	statistical process control
SQL	structured query language
TC	thermocouple
TDO	Technology Development Office

VHTR	very high temperature reactor
WG	with grain

# **NGNP Data Management and Analysis System Modeling Capabilities**

## **1. INTRODUCTION**

Research and development (R&D) activities are underway to support development of technology for the Generation IV (Gen IV) Very High Temperature Reactor (VHTR). A particular focus of the research is on those activities required to design and license the first Next Generation Nuclear Plant (NGNP). The research is being conducted by an international team of research laboratories, universities, and private companies. The Technology Development Office (TDO) at the Idaho National Laboratory (INL) oversees and coordinates this research. In FY 2008, the TDO established the NGNP Data Management and Analysis System (NDMAS) to manage the large body of data being generated by the research. Through the NDMAS, data generated from VHTR research can be stored in a controlled and secure electronic environment that ensures both its integrity and its availability for use by VHTR researchers. The NDMAS provides a significant capability for allowing users to study the data and explore relationships among the attributes and responses being studied. This modeling capability is the subject of this report. For the purposes of this report, “modeling capability” is defined as a set of tools and methods for investigating relationships among VHTR research data.

Using NDMAS, one can explore relationships in the VHTR research data at a number of levels. At the simplest level, researchers can view graphs of data and think about possible relationships that might exist between various physical quantities in the experiment.

Intuitive models that come from data visualization can be checked by empirical studies. One can estimate parameters, such as averages within groupings of data, and observe which groupings have better outcomes. Formal statistical tests can be performed to identify differences that are beyond the realm of normal variation. At a higher level, one can formulate mathematical relationships that might exist between various attributes or measured quantities, and fit these to the empirical data to see what relationships best represent the data.

More involved formal models go beyond just empirical patterns and include known physical relationships between the quantities under study. Physical and empirical models can be combined to even better characterize relationships among the measured responses.

A final level of modeling, involving simulation of dynamic conditions as they propagate in a complicated system over a period of time, is not part of the modeling capabilities within NDMAS. NDMAS modeling will, however, support the development of such models. Some of the experiments planned for the VHTR will produce data to tune and validate such models, and NDMAS modeling capabilities will facilitate the study of those data as well as other data generated by the VHTR R&D program.

A major NDMAS capability that supports such modeling is the ability to display analytical results on the Internet. NDMAS uses a SAS Enterprise Business Intelligence (EBI) Web portal to make the experimental data and analytical results available to the VHTR research community.

In Section 2, NDMAS modeling capabilities are described in more detail. Section 3 is a compendium of modeling examples that have been performed to date. This section is expected to expand in future revisions of this document as more data streams are added in NDMAS and more analyses are performed. Section 4 outlines ongoing modeling applications and possible modeling capabilities to be added in the future, and Section 5 provides conclusions and a summary of the modeling capabilities.

## **2. NDMAS MODELING OVERVIEW**

NDMAS modeling is presented in this section from the standpoint of what the models describe, how the modeling is performed by different groups of researchers, and how the results are or could be used to improve VHTR research.

### **2.1 Subjects of Modeling—Phenomena of Interest**

Since modeling seeks relationships between various experimental quantities, knowledge of the available data and associated processes is a necessary prerequisite for modeling. The types of data currently stored in NDMAS are described briefly in this section and are itemized in Appendix A. A detailed description of the research data is beyond the scope of this document.

NDMAS has the capability of storing and qualifying all the data generated in the VHTR research. The data are organized according to data collection project, data stream, and data package. Currently, five projects have been identified:

- Fuel development and qualification
- Materials testing and qualification—graphite technology development
- Materials testing and qualification—high temperature materials
- Design methods and validation
- Nuclear hydrogen initiative.

Data have been input to NDMAS for the fuel development/qualification and graphite technology development projects.

Various data streams are generated for each project. A data stream is a set of parameters or measurements collected from one source that can be input into NDMAS together. A data stream may consist of a single set of data that is input just once, or it may be a set of data that is input repeatedly for different time frames or experiments. The set of data submitted in each instance of input for a data stream is called a data package. For example, while fuel is being irradiated in the Advanced Test Reactor (ATR), process data are generated every 5 minutes showing various temperatures and gas flow rates for each capsule in an experiment. These data are collected and processed into NDMAS on approximate weekly intervals. Appendix A describes NDMAS data streams and the associated inputs for the fuel and graphite data streams, among others.

At the level of individual data points, each numeric or qualitative value is associated with an experimental unit such as a fuel particle, fuel compact, capsule, or test train. Related records describe additional attributes for these entities. All data in NDMAS are stored in a Structured Query Language (SQL) database. This database has a table that shows the hierarchical relationship between the experimental entities.

The NDMAS provides extensive web pages devoted to supplying and summarizing data from VHTR experiments and related analyses. A summary of the SAS datasets stored within NDMAS can be found in the “Dataset Descriptions” webpage, which is accessible after logging into the INL NDMAS web portal as described in Section 2.2.1. The summary is organized by data stream and type of analysis (i.e., base dataset or analysis data). For each data table, the summary shows the character fields along with their contents and the number of records having each value. A second table shows the numeric fields, with their mean, median, minimum, and maximum. The tables also provide the number of records, the number of nonmissing records, and the standard deviation of the mean for each quantity.

NDMAS supports modeling of relationships between quantities in particular data packages. It also facilitates modeling of data across data packages, such as from one reactor cycle to another. One can also model relationships among quantities from more than one data stream. ATR reactor operating conditions

data, for example, are combined with VHTR irradiation experiment data for routine plotting and for analyses of controls on temperature. Data from different experimental units, such as different fuel capsules, can also be visually compared using NDMAS. Particular modeling efforts can be geared to the objectives of each VHTR experiment, or to resolve particular questions posed by other VHTR researchers or stakeholders.

An important function that NDMAS provides for the modeling effort is to ensure that data used for the models are captured correctly, are accurate, and are suited for their intended use. These characteristics of the data are the focus of the data qualification section of NDMAS. After data are entered into the SQL data base, they are checked to ensure that they are correctly captured, i.e., that they are identical to the raw data files supplied to NDMAS. As applicable, accuracy tests follow. An example of an accuracy test is the calculation of the coefficient of variation (CV) for a set of data. If the CV is unusually large, the data set is flagged because possible outliers or transcription errors might exist. The overall suitability of the data is ensured by the fact that data marked as qualified were collected under the framework of NQA-1, Part I: “Quality Assurance Requirements for Nuclear Facility Applications” (ASME 2000), as implemented through the *Very-High-Temperature Gas-Cooled Reactor Technology Development Office Quality Assurance Program Plan* (VHTR TDO QAPP) (INL 2009).

## **2.2 Modeling Process for Various Groups of VHTR Researchers**

NDMAS modeling capabilities for particular researchers depend on the individual’s level of access to the system. A number of user-specified options allow remote users who view NGNP data using the INL NDMAS web server to customize the displays they obtain for their own analysis needs. A broader range of modeling capabilities exists for members of the NDMAS Development Team, who create the displays that show on the Web. A third analysis capability is for researchers to file requests for particular analyses to be performed by NDMAS team statisticians. A fourth level of capability is completely unbounded: users can download data for their own analyses using whatever tools they prefer.

### **2.2.1 Modeling Capabilities via the Webpages**

Several modeling capabilities are a direct part of the NDMAS webpages, found at the following link: <http://sasweb.inl.gov/Portal/displayLogon.do>

(Note that one must contact the Web services administrator in order to obtain a user ID and password in order to log in and access this webpage). The modeling capabilities include data visualization, data aggregation (summaries), and data expansion (drilling down to view more detail in the data). The capabilities vary according to the webpage the user chooses to display. The modeling capabilities in the webpages showing current VHTR data are noted in subsections below.

The web content changes over time. The current discussion reflects the status of the webpages as of August, 2009. Additional sections will be added as more pages are developed.

Each “page” (or tab) in the INL NDMAS web portal consists of one or more sections with teal-colored headers. The sections are called portlets. Arrows on the far right in the portlet headers allow the user to display or hide each section. The portlets related to modeling capabilities are discussed below. Note that, in browsing the INL NDMAS web portal, clicking the “Back” arrow causes an error that will require the user to log into the system again. When the “SAS Web Report Viewer” appears, the correct method for moving back to the list of reports is to click above the Viewer or NGNP heading where the word “Portal” appears.

#### **2.2.1.1 Fuel Graphical Summary**

The Graphical Summary page in the INL NDMAS web portal contains summary plots for each capsule in the first Advanced Gas Reactor (AGR) fuel irradiation experiment (AGR-1) currently

underway in the ATR. The first portlet after the “Information” portlet is the “All Cycles by Capsule” portlet. The graphs here show effective power (MW), flow rates for He and Ne gases, temperatures for various thermocouples, and release-to-birth (R/B) rate ratios for Kr-85m, Kr-88, and Xe-135 plotted by date for all cycles of the AGR-1 experiment. There is a graph like Figure 1 for each capsule.

The first panel of the graph shows the ATR reactor state by plotting the effective reactor power. It is the average of power values from the center, NE, and SE ATR lobes, which are the three of the five ATR lobes that are closest to the AGR-1 experiment in ATR position “B-10.” Because power is a reactor attribute, it is the same for each capsule. The other parameters are reported separately for each capsule.

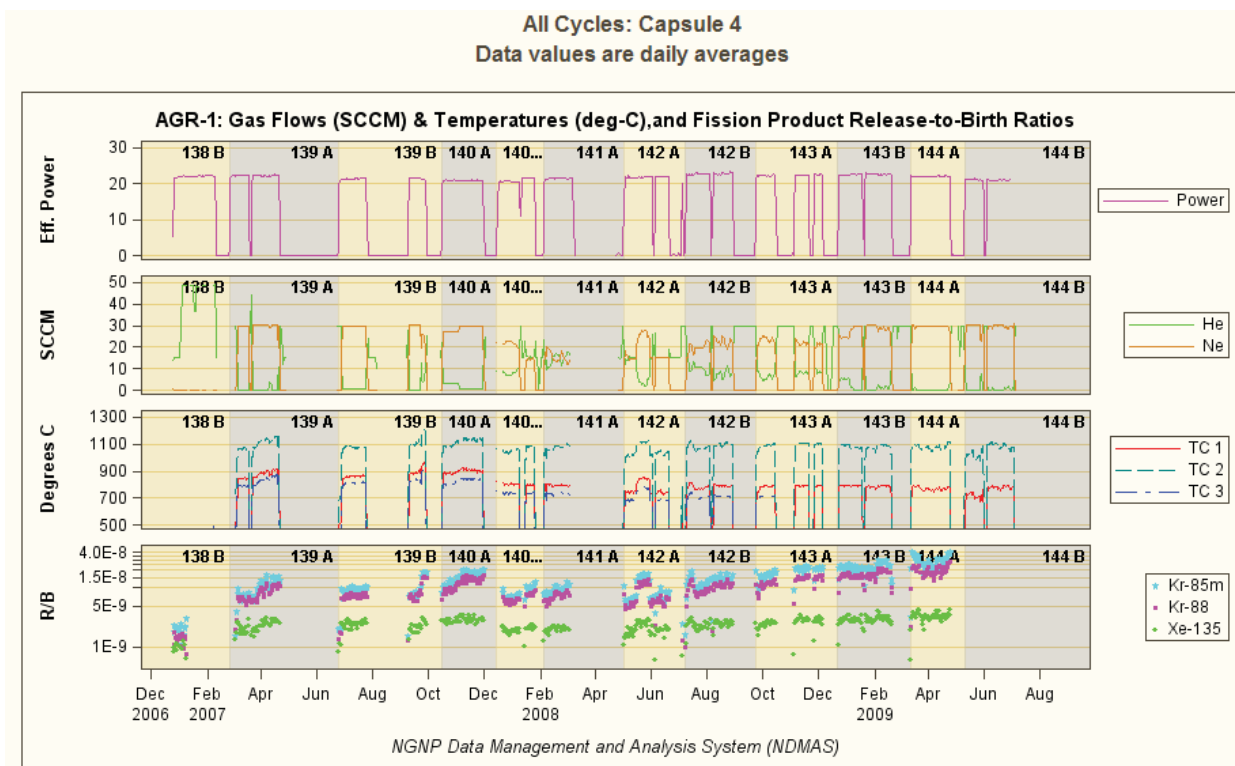


Figure 1. Graphical summary of Capsule 4 data for all cycles of the AGR-1 experiment to date.

The “Current Cycle” portlet on the Graphical Summary page provides the gas flow rates and temperatures for just the current cycle for each capsule. The recent values are easier to see here because the time scale is not as compressed.

The third Graphical Summary page portlet, “ATR Power Data,” provides more detail about the ATR effective power and other experiment-level power attributes. The average effective power is the same as the top portion of the capsules in the first display. The middle panel shows shim positions as degrees of rotation, while the third gives the thermal power for the five ATR lobes. All of these are daily averages plotted on a time axis.

The final portlet, (Fission Product Release by Capsule & Cycle) gives the fission product monitoring R/B ratios by capsule and reactor cycle. These are the bottom displays from the initial summary, grouped together so that changes from one capsule to another can be shown. Capsule 6 is at the top of the test train as installed in the ATR, nearest to the instrumentation recording devices, and Capsule 1 is at the bottom.

The Fuel Graphical Summary webpage does not provide direct access to the fuel irradiation experiment data, nor does it allow the user to manipulate the data for modeling. However, the displays facilitate thinking about relationships between ATR power, thermocouple, control gas flow rates, and fission product data. They allow between-capsule comparisons. They support intuitive modeling about



the overall effects of time as fuel burnup increases and boron content decreases from ATR cycle to ATR cycle.

### 2.2.1.2 Fuel Tabular Drilldown

The Fuel Tabular Drilldown webpage contains information about the same fuel irradiation attributes as the graphical summary. Information can be accessed on reactor power measures, gas flow rates, thermocouple temperatures, and R/B ratios. A series of reports in the first portlet display the data by ATR cycle, with capsule results grouped together as panels in one graph. A series of reports in the second portlet display the data by capsule over all cycles. An example from one of the reports is presented in Figure 2.

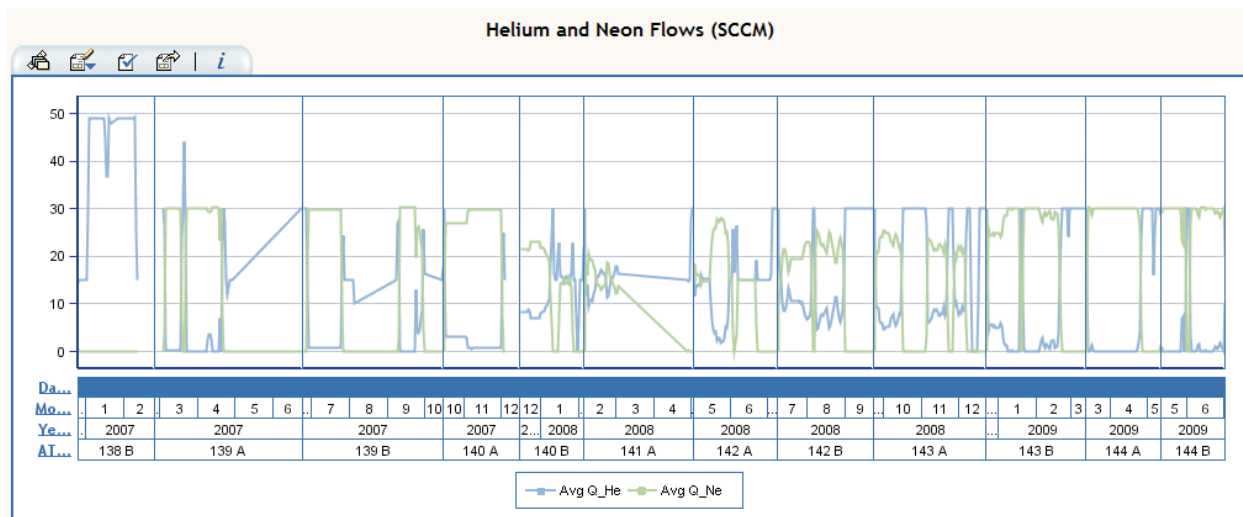


Figure 2. Example from Fuel Tabular Drilldown webpage.

The reports in this webpage of the NDMAS Web portal are unique because they display data from SAS EBI online analytical processing (OLAP) *cubes*. Cubes are data structures that allow rapid analysis because the data are hierarchically arranged with pre-calculated summary data at each hierarchy level. For AGR-1 data, this means that the data are readily examined at various time intervals, from hourly to daily, monthly, and yearly.<sup>a</sup> The data can also be easily subsetted to focus on particular intervals of time. For each data attribute, a user can observe averages and maximums for the specified time periods.

The time selections are controlled by clicking on particular entities (years, for example) in the X axis of the graph. Expand and drill-down options are provided. Both lead to more detailed displays, but the drill down option also subsets the data to focus on the period selected. Expanding or drilling down on a specific year reveals monthly data. Clicking on a specific month allows further expansion of the associated data as daily values are shown for each calendar day in the month. The expansion affects all the graphs on a page. Then, when daily results are displayed, clicking on a specific day causes those data to expand and reveal hourly results. The data can be reaggregated to return to previous displays showing a broader expanse of time by clicking on particular dates or months and selecting the “Collapse” option. When only hourly data appear, aggregation to the day level can be requested by clicking on the Day label on the left side of the X axis. Similarly, when only day data appear, aggregation to the monthly level can be requested.

<sup>a</sup> The most detailed data (e.g., the five-minute temperature data) are not accessible through the cubes.

Whatever is done in each manipulation to the graph being examined affects all the other graphs in the same report. One option accessed by the time labels on the left side of the X axis allows drilled-down data to be sorted by the attribute being displayed. This capability is useful for modeling considerations because one can observe patterns in how other attributes increase or decrease as the studied variable changes.

Further modeling support comes from the tab options at the top of each graph. The first tab relates to the data fields that are plotted, the second to graph options such as filtering and conditional highlighting, the third to graph properties such as the thickness and color of the lines, and the fourth allows export of the data. A final tab lists the full expanse of possible attributes that can be displayed.

The data itself appears following the graphs. The data display is at the same level of aggregation as displayed in the graphs. The aggregations can be controlled in the data display as well as in the graphs. In the data tables, the second tab gives table options such as how to filter and sort the data, and the third tab allows the user to change table properties such as the font and displayed table size.

The export tab, common to both the graphs and the tables, allows the user to export the data as a tab-delimited text file, or to export the formatted data directly into Excel<sup>a</sup>. This capability supports modeling as described further in Section 2.2.4.

### **2.2.1.3 FPMS Gross Gamma Data**

A sodium iodide detector in the AGR-1 sweep-gas flow line for each capsule monitors the associated gross gamma level. A seventh detector functions as an on-line spare. The detectors record the accumulated gamma count over a nominal detector dwell time of 3.5 seconds. The radiation comes from stray or ‘tramp’ releases from heavy metal contamination on the fuel particles and compacts. In addition, the gross gamma recorders pick up fluctuations associated with perturbations in the instrumentation and recording system. The system is not intended to provide quantitative estimates of fission product releases, but rather to provide an early indication of any fuel leakage that might occur in the experiment.

Two sets of plots can be viewed in the FPMS Gross Gamma Data webpage. In the first portlet (Interactive Gross Gamma Plots), the user can view graphs of gross gamma counts for the most recent seven days, any specified less-than-24-hour period, or any specified day or range of days, for any of the seven detectors. This capability is provided by the *Stored Process* feature in the INL NDMAS web portal. Stored processes direct the system to retrieve and format the data and then create the plots. In the second portlet, a standard set of plots shows Detector 4 data for the most recent seven days, the most recent day (less than 24 hours), and since the start of the most recent ATR cycle (see the example in Figure 3). Detector 4 is associated with Capsule 4, near the center of the AGR-1 experiment train.

The use of gross gamma data in modeling is limited because it is subject to numerous instrument perturbations and does not account for changes in gas flow rates. However, it does respond to changes in the irradiation experiment such as increases in neutron flux, and the data are available almost immediately after collection. Therefore it has considerable potential for real-time analysis of experimental data. The more accurate isotope-specific spectrometer results, which are displayed as R/B rate ratios, are probably more suitable for modeling (see next section).

---

<sup>a</sup> Since cubes combine different data streams, some interpolation of the raw data occurs to get the data on a uniform hourly time scale. Therefore, cube data downloads differ slightly from downloads of source data from single data streams (such as the downloads described in Section 2.2.1.4).

### Nal Gross Gamma – ATR Cycle 144B – Detector 4

From cycle start --05/11/09 to 07/22/09

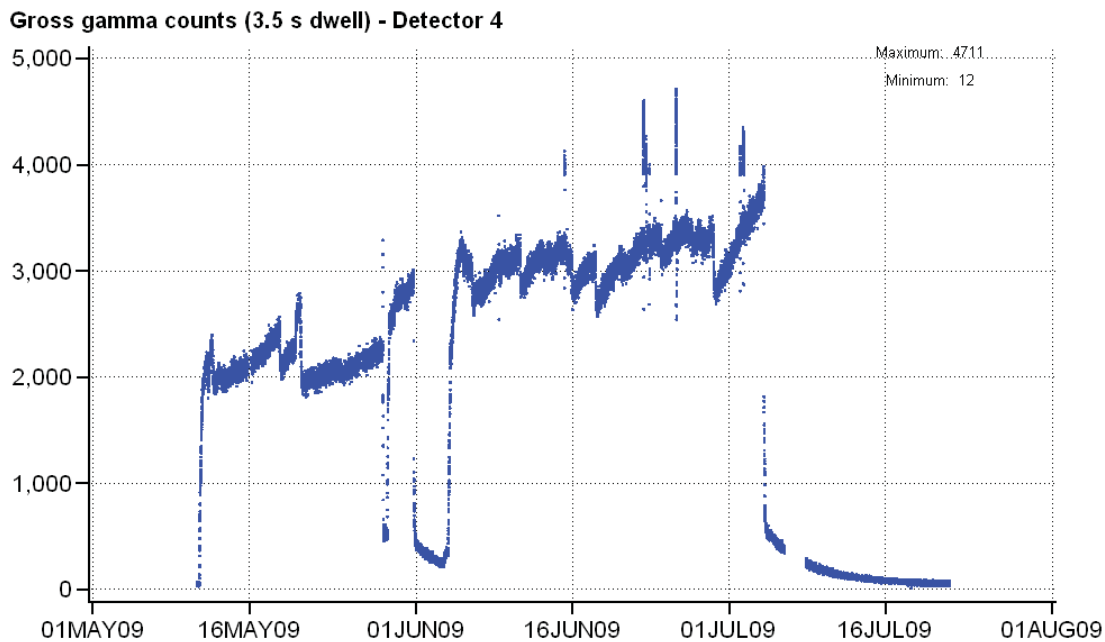


Figure 3. Example of gross gamma count plot for Detector 4.

#### 2.2.1.4 FPMS Release and R/B Data

The Fission Product Monitoring System (FPMS) has gamma-ray spectrometers in the sweep-gas flow lines for each capsule in addition to the gross gamma counters. The spectrometers measure five Kr isotopes (85m, 87, 88, 89, and 90) and seven Xe isotopes (131m, 133, 135, 135m, 137, 138, and 139). NDMAS stores four quantities for each of these radionuclides: release rate, R/B ratio, and error estimates for each of these quantities. The accumulated counts are recorded over a nominal 8-hour sampling period during the irradiation experiment in the ATR.

The birth rates used to calculate R/B ratios at each 8-h time interval are themselves calculated quantities. The main calculations are performed at the start and end of a reactor cycle and at two points in between. Eight-hour values to match the release rates are obtained by interpolation. Because the birth rate estimates are calculated at the end of each reactor cycle, the post-processed release and R/B data are not available for loading into NDMAS until the end of each ATR reactor cycle.

The FPMS Release and R/B Data webpage has two portlets that provide direct access to the isotope-specific FPMS data by reactor cycle. One portlet (FPMS Release Data) lists the release data, with capsule-specific isotope data for each cycle. The other portlet (FPMS R/B Data) lists the R/B ratio data. There is also a link that contains all the FPMS data loaded into the SQL database (currently, over 11,000 records).

The FPMS data portlets use the SAS EBI *Data Exploration* tool, which provides a significant modeling visualization and downloading capability. The user can select and order available “categorical” and “measurement” variables to develop a customized table (Figure 4). Then the data can be filtered and sorted as desired by the user. In the query capability of these portlets, one can even add totals, percentages, and other calculated fields (e.g., the ratio of two isotopes). Ranking the data according to a specified field is another capability. Simple line plots of the data can also be made within the display or

the data can be downloaded to Excel and plotted using other scientific plotting software. Figure 5 is an example of such data plotted using JMP.<sup>a</sup>

	Filepath	Capsule	Specid	Date	Time	Kr 85m Rat	Kr 85m Rer	Kr 87 Rat
1	\\Sasngnp\ngnp\NGNP_Data\AGR-1\FPMS data\Clean\BirthRates\143A	1	G1809240300	09/24/2008	3:08	2.8151E-9	8.4	2.06301E-9
2	\\Sasngnp\ngnp\NGNP_Data\AGR-1\FPMS data\Clean\BirthRates\143A	1	G1809241100	09/24/2008	11:08	4.19189E-9	7.5	2.77236E-9
3	\\Sasngnp\ngnp\NGNP_Data\AGR-1\FPMS data\Clean\BirthRates\143A	1	G1809241900	09/24/2008	19:08	1.87379E-8	7.2	9.11354E-9
4	\\Sasngnp\ngnp\NGNP_Data\AGR-1\FPMS data\Clean\BirthRates\143A	1	G1809250300	09/25/2008	3:09	1.16371E-8	9.4	7.4466E-9
5	\\Sasngnp\ngnp\NGNP_Data\AGR-1\FPMS data\Clean\BirthRates\143A	1	G1809251100	09/25/2008	11:09	1.22486E-8	8.1	7.45577E-9
6	\\Sasngnp\ngnp\NGNP_Data\AGR-1\FPMS data\Clean\BirthRates\143A	1	G1809251900	09/25/2008	19:09	1.19124E-8	9.2	7.71921E-9
7	\\Sasngnp\ngnp\NGNP_Data\AGR-1\FPMS data\Clean\BirthRates\143A	1	G1809260300	09/26/2008	3:09	1.41099E-8	7.2	8.9484E-9
8	\\Sasngnp\ngnp\NGNP_Data\AGR-1\FPMS data\Clean\BirthRates\143A	1	G1809261100	09/26/2008	11:09	1.14846E-8	9.1	7.21842E-9

Figure 4. FPMS R/B data table for ATR Cycle 143A.

The third portlet provides statistical distributions for the logarithms of the R/B ratios for the three most important isotopes (Kr-85m, Kr-88, and Xe-135). The displays give histograms for each cycle along with box plots that are color-coded to show which capsules apply for any outliers. Each plot is followed by a small table showing the median and other key percentiles of the distributions. Figure 6 is an example of this display for Kr-85m.

Two additional graphs appear in the third portlet for the Kr-85m isotope. Capsule-specific Kr-85m median R/B ratios are plotted for each ATR cycle. In one graph, median data for each capsule are connected. In the other, needles connect the lowest and highest values for each cycle (Figure 7). These plots show, for example, that Capsule 6 had relatively low median Kr-85m ratios early in the experiment

<sup>a</sup> The particular data in Figure 5 show an anomaly in the data collection system for Kr-88 release activity in Capsules 2 and 3. A hardware problem caused an undesired shift in the spectrum, which is being addressed by project personnel. The NDMAS modeling/analysis tools help identify measurement anomalies.

and relatively high ratios in the more recent cycles. Plots like these facilitate thinking about possible relationships between the R/B ratios, capsule differences, and time or cycle impacts.

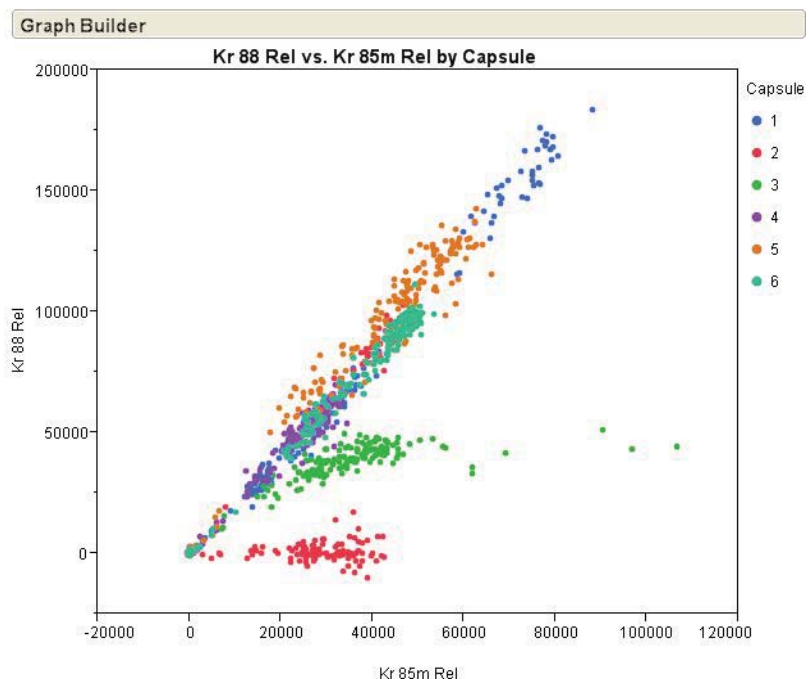


Figure 5. Kr 85m and Kr-88 release data (atoms/sec) from Cycle 143A plotted using JMP® software.

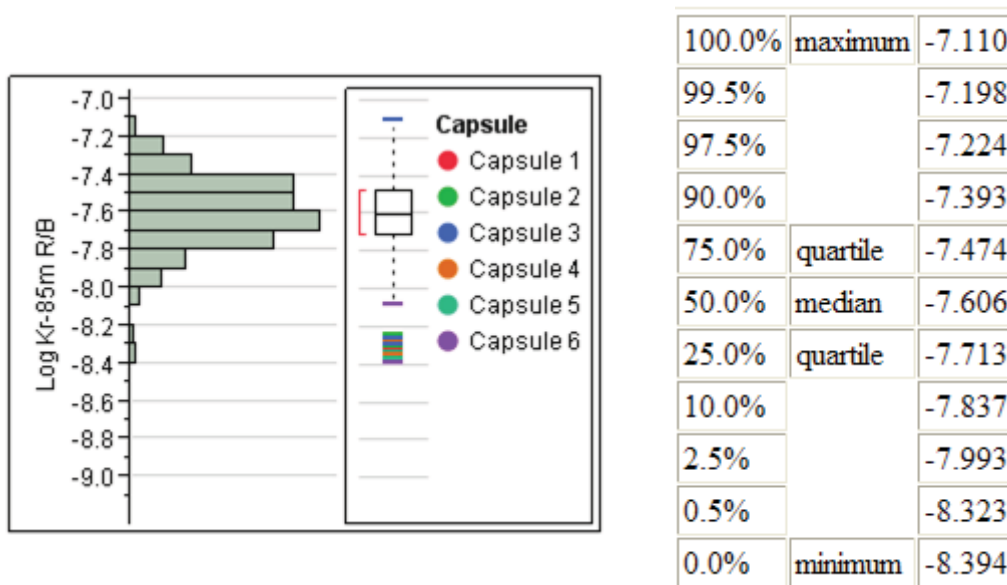


Figure 6. Distribution for an example FPMS R/B ratio.

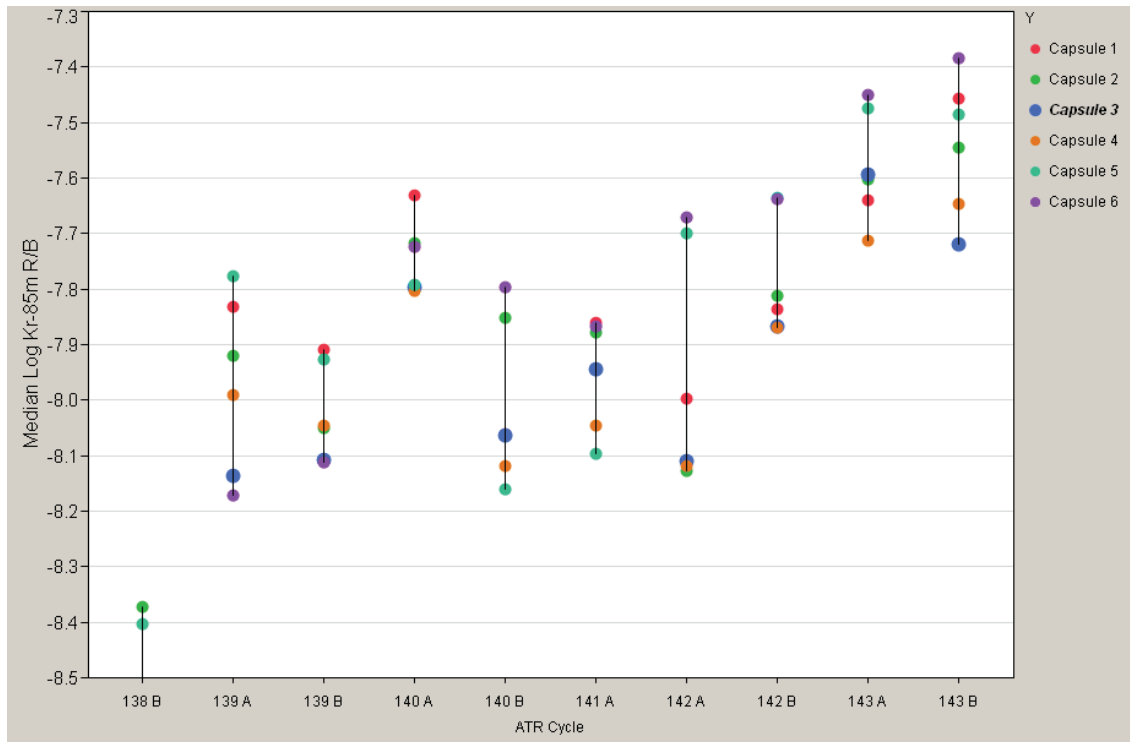


Figure 7. Medians for the logarithm of the Kr-85m R/B ratio, grouped by capsule and ATR reactor cycle.

The fourth portlet (R/B Correlations) shows modeling using data from two data streams. R/B data from the two main Kr isotopes are plotted as a function of capsule temperature as measured by various thermocouples for ATR Cycles 139A through 143B. The data stream merging process requires interpolation of data recorded at one time sequence onto the time sequence of another data set. NDMAS currently performs piecewise constant interpolation of the FPMS datasets onto the time sequence of the temperature data, where each parameter in the interpolated dataset is assumed to be constant between recording times. In future modeling, other interpolation methods can be used to construct more accurate datasets as necessary.

In the R/B Correlations portlet, a separate link exists for each isotope. Within each link, a row of five graphs exists for each reactor cycle. Each graph contains a scatter plot of daily average data, color-coded according to the capsule. Kr ratios less than  $5.E-9$  and Xe ratios less than  $1E-9$  were omitted. The plots using TC-4 and TC-5 have just one set of capsule data because these TCs only exist in Capsule 6. The cycle displays have fewer plots for later cycles, after TC failures occurred. Many of the graphs show an approximately linear relationship for the R/B ratio as a function of temperature. This situation exists particularly for Cycle 140A (Figure 8). The plots are similar for the Kr and Xe isotopes, and show that the R/B ratios respond to even small changes in temperature.

Another link in the “R/B Correlations” portlet gives the correlation coefficients between thermocouples and between each thermocouple and the Kr-85m R/B ratio by cycle and capsule. It then gives a *scatterplot matrix* for the data going into each correlation calculation. A scatterplot matrix shows the data in a table of little graphs (Figure 9). The matrix is of dimension  $n \times n$ , where  $n$  is the number of variables being displayed. Cells on the diagonal label the variable being plotted for each row and column. All the pairwise scatterplots that can be shown in the data appear as little graphs in the matrix. The R/B data in the portlet are in the bottom row and rightmost columns of both the listed correlation matrices and the matrices of little scatterplots. Matrices of scatterplots provide another useful visualization tool.



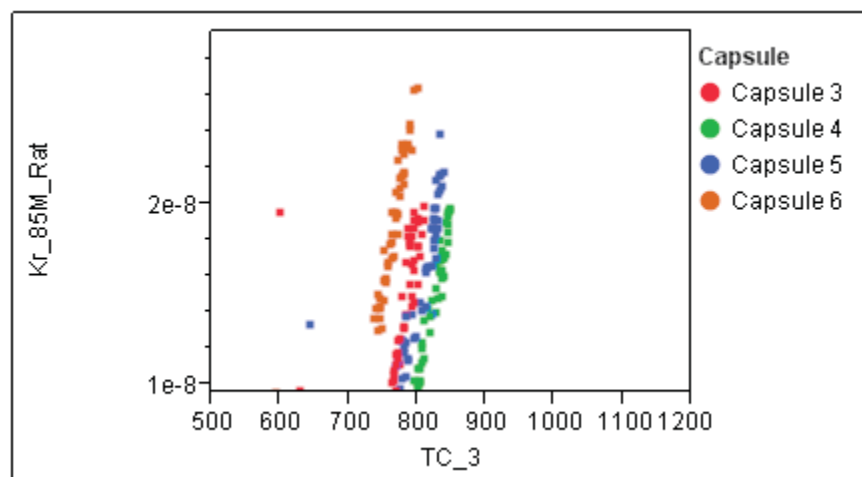


Figure 8. Kr85m R/B ratios as a function of TC #3 readings in four capsules (ATR Cycle 140A).

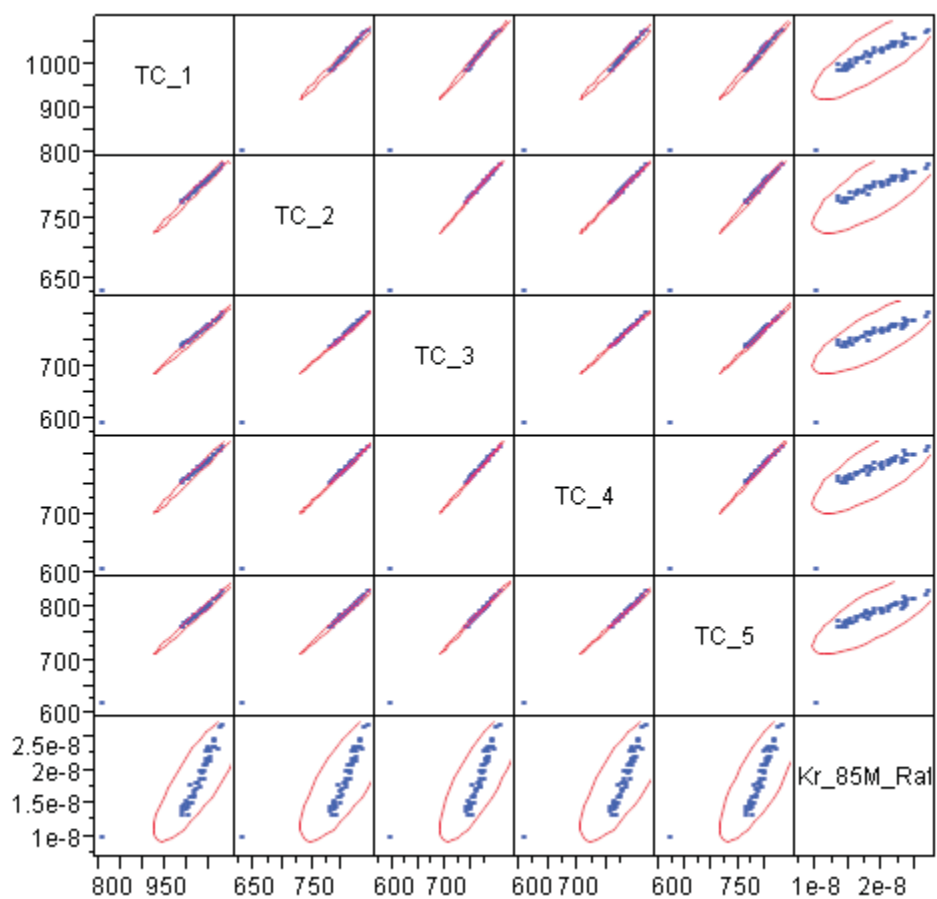


Figure 9. Scatterplot matrix with TC readings and Kr-85m R/B ratios for Capsule 6 in ATR Cycle 140A.

The last portlet (FPMS Plots) has three graphs that show the data across time and across capsules. The first presents R/B ratios for the three main isotopes (Figure 10), similar to the FPMS graphs in the Graphical Summary page. Another graph shows Kr-85m birth rates as calculated from the measured release rates and the processed R/B ratios supplied by the FPMS technical staff. The graph shows connected piecewise linear segments for each cycle. Where the lines change, new birth rate calculations were performed. The lines connecting the points are interpolations. The last graph shows R/B data for the other Kr and Xe isotopes (excluding Kr-85m, Kr-88, and Xe-135) supplied in the FPMS source files.

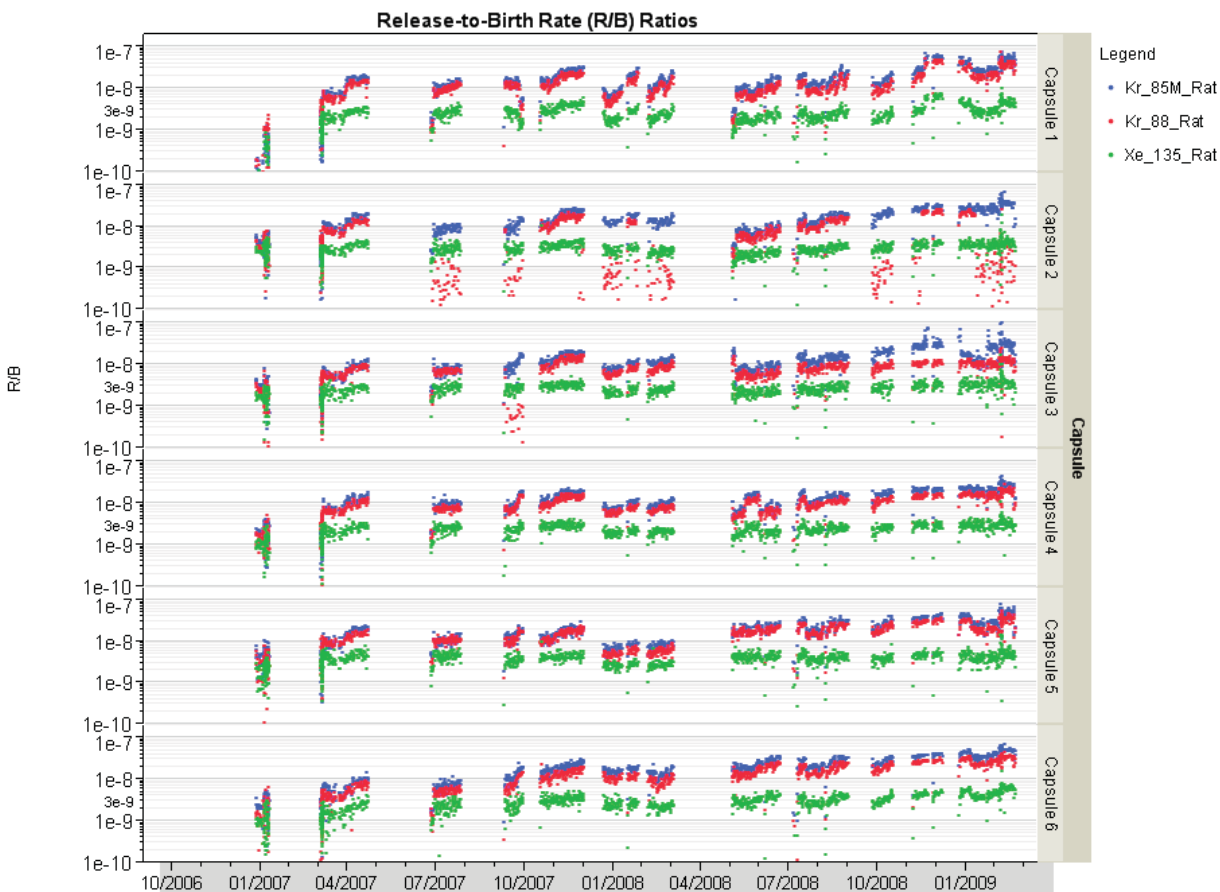


Figure 10. Three R/B ratios in time, with panels for each of the six capsules.

### 2.2.1.5 Fuel Thermocouple Analysis

The "Fuel TC Analysis" webpage shows outputs from modeling that are intended to assess the accuracy of the fuel irradiation experiment thermocouple (TC) readings. Knowledge of the temperatures experienced by the fuel, along with the neutron flux, is important for assessing the results of the AGR-1 experiment. A primary purpose of the irradiation experiment is to determine which fuels perform best in the high-temperature, high-flux environment of a VHTR.

The temperature data sets provide an important indication that the experiment is progressing as planned. The data streams are also important for experiment control, because the gas transport system uses these data to adjust the mixture of Ne and He in each capsule to control experiment conditions. Helium has a higher thermal conductivity than neon, and thus transfers thermal energy more rapidly between the capsule and the much colder water in the reactor vessel, leading to decreased capsule temperatures. Neon has a significantly lower thermal conductivity, so capsule temperatures can be increased by increasing the neon/helium ratio of the gas flow mixture.



A primary means of assessing the accuracy of the TC data relies on numerical simulations conducted by the AGR-1 technical staff. Measured temperatures are compared to calculated thermocouple temperatures to help evaluate the integrity of the thermocouples. The calculated temperatures are determined for one or more times during each reactor cycle. Steady-state fission power heating rates are calculated for the test fuel stacks, using a combination of the MCNP and ORIGEN2 nuclear reactor simulation codes (Chang and Lillo, 2007). These calculations employ reactor operating conditions data provided by ATR operators. The heating rates are then used as source terms in a 3-D heat transport model of the AGR-1 experiment capsules (Ambrosek, 2005a), to calculate temperatures in the fuel stacks and at the thermocouples. These complex evaluations are beyond the scope of NDMAS modeling. They have the advantage of accounting for a wide range of evolving conditions in both the ATR and in the experiment itself, including changes in power levels induced by changes in the configuration of the ATR, fuel burnup within the capsules, and boron depletion in the graphite holder assembly. Where thermocouples record temperatures significantly different from readings predicted by numerical simulation, the thermocouples may be judged to have failed.

Measured temperatures have been supplied by the TCs every hour during the first cycle in the experiment, every 10 minutes during the second cycle, and every 5 minutes during the rest of the experiment. Measured temperatures are supplemented, and checked against, temperatures calculated via simulation of neutron transport and heat transport, which are typically performed every few weeks.

Because of the importance of the TC readings, much of the current NDMAS modeling effort has focused on how to determine whether or not they are accurate. The “Fuel Thermocouple Analysis” page shows the results of some of these analyses. Like the graphical summary pages, it does not provide direct access to the data, nor does it allow the user to manipulate the data for modeling. However, the displays facilitate thinking about relationships in the data, allow between-capsule comparisons, and support intuitive modeling about the overall effects of time on temperature as fuel burnup increases and boron content decreases from ATR cycle to ATR cycle.

There are four portlets in the Fuel TC Analysis page. The first provides some information about the 18 TCs installed in the AGR-1 irradiation experiment test train, including their design and where they are installed. Half of the TCs have experienced failure. The portlet provides failure dates and other information about the failures.

The second portlet shows daily pairwise correlations between TC readings for TCs in the same capsules. For each pair of TCs in a capsule, ordinary Pearson correlation coefficients are calculated for each day, using pairs of 5-minute readings for which both readings are at least 100°C. Most of the correlation coefficients are based on 288 temperature pairs. TC readings within a single capsule are expected to be very highly correlated, although measured temperatures tend to be higher in the center of the test train than on the edges. The displays in the portlet, produced by the SAS “JMP” software, have one pair of panels for each pair of TCs. The top panel shows the correlation coefficients, while the second panel shows the two daily average temperature profiles. Based on there being from two to five TCs in a capsule, there are from one to 10 such pairs that can be compared for each capsule. There are a total of 21 within-capsule TC pairs. The legend refers to “First TC,” and “Second TC.” The lowest-numbered TC is always the first one. The data are plotted against a time axis that spans the duration of the AGR-1 experiment (Figure 11 gives an example, with the time axis copied from the bottom of the series of panels). Disqualified temperatures are plotted using dotted lines, and correlations with one or more disqualified entries are shown in purple instead of black.

The within-capsule correlation displays show that the correlations tend to be high, except when the ATR reactor transitions to a shutdown power status and when catastrophic failures in the TC readings occur that reduce one set of TC readings to near zero. The displays also show dotted lines in the temperature graphs for instances where the TC readings have been declared to be failed, even though they continue to give high temperature readings. A purpose of studying these data is to see if a statistical test

can be developed that shows or detects that a TC failure has occurred when it still generates realistic output.

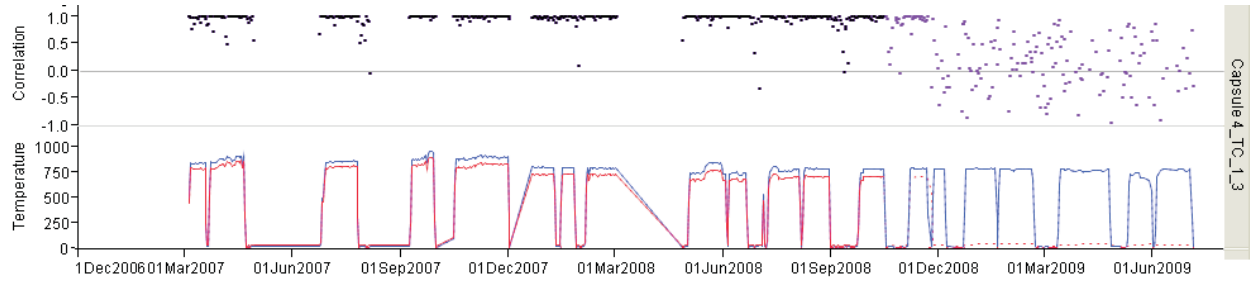


Figure 11. Daily correlation coefficients and temperatures for TC\_1 (blue) and TC\_3 (red) in Capsule 4, with purple correlation coefficients showing disqualified data for one or both TCs.

The third portal shows TC correlations and readings, like the second. However, the correlations are for TC pairs with each TC in a different capsule. Somewhat lower correlations are expected for between-capsule comparisons. A representative TC was selected from each capsule for the between-capsule correlation comparison. With six capsules, there are 15 pairwise comparisons. Figure 12 is an example of the between-capsule correlation coefficient and average temperature display (using two TCs that have not failed).

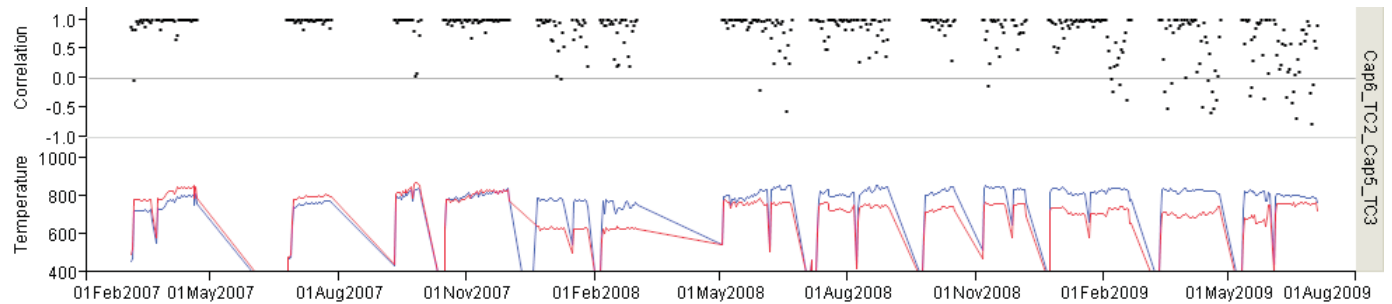


Figure 12. Daily correlation coefficients and temperatures for TC\_2 in Capsule 6 (blue) and TC\_3 in Capsule 5 (red).

The between-capsule correlations are of interest in comparing capsule temperatures as well as for possible additional TC accuracy evaluations. The existence of high between-capsule correlations is to be expected because fission heating rates in each capsule are responding to the same primary influences, the neutron flux imposed by the reactor. The secondary control of temperature, via modulation of the mixture of helium and neon flowing to each capsule, is most of the time an automated response to the monitored TC readings. As long as the temperatures across capsules change in a similar way, the gas flows that respond to those changes will also follow the same pattern. In turn, with similar gas flows, the temperatures across capsules remain highly correlated. However, periods showing increased between-capsule correlations, with no change in within-capsule correlation, may indicate formation of a new TC junction. For such a failure, TC readings are influenced by temperatures at the new junction as well as at the junction where the TC is installed.

The last portlet shows actual and model-predicted TC readings (Figure 13). A panel appears for each capsule. Seven of the TCs have failed in the harsh environment of the AGR-1 test train, and two installed TCs failed during fabrication. Therefore, empirical models were sought to predict the temperatures that might have been seen by the failed TCs. If fuel experimental conditions are generally the same throughout the test train, and the dominant controls on temperature are ATR operating conditions rather than capsule-

specific behavior such as fuel and boron depletion rates, then the temperature at a failed TC position might be a function of the other temperatures in the test train.

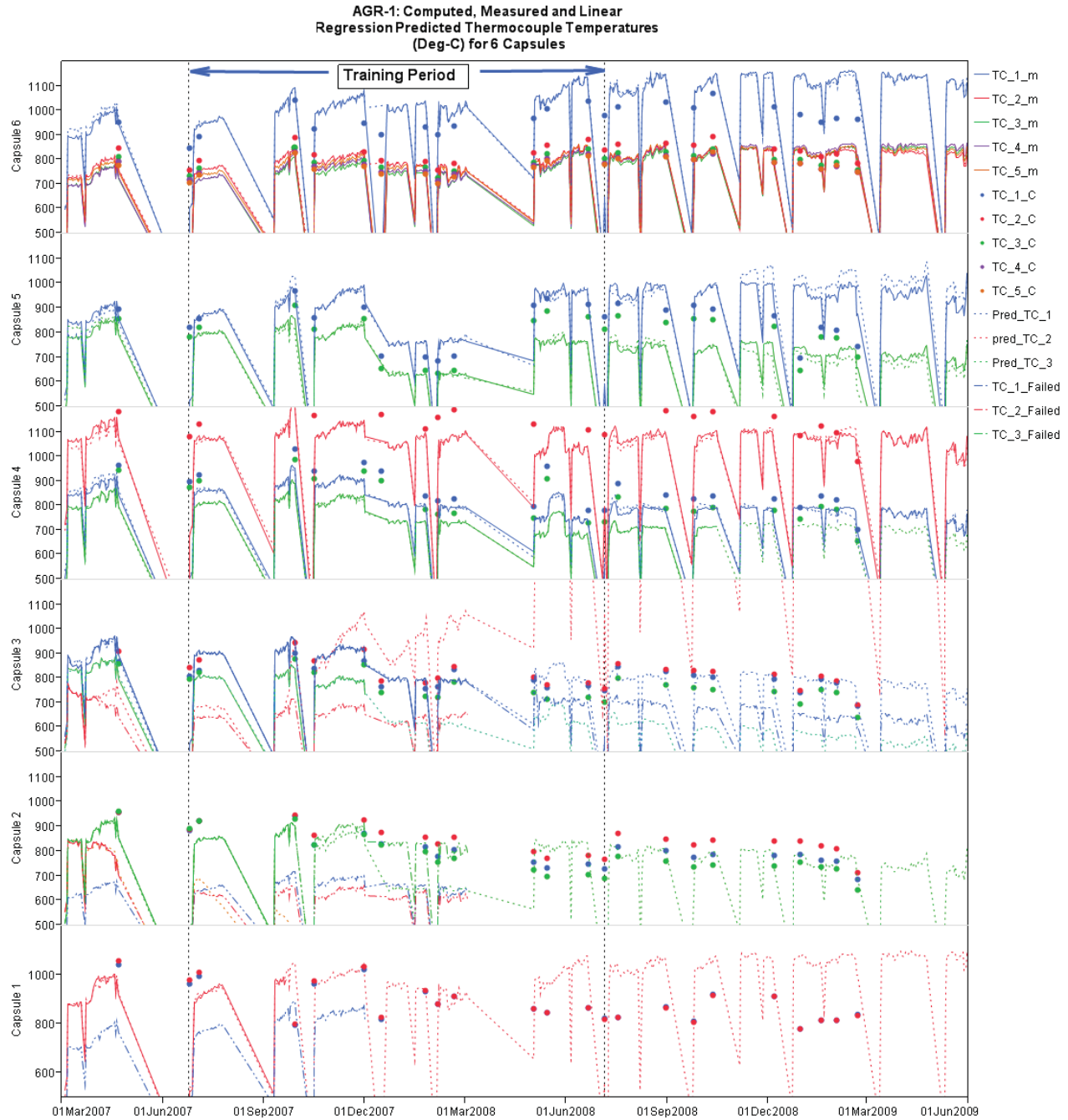


Figure 13. Measured and predicted thermocouple readings, with thermal physics calculated temperatures.

The models were first developed for the operating TCs in order to test the feasibility of such predictions. A regression model was fit for each of six operating TCs, using the other eight TCs as predictor variables. No models were fit for TCs 3, 4, and 5 in Capsule 6, which record readings very similar to TC 2 in Capsule 6. The regression coefficients were estimated by minimizing the sum of the squares of differences between the observed TC readings and the predicted TC readings. The data used to

estimate the model coefficients was from the “Training Period” labeled at the top of Figure 13. The first two ATR cycles in the AGR-1 experiment were omitted from the training period because their performance was atypical of later cycles. Experimentation led to selection of the end of ATR Cycle 142A (7/15/2008) for the end of the training period. After fitting the models using data in the training period, predicted values were generated for the more recent period. These are the dotted lines in the panels for Capsules 6, 5, and the red and blue plots in Capsule 4. These dotted lines are seen to fit the actual TC readings fairly closely, although some are uniformly higher than the observed TC readings and some are uniformly lower.

No model was constructed for the two TCs that failed on fabrication because there was no period with qualified data from these TC that could be used to train the model (i.e., estimate the equation coefficients). Two other TCs failed fairly early in the experiment and had little training data: TC\_2 in capsule 3, and TC\_2 in Capsule 2 (both of which are plotted in red). The red dotted line in the Capsule 3 panel shows that this model predicted high, off-scale temperatures. The model for TC\_2 in Capsule 2, on the other hand, led to low off-scale temperatures for the time period after September of 2007.

Models for the remaining five failed TCs used the data up to their failure date for training. The results can be assessed by comparison with the calculated temperatures (Ambrosek, 2009). These are shown on the graph as dots, with labels ending in “-C.” They are believed to be accurate. The best temperature prediction model is for TC\_1 in Capsule 3. Here, the blue dotted lines remain near the calculated values while the actual observations (from the drifting, inoperable TC) were decreasing.

The predicted temperature modeling may be useful, especially if it can be refined further. In that case, when instrumentation from a capsule is lost, its temperature could be approximated using the temperature data from other capsules. The predicted temperatures from the regression models are much easier to evaluate than the detailed calculated models. This modeling effort is discussed in more detail in Section 3.1.1.1.

### **2.2.1.6 Fuel Data Cycle Summary**

The last AGR-1 fuel irradiation data page summarizes the irradiation experiment conditions for each ATR cycle. The page has five portlets. The first provides background information about the TC failures that have occurred in the experiment, like the first page in the Fuel TC Analysis page. The remaining portlets provide a common output for a variety of parameters, including TC readings, gas flows, logarithms of R/B ratios, and overall reactor power levels. For each parameter under study, four attributes are displayed in four panels of a graph such as the one in Figure 14.

The top panel shows the mean for each ATR cycle for the parameter under consideration, for each measuring device. Each mean is the average of daily averages. Each point is surrounded by a lower and upper confidence bound. These bounds are calculated from the daily average data under the assumption that each set of daily averages is a sample from a normal distribution. Under this assumption, the interval from the lower 95% bound to the upper 95% bound covers (includes) the true mean of the distribution 95% of the time. Thus, the plot not only shows the mean values but gives an indication of how the means of the daily means might vary from random variation.

The second panel shows the maximum values that the daily average parameters achieved during each cycle.

The third panel provides another indication of variation in the data within a cycle. The coefficient of variation (CV) for a set of data is defined as the ratio of the estimated population standard deviation and the sample mean. Thus, the CV is a measure of the noise in the daily averages, expressed as a fraction of the overall average of the quantity being measured. The CV values facilitate comparisons of the variation between the different TCs or gas flows or log R/B ratios within a cycle and of particular measurements across reactor cycles.

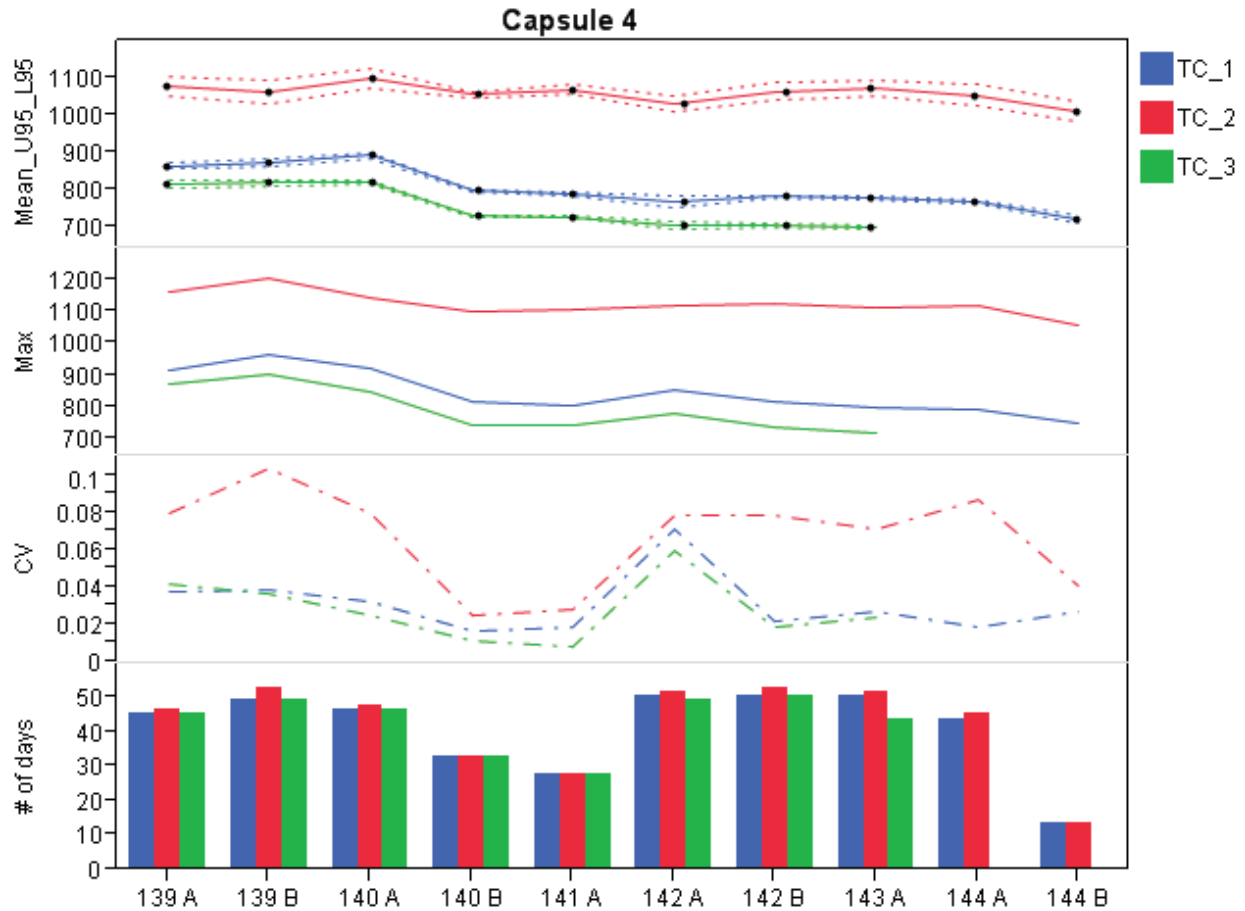


Figure 14. Capsule 4 TC data summary for each cycle.

The final panel shows the number of daily averages going into each calculation. When a TC fails, the numbers drop to zero. For the temperatures, another pattern influences the number of days. The daily average temperatures entering the calculations for the plots are filtered so that the plots focus on periods of reactor operations. TC daily averages less than 560°C are omitted. Therefore, the highest TC reading often has slightly more data points than the others.

The webpage portlets present graphs like those described above. The first portlet has just one trace in its panels and shows statistics from the average daily effective power levels for the reactor. The remaining portlets contain separate reports for each capsule. The reports in the second portlet describe temperatures, those in the third portlet describe control gas flow rates, and those in the last portlet describe the logarithms of the R/B ratios.

The control gas flow rate reports have two series of graphs. The second graph in the panel shows He and Ne flow rates, as described above. The first graph shows the Ne fraction, defined as the average daily Ne flow rate divided by the sum of the average daily Ne flow rate and the average daily He flow rate. Like the graphs for reactor effective power, these panels each have just one plot (although there is a separate plot for each capsule). The Ne fraction is of interest because having a higher fraction of Ne in the capsules allows more of the heat to remain in the capsules, generally leading to higher temperatures. A number of these graphs show increases in the average of the daily average Ne fractions in the four most recent cycles (see Figure 15). These increases might be expected because, as the irradiation experiment continues, fuel burnup occurs and the fission rate in the fuel decreases. Thus, there is less need for He gas (that removes heat) in the later stages of the experiment.

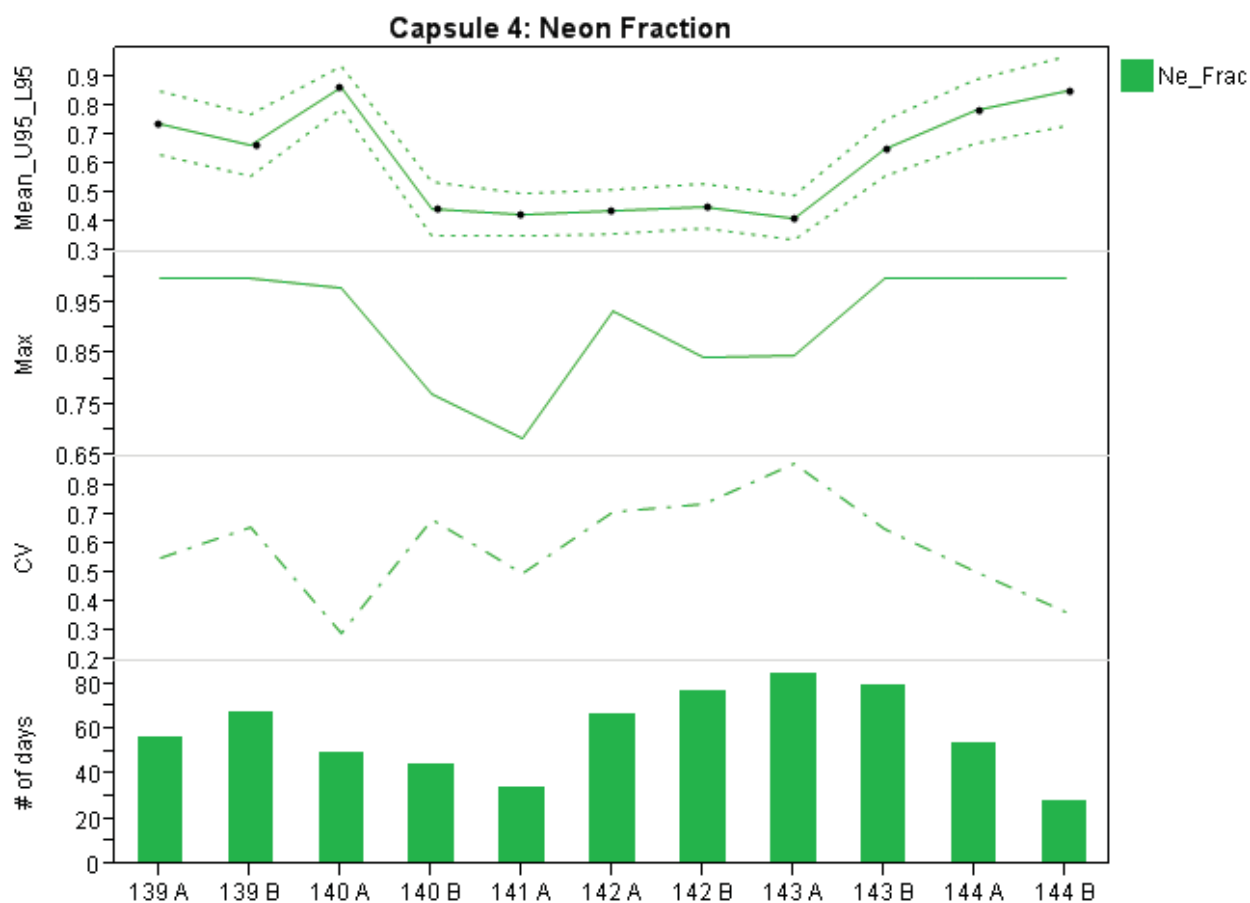


Figure 15. Capsule 4 data summary for Ne fraction for each cycle.

A final feature of the Cycle Summary webpage is that a table with the plotted data appears alongside each graph. Like the data exploration pages described above, these data can be downloaded for further analysis. For example, a user can obtain the data from each capsule and then make between-capsule comparisons of the cycle averages.

### 2.2.1.7 Graphite Characterization Data

The AGC-1 (Advanced Graphite Capsule-1) test has provided initial characterization data for 469 graphite specimens. The primary modeling that is envisioned with these data will be to compute the change in the various attributes of the graphite specimens resulting from irradiation in ATR. Irradiation is scheduled to begin in August 2009. Still, relationships between the variables can be explored with the existing data shown in the webpage. Two primary tools for this exploration are box plots and the “Graphite Data Exploration” option contained in the “AGC Characterization Data” portlet.

The “Graphite Box Plots.srx” report provides a static series of box plot graphs. Each graph shows a particular measured value of the graphite specimens of a particular type. The two types of specimens are “Creep” and “Piggyback.” The data are further grouped by graphite grade. For each grade for a particular specimen type, the associated population of values is described by a little box plot. The boxes span from the 25<sup>th</sup> to 75<sup>th</sup> percentile of the associated data, with extensions showing the 5<sup>th</sup> to 95<sup>th</sup> percentiles. The median is marked in the middle of each box. “X” markers show minimums and maximums that lie outside the range spanned by the 5<sup>th</sup> and 95<sup>th</sup> percentiles. These plots exist for physical parameters such as mass, length, and density, as well as several measures of elastic modulus, coefficients of thermal



expansion, thermal diffusivity, and electrical resistivity. These plots provide a modeling capability because they show the variation present in the data sets and allow comparisons across specimen types and graphite grade. Figure 16 shows an example.

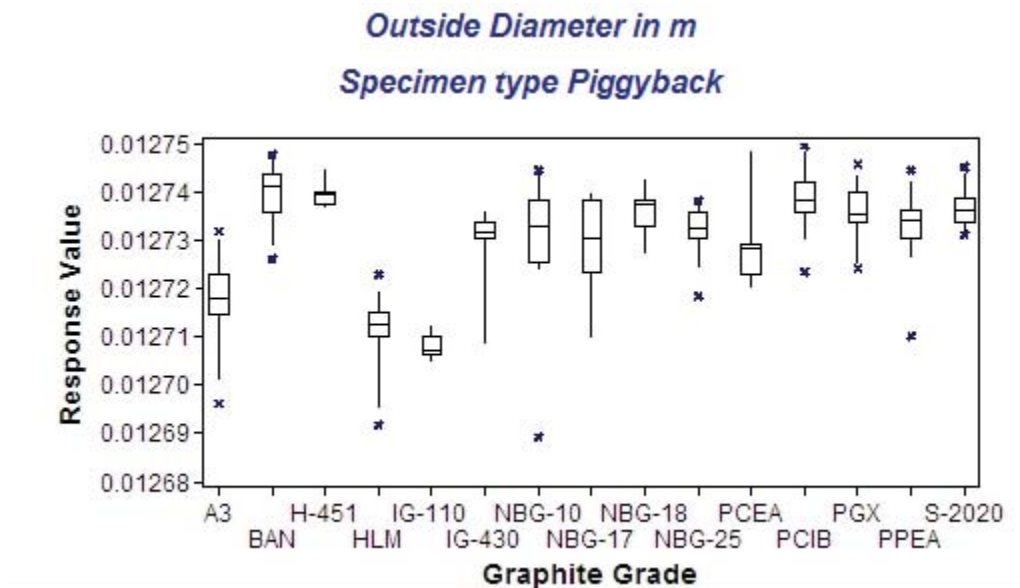


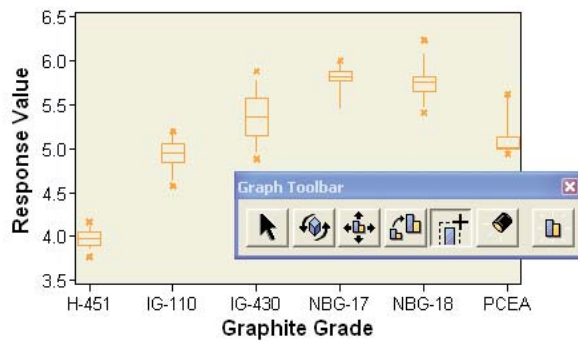
Figure 16. Box plots of piggyback graphite specimen diameters for different graphite grades.

The HTML Box Plots portlet near the bottom of the page provide further modeling capabilities using the box plots. Here, any single plot of interest is easily displayed using a Table of Contents section on the left side of the portlet. Unlike the static graphs in the report just discussed, the displayed graphs are ActiveX graphs. Placing the cursor over a box plot or plotted x in these graphs will bring up a little window that lists the value(s) of the data. The graphs can also be customized on the fly, with such actions as filling in the boxes and connecting them. Titles and colors can be changed. A graphic toolbar allows the graph to be moved inside its window, expanded, shrunk, and subsetting (Figure 17). One can, for example, make the graph show just one box plot for a single graphite grade, if desired. These flexibilities enhance the user's ability to visualize the data and the relationships between different graphite grades across the span of the measured characteristics.

The second modeling capability shown in the AGC Characterization Portlet is the graphite Data Exploration feature. This feature displays many of the measured graphite variables in a table that can be explored and graphed in the same way as the capabilities in the FPMS Data Exploration portlets. The user exploring the graphite data removes all fields from the "Selected Items" list on the left side of the screen, adds a few items, and clicks the "Apply" button. The SAS system aggregates the data to the level of the unique attribute values present in the selected columns. If "Specimen Number" is included in the Selected Items list, then actual response values are reported. If "Specimen Number" is not included, an average value for the selected aggregate is reported.

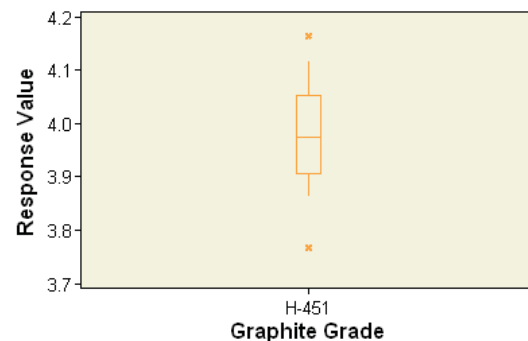
If the resulting displayed data do not have too many values, the system will display the results in a graph as requested by the user. On the other hand, if the system cannot make a graph showing all the unique categories that will fit on the webpage, it will display an error message about not being able to display the data.

Plot for Coefficient of Linear Thermal Expansion ( $\mu\text{m}/(\text{m } ^\circ\text{C})$ )  
Specimen type = Creep



Box 25 to 75 percentile  
Whiskers 5 to 95 percentile

Plot for Coefficient of Linear Thermal Expansion ( $\mu\text{m}/(\text{m } ^\circ\text{C})$ )  
Specimen type = Creep



Box 25 to 75 percentile  
Whiskers 5 to 95 percentile

Figure 17. Example of use of ActiveX graph Toolbar to expand one box plot.

As an example of a graphite data exploration display, the Specimen Type, Graphite Grade, and Orientation attribute variables were selected, in that order, and the Poisson's Ratio measure was selected in the data exploration window. In the data table that resulted, the data were sorted by Poisson's Ratio. Then the table was changed to a bar chart. The display in Figure 18 is the result. The chart shows the trend in Poisson's Ratio across graphite grades and allows comparison of Poisson's Ratio between piggyback and creep specimens for the same graphite grade for the same specimen orientation (AG against grain, WG with grain).

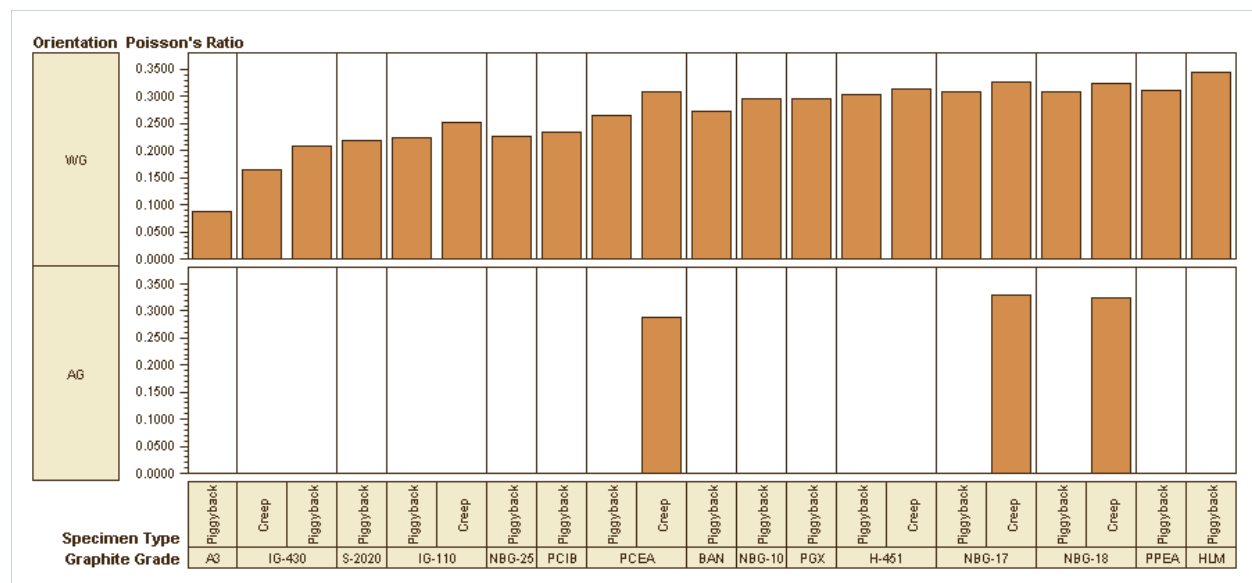


Figure 18. Graphite data exploration using Poisson's Ratio (grouped by graphite grade, specimen type, and with or against grain orientation).

Another example of Data Exploration is when two methods were used to measure elastic modulus on the graphite specimens, sonic resonance using ASTM C 747-93 (Reapproved 2005), and sonic velocity using ASTM C 769-98 (Reapproved 2005). To compare the correlation between the two methods, the Graphite Data Exploration portal can be used to plot the average elastic moduli for each graphite grade



and orientation as shown in Figure 19. These plots can only be made using summarized or filtered data in the Data Exploration. There are too many individual specimen measurements to plot the raw data for all graphite grades together. Data Exploration tools provide some ability to view the data and the relations among the data, but those abilities are limited. More powerful modeling capabilities are available through SAS and JMP tools. Data Exploration is the best interface for selecting data to download for such studies.

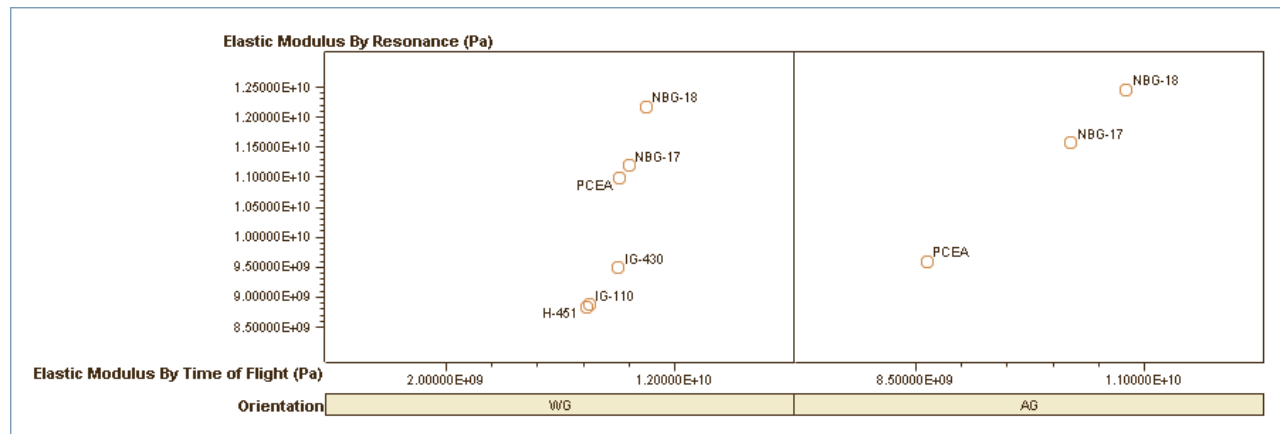


Figure 19. Averages, within graphite grades for each specimen orientation, for elastic modulus measured using sonic resonance compared with elastic modulus measured using sonic velocity.

### 2.2.1.8 Live JMP Reports

For users who have “JMP,” a SAS software product, installed on their PCs, the Live JMP Reports page provides additional modeling capabilities. The page contains a portlet that explains how to set up the JMP software, and a portlet with links to Live SAS JMP outputs. These are stored processes from JMP that invoke JMP on the user’s PC. The processes retrieve the data and display graphical summaries. The user is then free to pursue other modeling with the downloaded data. JMP offers an extensive array of modeling tools, which are discussed briefly in Appendix B.

### 2.2.1.9 Summary of Data Modeling from the INL NDMAS Web Portal

In the examples that have been discussed above, several capabilities for website users to view data and visually explore relationships have been presented. The primary modeling capabilities are:

- Data visualization through ordinary graphs
- Data visualization through lattice graphs that show several plots grouped according to a common attribute; the differences that define the groupings (such as different experiment capsules) can be compared.
- Tabular drill-down views of the data using SAS EBI “cubes”
- Data Exploration panels that allow the user to select particular variables, observe aggregated results, and download data
- Customized graphs for particular time periods, obtained using Stored Processes
- Box plots and histograms that show data distributions
- ActiveX graphs that allow additional customization of the observed displays.

Additional capabilities are being developed.

### 2.2.2 Modeling Capabilities for the NDMAS Team

The NDMAS team has direct access to the data in the structured query language (SQL) “Vault.” Data sets judged most useful are shown in the INL NDMAS web portal, but all the data in the system are accessible to the NDMAS development team.

In NDMAS, the data are stored as described in Figure 20. The vast majority of the data enter the system from electronic records such as text files or Excel spreadsheets. In Figure 20, these are schematically shown in the “Source” rectangle. Enterprise Guide (EG) is a tool provided by SAS for data manipulation and analysis. “Projects” have been created in EG to process each data stream and load it into an SQL Server database. This data repository is represented in the “Storage” box in Figure 20 as a tall cylinder, because ultimately, each datum is placed in a separate record. There are literally millions of short records in the main data table. Isolating each data value allows the data qualification activities of the data base to flag and resolve individual problems. The Vault also provides for data security and change control.

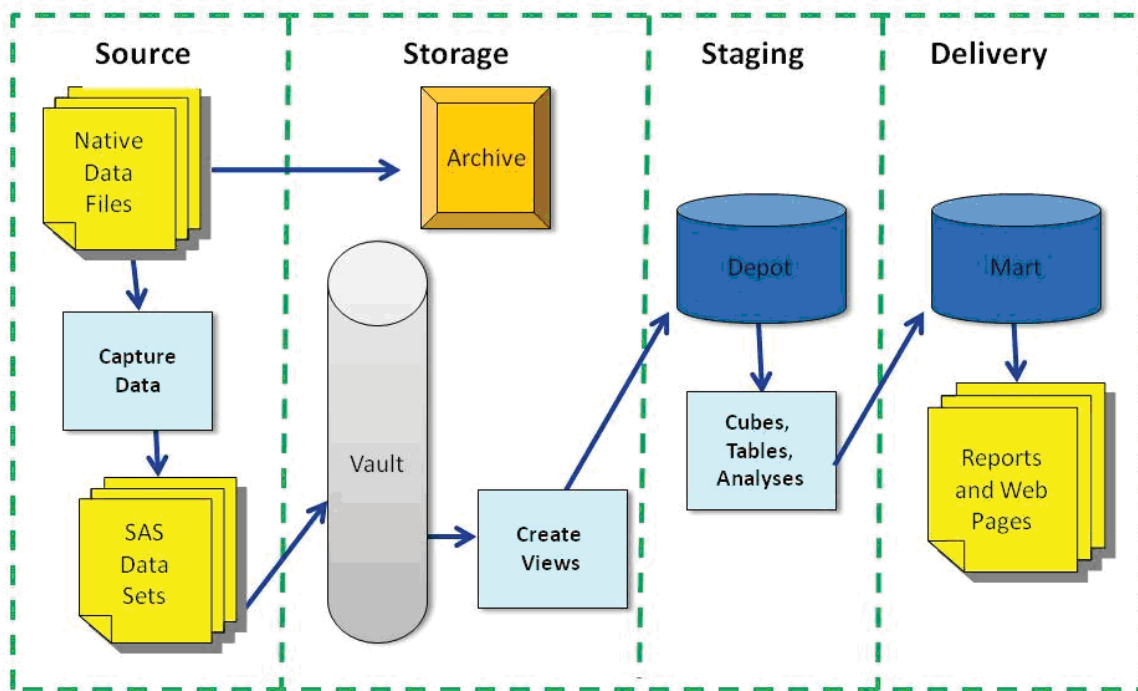


Figure 20. Four major steps in NDMAS data processing.

NDMAS developers extract the data from the Vault as tables, generally with multiple measurements in each record such as experiment parameters (temperatures, gas flows) in a particular capsule at a particular point in time. These more “horizontal” data views are contained in the “Depot” shown in the Staging box in Figure 20. These are the primary data sets used by NDMAS team members for modeling and analysis. The “Mart” in the Delivery box is a mirror image of the external NDMAS server, and provides the production capabilities described in Section 2.2.1. The Mart is separate from the Depot in order to ensure that errors or problems that occur in developing models will not affect the reliability of the production webpages. Results of the modeling are displayed from the Mart.

Some general guidelines for using Enterprise Guide to create models using the NDMAS data are given in Appendix B.

As observed in Section 2.2.1.8 above, additional modeling capabilities are provided by the SAS “JMP” product. These are also described further in Appendix B.

### **2.2.3 Modeling Capabilities via Analysis Requests**

Users who need particular studies to be performed using the VHTR data can request these analyses from the NDMAS staff. The analyses can be scheduled and performed. Results can be displayed on the INL NDMAS web portal and/or in reports, as desired by the person making the request. For the reports displayed in the portal, a report distribution capability of the server allows users to create guidelines on who has access and to what content. Modeling reports can thus be distributed to particular users on the Internet based on assigned groupings.

### **2.2.4 Modeling Capabilities via Downloads**

The INL NDMAS web portal provides several options for downloads of the data. Users can also request particular data sets and the NDMAS team will deliver them (pending appropriate release approvals). The results can be in Excel spreadsheets or many other formats, as desired by the user. Such data can be combined with other data and used for modeling to further the state of VHTR research in whatever way the user has in mind.

An example of the modeling capability available from a download is described in Section 3.1.2.

## **2.3 Uses of the Applications**

NDMAS modeling capabilities have many potential uses. A partial list follows.

- Scientific understanding is, of course, a fundamental reason for any attempt to identify relationships between variables.
- Data visualization for webpage outputs helps researchers grasp the patterns in the observed data. In the modeling, these patterns are distilled from sometimes thousands of records.
- Accuracy tests for input data streams are a current use for many of the models. Some of the tests are based on simple models, such as the idea that the coefficient of variation (the standard deviation divided by the mean) should remain within certain bounds. Others are based on functional relationships established by a regression analysis. Once a pattern has been established, significant deviations from the pattern give rise to alerts for increased data review. Such deviations either indicate errors in the data collection process, or significant changes in experimental conditions.
- The alerts or early warnings of possible anomalies or instrument failure based on departure from prior patterns can be useful during the experiments. In some cases, experimental conditions can be adjusted or corrected as a result of the accuracy tests. The timeliness of data processing in NDMAS also facilitates this potential use of the models.
- Hypothesis tests of the experimental results can be developed and evaluated. The tests can help identify the features of the experimental design that make a difference, or the features that lead to the best performance. Random variation is always present. The statistical modeling can help distinguish whether the measurement results of one process are really likely to be an improvement over the measurements from a different process, even in the presence of this variation.
- The models can help identify limits defining envelopes for safe operation.
- Alternately, the data can be used to characterize reliability, given particular operating limits.
- The statistical modeling can lead to response surfaces that allow users to predict future phenomena based on operating conditions that have been studied in prior ATR reactor cycles or VHTR experiments.
- The statistical models can support VHTR licensing.

### 3. EXAMPLES OF CURRENT MODELING APPLICATIONS

Examples of modeling applications for each major NGNP project are listed in this section. The modeling examples discussed here are generally more involved than the displays available from the INL NDMAS web portal that were discussed in Section 2.2.1.

Currently, NDMAS is populated with data from two projects, the fuel irradiation study and the graphite characterization. NDMAS will be expanded and sections will be added to future versions of this report as more data streams enter the database and more models are developed. Within projects, the examples are organized based on the response variable under study. The following attributes are discussed for each example:

- Purpose
- Input data
- Data preparation
- Modeling method
- Discussion of method details or particular issues, as applicable
- Results and their interpretation.

#### 3.1 Models Related to Fuel Irradiation

Two measurements that have been studied are the temperature readings from the TCs and the fission product R/B ratios.

##### 3.1.1 Capsule Temperature Models

Understanding temperature fluctuations has been a major focus of fuel irradiation monitoring because one of the primary purposes of the experiment is to test the fuel performance in a high-temperature environment. The time- and volume-averaged temperature in AGR-1 fuel capsules is intended to be approximately 1,150°C during ATR full-power operations (more specifically, from 1,075 to 1,180°C). The temperature is moderated by a gas flow control system that forces a mixture of helium and neon gases through the experiment capsules. Adjusting the gas mixture adjusts the thermal conductance between the fuel and, ultimately, the cooling water in the primary reactor vessel. Neon is a poor conductor of heat compared with helium, so the system increases the helium-to-neon ratio to decrease temperature and decreases that ratio to increase temperature. During the course of the experiment, the fuel being tested experiences burn-up, leading to decreased fission heating rates in the capsules. Some of this decline is compensated by the use of boron, which has a large cross section for neutron absorption, in the graphite holder assembly. Boron, however, is also depleted over time, leading to increased neutron flux to the fuel. There is thus a tendency toward initially increasing temperatures, while boron depletion is the dominant effect, followed by decreasing temperatures when the fuel depletion effect begins to dominate. These long-term changes in the fission rate of the fuel affect larger temperature differences than can be compensated for with gas flow. Thus, toward the end of the experiment, the desired temperature may not be reached, even if the control gas is 100% neon.

Each capsule stacked vertically in the assembly that forms the AGR-1 test train has three fuel stacks and from two to five thermocouples (TCs). Each fuel stack contains four fuel compacts with coated fuel particles. Figure 21 shows the locations of the thermocouples and also provides information about their design. The ability to measure temperatures in the test train during irradiation is critical to the ability to study and control the temperature in the fuel. Determining whether the TC data are accurate and how the

temperatures fluctuate from one capsule to another is an important activity to ensure that the test meets its goals.

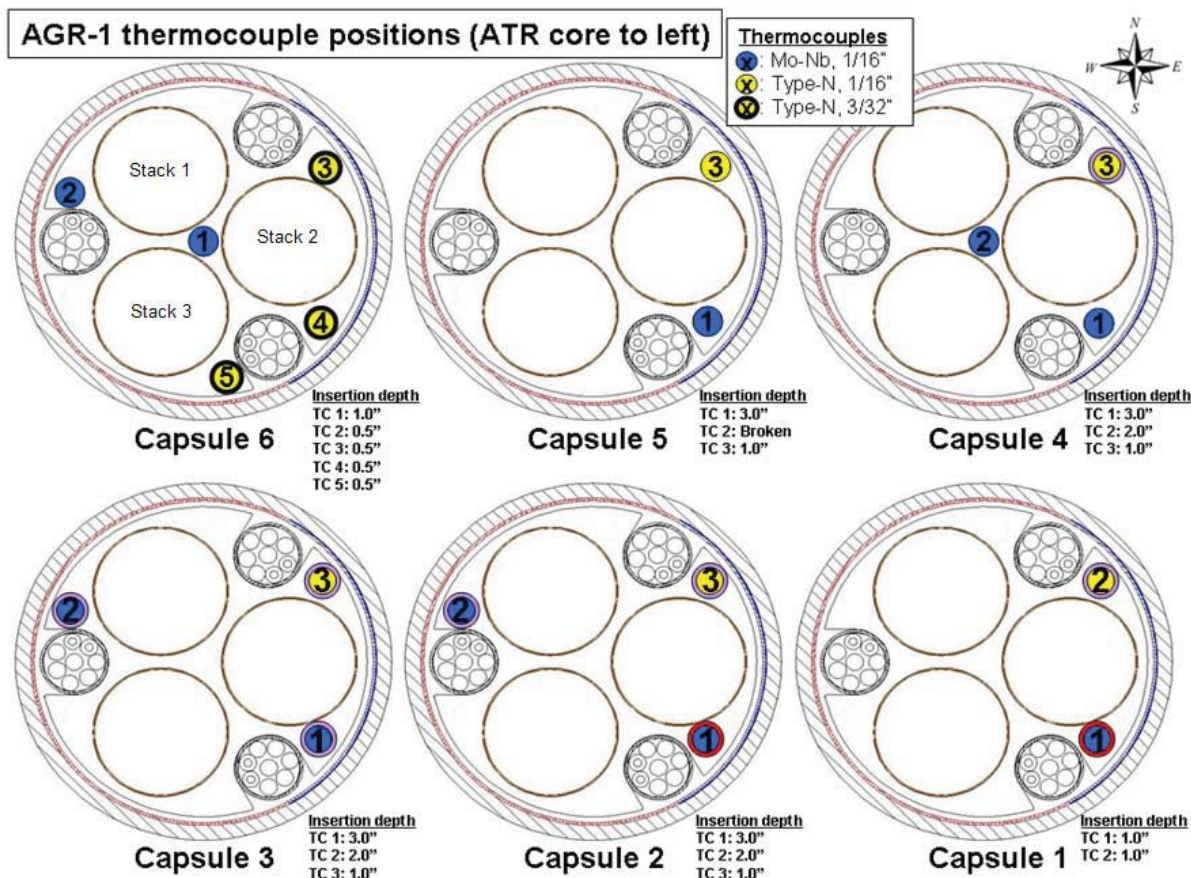


Figure 21. AGR-1 fuel irradiation experiment thermocouples. A red ring around a TC marker indicates that the TC failed during fabrication. Light purple rings represent TC failures during the experiment.

Thermocouples in high-radiation environments are prone to both drift and failure, due to the effects of transmutation, structural damage, and radiation-induced electromotive forces (Ambrosek 2005b). During the AGR-1 experiment, three phenomena occurred that have had a significant impact on the temperature data. First, three TCs were broken in fabrication. One of these failures was noticed during the installation process and that TC was not installed. The other two provided readings that are clearly related to temperatures in the capsule train, but those data have been declared invalid. The second phenomenon is that two of the installed TCs failed at certain points in time and started giving outputs near zero. This type of failure, herein referred to as a ‘catastrophic’ failure, is easy to recognize in the data. The third phenomenon has disqualified data from five of the TCs in a more subtle departure from a correct temperature reading. Two possible scenarios have been identified. One is junction failure, which is defined as registration of temperatures from locations outside the intended location, such as may occur via formation of a new junction between the wires in a position closer to the instrumentation collecting the data. Where new junctions develop, the thermocouple in one capsule may reflect changes in another capsule, close to where the new junction has formed, as well as in the original capsule. The second scenario is drift failure, herein defined as TC readings that respond to temperature at the desired location but with decreased accuracy. Table 2 summarizes the TC failures that have occurred in the AGR-1 irradiation experiment as of June 30, 2009.



Table 2. Failure status for AGR-1 fuel experiment thermocouples (TC) by capsule.

Capsule Number	Thermocouple Number				
	TC_1	TC_2	TC_3	TC_4	TC_5
6 <sup>a</sup>	OK	OK	OK	OK	OK
5	OK	Fabrication failure (not installed)	OK	—	—
4	OK	OK	Drift or junction failure, 10/16/08 Flat <sup>b</sup> since 11/20/08	—	—
3	Drift or junction failure, 3/9/08 Not flat	Drift or junction failure, 4/1/07 Flat since 4/29/08	Catastrophic failure, 12/02/07	—	—
2	Fabrication failure, 11/30/06 Flat since 4/28/08	Drift or junction failure, 4/22/07 Flat since 4/28/08	Drift or junction failure, 9/30/07 Flat since 4/28/08	—	—
1	Fabrication failure, 11/30/06 Flat since 12/02/07	Catastrophic failure 9/22/07	—	—	—

a. Capsule 6 is at the top of the test train, closest to the instrumentation. It is the only capsule with five TCs.

b. “Flat” means that the readings dropped to near zero, demonstrating failure of the TC. “Catastrophic failure” applies to TCs whose readings suddenly became flat, with accurate prior readings. The other failures were fabrication, drift or junction failures identified by the NGNP experiment team, and are not directly obvious from the subsequent data (until it became “flat”).

There are three sets of parameters in the NDMAS fuel irradiation data that can be used in empirical and/or physical models to study capsule temperatures. The simplest quantity that is similar to the temperature at one TC is the temperature at other TCs. The second quantity that is known to affect capsule temperature is the gas flow mixture. It is the primary local effect, although when the control is automatic, it is just responding to the primary conditions in the ATR that affect the heat generation. The third set of parameters contains ATR configuration attributes that drive fission power such as the position of control cylinders and regulator rods.

The models below are presented in that order. First, a simple model giving a prediction of temperatures based on other temperatures is presented. Comparison of temperatures that might lead to detection of unwanted TC junctions is also discussed. The neon fraction in the control gas is considered in the next set of models. Fission power data computed from reactor operating data was directly available for one cycle and was used in a model for temperature that was suggested from physical process (heat transfer) considerations. In the next set of models, the issue of which ATR operating configuration measures most affect the temperature is considered. The models address the question of whether temperature is well correlated with ATR configuration attributes and ATR power measurements, and whether these correlations are consistent from cycle to cycle.

In most of the ATR power parameter examples, the focus has been on using ATR variables which describe the configuration of the reactor, like control cylinder positions, as opposed to reactor measurements like power at the lobes. This choice is, in part, due to preliminary analyses, which indicated better correlation with the former than the latter, and in part on the goal of being able to predict capsule temperature for an upcoming cycle, based only on controlled operating conditions planned for the ATR.

The possibility of splitting the temperature modeling into two phases is also under study. The first phase would be to predict fission power from ATR configuration parameters. (Only one cycle of fission power data exists for the development of this model). The second phase would be to find a model that combines the fission power information with the Ne fraction in the control gas and/or other parameters to provide a good predictor of TC temperature.

The statistical or empirical modeling of temperatures in the capsules is currently in a developmental stage. The models are primarily for data exploration. The NDMAS modeling team hopes to eventually develop techniques that can contribute to the understanding of TC performance and the identification of factors showing the occurrence of fabrication, drift, or junction failures. The current results are all considered preliminary.

### 3.1.1.1 *Prediction of Temperature in Capsules with no Working TCs*

**Purpose.** To determine whether temperatures in capsules lacking functional TCs can be predicted using TC readings from other capsules during reactor operations. This model is shown in the last portlet discussed in Section 2.2.1.5 (Figure 13), but it is outlined in more detail here.

**Input Data.** AGR-1 qualified TCs readings.

**Data Preparation.** The TC data were extracted from the NDMAS Vault. To ensure that they describe power operations, reading less than 100°C were omitted. Because the first fuel cycle (138 B) had only five TCs that reported temperature data, the first fuel cycle was dropped from the data analysis. The detailed temperature readings collected every five minutes were used in the analyses.

**Modeling Method.** Simple linear regression was used to model each failed TC temperature reading as a function of the other working TC readings. Let  $T_i^{X-Y}$  be a reading from TC number “X” in capsule number “Y.” The equations were of the following form, where the term on the left is a predicted reading for a failed TC and the remaining terms contain data from the working TCs:

$$PredT_i = \beta_0 + \beta_1 T_i^{1-6} + \beta_2 T_i^{2-6} + \beta_3 T_i^{3-6} + \beta_4 T_i^{4-6} + \beta_5 T_i^{5-6} + \beta_6 T_i^{1-5} + \beta_7 T_i^{3-5} + \beta_8 T_i^{1-4} + \beta_9 T_i^{2-4}$$

To estimate the parameters, qualified data from the period before TC failure were entered in the model. The model was also applied to most of the TCs that did not fail, in order to see how well it predicted the subsequent observed values. For these models, the term on the right corresponding to the TC being estimated was, of course, not included. The models were fit using ordinary least squares; that is, the coefficients were selected to minimize the sum of the squares of the residuals in each model. The SAS procedure, “REG,” was used in Enterprise Guide to fit each model.

**Discussion of Method Details.** One modeling issue was the selection of an optimal “training period.” Data in this period are used to estimate the regression equation coefficients. In experimenting with the model, various training periods were used. The data immediately prior to failure are clearly relevant. Data early in the experiment, however, could be less useful. For the figure in the INL NDMAS web portlet (Figure 13), data from Cycle 139A were excluded in addition to Cycle 138B because changes in AGR-1 thermal conditions over time due to depletion of boron in the graphite and to fuel burn-up might lead to changes in the relationship between a TC’s readings and those of the other TCs used as independent variables in the regression model. This possibility is especially true at the beginning of the AGR-1 irradiation period.

Experimentation led to selection of the end of ATR Cycle 142A (7/15/2008) for the end of the training period in the figure on the webpage. As with the start of the period, other end dates were also considered for the operating TCs. Training periods for the failed TC models ended on the failure dates.

After fitting the models using data in the training period, predicted values were generated for the more recent period. These are the dotted lines in the panels for Capsules 6, 5, and the red and blue plots in Capsule 4. These dotted lines are seen to fit the actual TC readings fairly closely, although some are uniformly higher than the observed TC readings and some are uniformly lower.

A second issue is the number of variables to include in the model. For this first set of analyses, all the variables were retained. Nearly all of the coefficients were statistically significant at the 95% confidence level. That is, the probability that a coefficient could have been estimated to be zero, based on the variation in the data used to estimate the coefficient, was less than 0.05. This determination comes from a Student's t test with one degree of freedom. The cutoff for a significant coefficient is that the absolute value of the coefficient divided by its estimated standard deviation be greater than 12.7. All the coefficients were significant for five of the six functioning TC models and for four of the seven failed TC models.

**Results and Their Interpretation** . The overall results of the modeling are shown in Figure 13. The predicted values were examined closely for TC\_3 in Capsule 4, which has the most qualified data among the failed TCs. Its failure occurred in October of 2008, in Cycle 143A. The close fit between the predictions and the qualified data is shown in Figure 22. In the figure, the end of the training period was taken to be 7/5/2008, before the failure date, so that there would be qualified data to compare with model predictions. The top part of the figure shows the model values and observed readings for the experiment from Cycle 139A through to Cycle 144B. The blue line shows the TC readings while the red lines show the model and its prediction limits. In Frame (c), the figure shows a close fit for the model's predictive ability for the first half of Cycle 143A.

Not all of the models fit so well. Having more data available for the prediction helps. The predictions were poorest for TC\_2 in Capsule 3, and were also poor for TC\_2 in Capsule 2. Both of these TCs were the earliest to fail during the experiment. No models were formed for the two TCs that failed on installation and had no qualified data for the regression models. More development work is planned for this modeling effort (see Section 4.1.1.4).

### **3.1.1.2 Potential Use of TC Correlation Coefficients to Monitor TC Performance**

**Purpose.** To examine patterns in correlation coefficients for pairs of TCs in the same capsule and in different capsules to identify possible anomalies such as the formation of unwanted junctions in the TCs.

**Input Data.** The thermocouple readings from the AGR-1 experiment, along with an indication of whether the data are qualified.

**Data Preparation.** Standard Pearson correlation coefficients were computed between each pair of TCs for each day of ATR operation (with temperatures greater than 100°C). The coefficients were labeled according to whether they were based on qualified data or data with at least one TC not qualified. They were also labeled by capsule for the within-capsule pairs and by both capsules for the between-TC pairs.

**Modeling Method.** For this preliminary investigation, the data were plotted (see Figure 11 and Figure 12 in Section 2.2.1.5). The qualified TC correlations were analyzed further. An expected shape for the correlation distribution within capsules was established using the within-capsule data. Generally, correlations between capsules are expected to be lower than correlations within capsules. TCs with unusually high correlations between capsules may have formed a junction near the associated capsule. For this failure mechanism, the associated capsule must be located higher in the test train, since the leads feed in from the top of the test train.

**Discussion of Modeling Details.** Averages were calculated for between-capsule and within-capsule correlations. Additional ways of comparing the correlation coefficients are still under development.



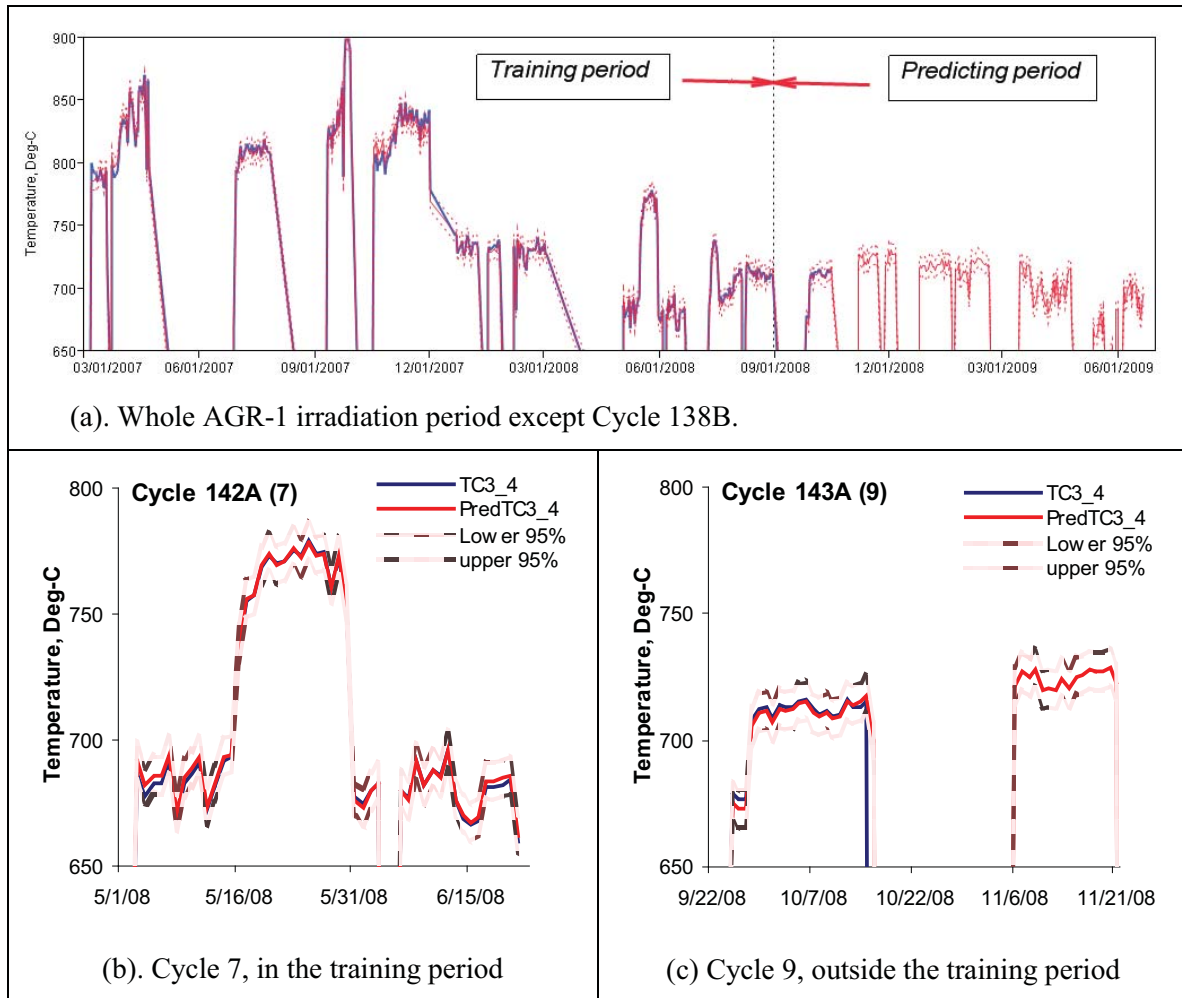


Figure 22. Observed and predicted temperatures for TC\_3 in Capsule 4, with 95% prediction limits.

**Results and Their Interpretation** . Figure 23 shows the average within- and the average across-capsule daily correlation coefficient as a function of capsule. Capsules 1, 2, and 3, which have the majority of the failed TCs, also have the highest average between-capsule correlation. These averages are greater than the with-in capsule averages (although Capsule 1 has no within-capsule correlation coefficient since only one TC there had any qualified data). Further research is needed to determine whether these high correlations are indicative of junction failures.

### 3.1.1.3 Temperature as a Function of Ne Fraction and Fission Power

**Purpose.** To determine whether TC readings can be predicted using Ne fraction and fission power.

**Input Data.** Fission power in MW was calculated for two positions in each of the four fuel compacts in each of three stacks, for each capsule in the AGR irradiation experiment. A total of 144 values were obtained. This analysis was performed in daily time steps for the days in Cycle 139B (the third ATR cycle in the experiment). Data are present for 55 days. The calculations were performed by J. Sterbentz (2009) using ATR operating condition parameters with MCNP and other ATR neutronics codes. Qualified temperature and gas flow data came from the NDMAS Vault.

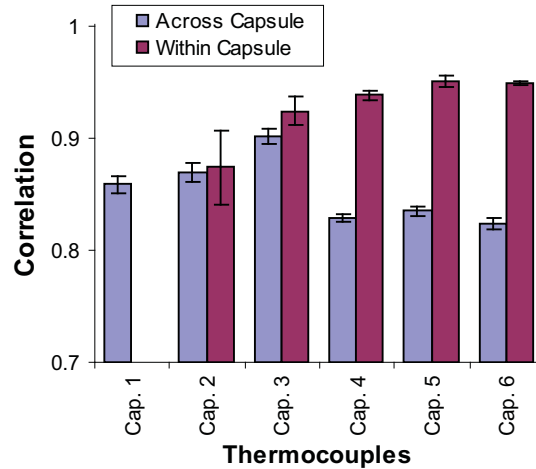


Figure 23. Averages of daily correlation coefficients within capsules and across capsules.

**Data Preparation.** The fission power data were read from an Excel spreadsheet into the NDMAS Vault. They were averaged for each stack in each capsule. The plots in red on the left side in Figure 24 show the Capsule 4 fission power data. The Ne fractions and temperatures were also averaged at a daily level. The Capsule 4 daily average temperatures appear as the blue curve on the left plot in Figure 24. (The fission powers are scaled so that the vertical axis in the figure can be used for both types of data.) Ne fractions (computed as Ne flow rate divided by total control gas flow rate) are shown in green on the right side in the figure. For the regressions, the fission power data were averaged across stacks (the three red lines in the left figure) to get one value for each day. The data were merged into a data set with daily temperatures, fission powers, and Ne fractions.

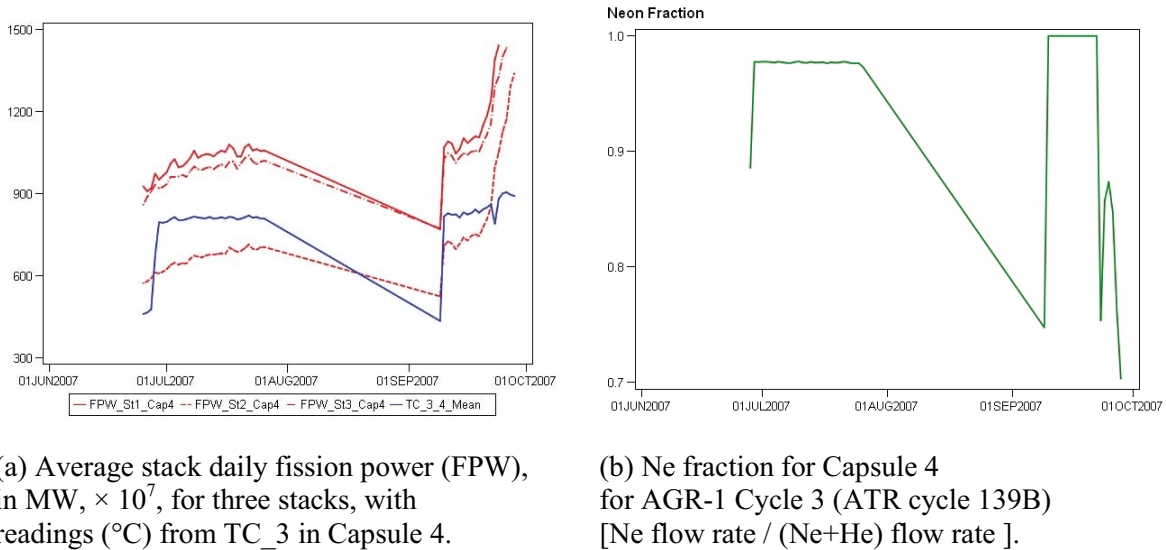


Figure 24. Cycle 139 B data for regression model.

**Modeling Method.** The initial modeling described here focuses on the behavior of TC\_3 in Capsule 4. Two relationships motivated the form of the regression equation. First, heat balance considerations lead to

$$Q = C (T_{in} - T_{out}) \quad (2)$$

where  $Q$  represents heat added to the capsule from fissions in the fuel,

$C$  is the gas mix thermal conductivity, and

$T_{in}$ ,  $T_{out}$  are inlet and outlet cooling gas temperatures.

The heat added is directly related to the fission power. The change in temperature can be regarded as some linear function of the TC readings.

The thermal conductivity ( $C$ ) is directly related to the Ne fraction, since increases in He in the gas mix increase heat removal. The relationship is demonstrated in Figure 25. In the figure, temperature, gas mixture, and thermal conductivity data presented in EDF 5138 (Ambrosek, 2005a) were fitted using a second degree polynomial. Although the correlation of Ne fraction (1-He fraction) and thermal conductivity is negative, it is still suitable for the regression equation. Gas conduction is the primary heat transfer mechanism in the capsules. Equation (2) leads to the inclusion of a  $Q/C$  term in the regression model.

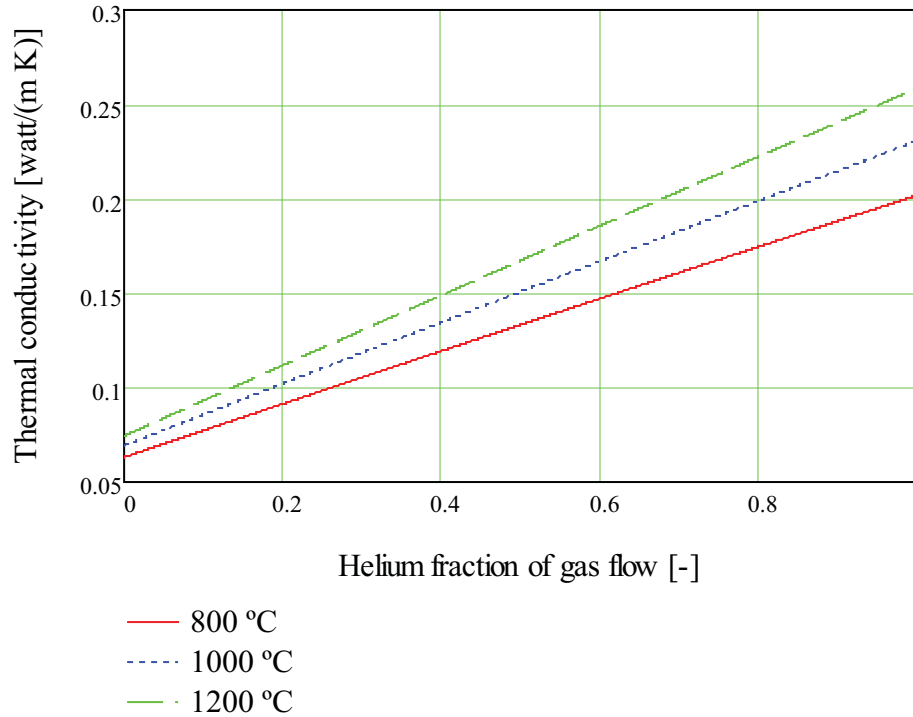


Figure 25. Thermal conductivity as a function of He fraction and temperature.

The second relationship comes from additional empirical correlations between thermal conductivity and temperature raised to a power. For example, the Handbook of Physical Properties of Liquids and Gases [Vargaftik, 1996, p. 1014] suggests a thermal conductivity correlation for temperatures between 600°C and 5000°C in a pure neon gas. The equation shows thermal conductivity as proportional to the temperature raised to the 0.63 power. Inverting this relationship leads to an equation with temperature proportional to thermal conductivity to the 1.6 power. Other references cite slightly different correlations, and the AGR-1 application is not identical to the conditions in the Handbook. Figure 25 shows that this

relationship does not hold rigorously in the AGR-1 environment since temperature can change (along one of the horizontal grid lines) without changes in the thermal conductivity. However, the possibility of some relationship leads to the inclusion of a  $C^{1.6}$  term in the model.

Based on these two relationships, the following equation is proposed for representing the TC readings

$$T^{3-4} = \beta_0 + \beta_1 Q + \beta_2 Q/C + \beta_3 C + \beta_4 C^{1.6} \quad (3)$$

This equation is nonlinear in the measured parameters, with  $Q$  as fission power and  $C$  as Ne fraction. However, it is linear in the estimated beta coefficients, so it can be fit using ordinary least squares linear regression. The  $Q/C$  ratios and  $C^{1.6}$  values were computed from the  $Q$  and  $C$  data and added to the data set entering the calculations.

**Discussion of Method Details.** Selection of the training period was a major consideration in this analysis. In the raw data shown in Figure 24, there is much more variation in the fission powers and Ne fractions and corresponding temperatures on the right side of the two graphs than on the left. An important principle in the statistical modeling is that the training period data used to fit the regression coefficients be representative of the period to which the results will be applied. Therefore, the training period used the most recent half of the data points, and the merits of the model were evaluated by observing its predictions for the first half of the data.

A second model was also fit to the data. Here, one additional term was added: a 5th coefficient times an observed qualified temperature readings from one of the other TCs in Capsule 4. TC\_1 was selected. Cycle 139B occurred prior to the failure of this TC.

**Results and Their Interpretation .** The model provides a very good fit for the data, as shown in Figure 26. All the regression coefficients were statistically significant. The  $R^2$  coefficient of determination, which is a measure of how well a regression model fits, was 0.99 (1 applies if all the data lie on the regression line). The mean squared error, which is the variance of the residuals and is the minimized quantity in the regression, was the square of 8.1°C. The figure shows that the fit in the first half of Cycle 139B was good.

Adding the qualified TC\_1 temperature measurements from Capsule 4 to the model made it fit even better. The  $R^2$  was 0.9997 and the square root of the mean squared error was 1.2°C. The results are shown in Figure 27.

The biggest limitation of this model is that the power data were available for only one cycle. If more fission power data were available, it might be useful to extend this model to the other cycles. Future modeling may also include nonlinear regression that allows a direct estimate of exponents for thermal conductivity in the model.

### 3.1.1.4 Correlations of Temperature with ATR Power Parameters

Fission heating power in the fuel stacks in the AGR-1 experiment is largely controlled by the configuration of the ATR and the resultant neutron flux to the B-10 position, modulated by decay of fuel capsules and depletion of boron in the graphite carrier. Fission heating power, in turn, effectively controls temperature in the capsules, with secondary control provided by the thermal conductivity of the gas mixture flowing through each capsule. Further temperature change is effected by physical changes in the fuel stack assembly, such as gap growth around the fuel assembly caused by shrinkage of the fuel compacts and graphite carrier. To the extent that these relationships can be described by simple mathematical functions, those parameters can provide an independent estimate of TC temperatures that may be useful for identifying thermocouple drift and/or failure and for estimating TC temperatures in a

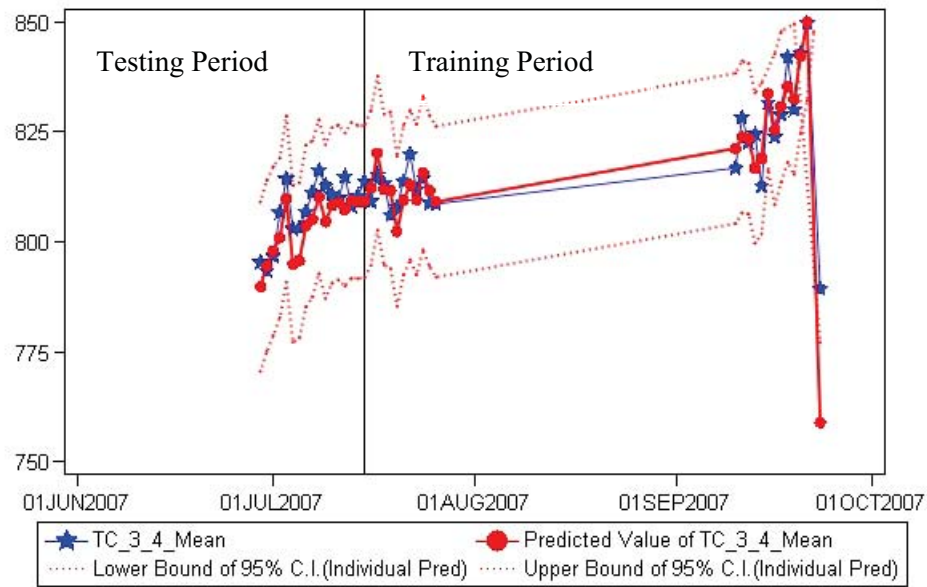


Figure 26. Predicted temperature readings for TC\_3 in Capsule 4 in ATR Cycle 139B, with prediction-based confidence bounds.

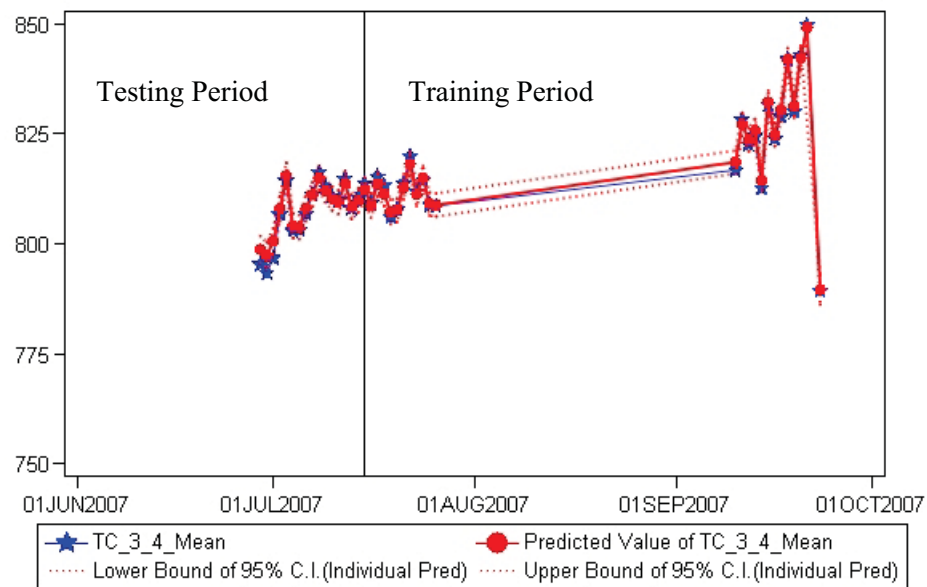


Figure 27. Predicted temperature readings for TC\_3 in Capsule 4 in ATR Cycle 139B, with model including TC readings from TC\_1 in Capsule 4.

future cycle, based on the planned ATR configuration. The first phase in studying these relationships is to take an overall look at how the parameters are correlated with the temperatures.

**Purpose.** To examine correlation between thermocouple temperatures and ATR operating condition parameters in order to determine what combinations of variables might provide an independent measure

of thermocouple temperature. The distribution of power within the ATR may also vary with cycle in a manner not reflected in operating conditions parameters because of fuel loading and the number and arrangement of experiments installed. To examine how such changes might affect the relationship between operating parameters and thermocouple temperatures, correlation is examined on a per cycle basis.

**Input Data.** Streams of TC readings, gas flow rates, and ATR lobe powers and shim positions extracted from the NDMAS Vault. The cycle numbers associated with the data were preserved. Because Capsule 6 likely provides the most reliable temperature record, irradiation data from that capsule were used for the data exploration.

**Data Preparation.** The fuel irradiation and ATR operational parameter data streams were merged by time. Data were filtered to include only full power data and to exclude data from Cycle 138B.

Two ATR configuration parameters were calculated from the basic ATR parameter data. The “REGcombined” attribute is a measure of regulator rod insertion depth. The ATR reactor has two regulator rods. One is fully inserted while the other is inserted approximately half-way (approximately 20 inches) during reactor operation. Both rods are extracted during shutdowns. The exact insertion depth of the rod that is not fully inserted is frequently adjusted. This insertion depth is tracked as a single variable, “RegCombined,” without tracking which rod is moving. The use of this variable instead of the two separate rod positions tacitly assumes that both regulator rods have the same effect. RegCombined is only used for first-pass examinations.

The second derived parameter is “PowerDays.” This quantity is the cumulative product of the effective power and the time interval associated with the power data.. The time-integrated power thus represents cumulative energy applied to the system. The units are MW-days.

**Modeling Method.** The data were sorted by ATR cycle and correlation coefficients for the correlation between each variable and a specific TC were calculated by cycle, using the detailed 5-minute data. The TC selected for the calculations was TC\_2 in Capsule 6.

**Discussion of Method Details.** The results presented summarize correlation coefficients between capsule temperatures and parameters believed to exert significant control or correlation with those temperatures. Correlation coefficients are, however, poor indicators of non-linear mathematical relationships. Future efforts may examine correlation ratios, or other statistical measures that better characterize any non-linear relationships that may exist.

**Results and Their Interpretation .** Figure 28 shows the results of the study by cycle. In the top part of the figure, the cycle labels are 139A, 139B, 140A, 140B, and 141A, respectively. In the bottom part of the figure, the cycle labels are 142A, 142B, 143A, 143B, and 144A, respectively. For each cycle, the parameters being compared with TC\_2 in Capsule 6 are, in order, Ne fraction (NeFrac), total gas flow rate (sccm) (Q\_Total), ATR lobe powers [in order, center (LC\_C), NE (LCNE), NW (LCNW), SE (LCSE), and SW (LCSW)], an indicator of the regulator rod positions (Regcombined), four ATR control cylinder positions [in order, controlling the NW (N1D2), SE (S1D2), NE (E1D2), and SW (W1D2) corners of the ATR], and power days (PowerDays).

The figure shows that Ne fraction remains highly correlated throughout the experiment. Correlations with the control cylinder positions (the “xiD2” variables) were also generally high throughout the experiment except for low values primarily in Cycle 141A. Correlation with thermal power at the four lobes (LCxx) and reactor center (LC\_C), in contrast, is generally poor and often negative. This suggests that power at the B-10 position is more sensitive to control cylinder position than to power at the lobes. The correlation of the temperature with power days tends to decrease as the experiment proceeds.



## Correlation coefficients by cycle, Capsule 6, TC\_2

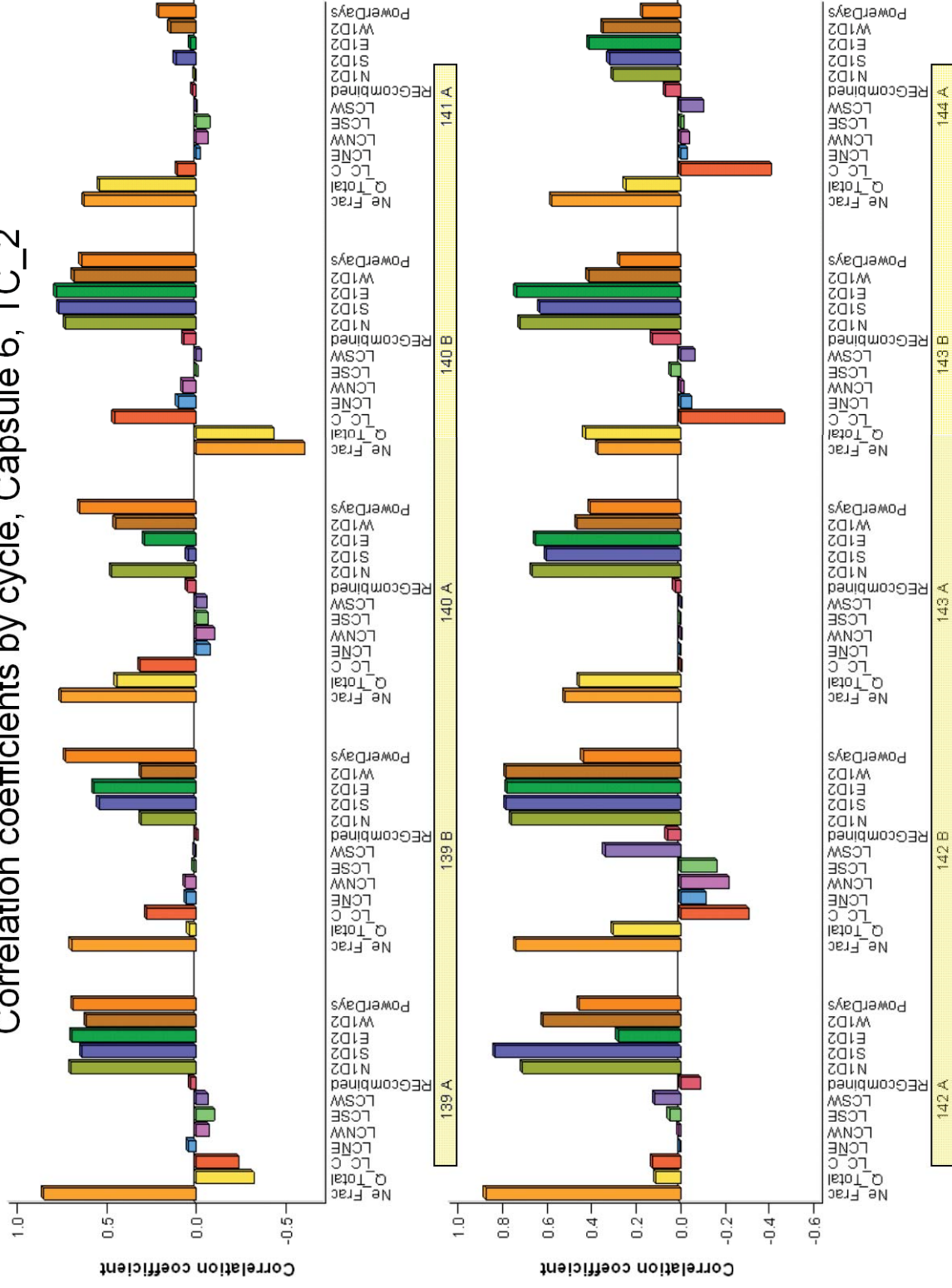


Figure 28. Correlations of variables with temperature, by cycle.

### 3.1.1.5 Regression Model for TC Readings Using Reactor and Experimental Controls

**Purpose.** To use ATR- and AGR- controlled parameters, like control cylinder positions and gas flow rates at each capsule, as a means of predicting TC temperatures.

**Input Data.** The merged stream of TC, gas flow rate, and ATR lobe powers and shim positions from the NDMAS Vault. For the data exploration, irradiation data from Capsule 4 were selected.

**Data Preparation.** Data were filtered to include only full power data, to exclude data from Cycle 138B, and to examine data from one capsule at a time. In addition, a training data set was separated from the larger dataset, so that model predictions for the training period could be compared to predictions for data beyond that period. In these examples, the training period encompassed data from March 1, 2007 to January 1, 2008.

**Modeling Method.** Ne fraction, all the control cylinders, lobe powers, and both regulator rod positions were considered for a regression model prediction the readings from TC\_2 in Capsule 4. The automated variable selection options in the SAS REG procedure were used to automate the process of evaluating the relative importance of these variables in the model. The procedure finds the best n-parameter model for values of “n” up to the number of independent variables provided.

**Discussion of Method Details.** (No particular details exist for this preliminary model).

**Results and Their Interpretation .** Results demonstrate (Figure 29A) that  $R^2$  values increase significantly when the first three parameters are added, but only marginally thereafter. Examining F-statistics for the model that incorporates all thirteen terms (Figure 29B) indicates that the control cylinder positions, combined with gas flow composition, provide the best linear model for TC temperatures, and that regulator rods and thermal power measurements add only marginal value.

The full model result shows in Figure 30. The dotted gray line is the model result for the observed TC\_2 temperatures in Capsule 4, shown as the solid red line. Temperatures for the other two Capsule 4 TCs are also shown in the graph. The training period is shaded. The model fit is much better for the training period than for the subsequent testing period.

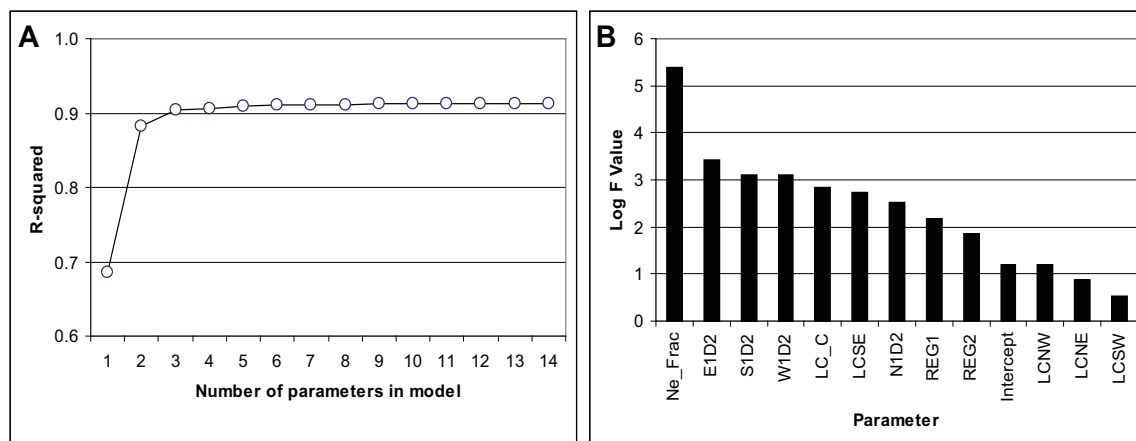


Figure 29. Determination of the number of terms to include in a model for readings from Capsule 4, TC\_2.



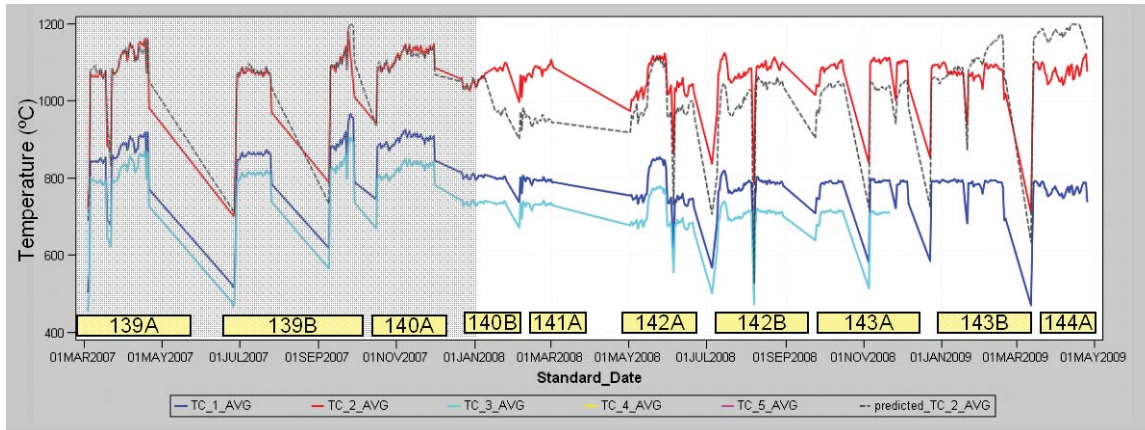


Figure 30. Capsule 4 TC\_2 model (gray dotted line) using all control cylinder, lobe power, and regulator rod depth variables and the measured TC\_2 temperature (red line). Other measured temperatures are provided for reference.

### 3.1.1.6 Temperature as a Function of Ne Fraction and Two Reactor Controls

**Purpose.** To develop temperature models using Ne fraction and the control cylinder positions, which were the most important variables in the previous model.

**Input Data.** The merged stream of TC temperatures, gas flow rate, and ATR lobe powers and shim positions from the NDMAS Vault. For the data exploration, the Capsule 6 irradiation data set was used.

**Data Preparation.** As in the previous example, data were filtered to include only full power data, to exclude data from Cycle 138B, and to examine data from one capsule at a time. In addition, the March 1, 2007 to January 1, 2008 period was separated out as a training data set.

**Modeling Method.** Proc GLM (General Linear Model) in SAS was used to perform a series of ordinary linear regressions and to compare the results. TCs 2 through 5 in Capsule 6 provide nearly identical readings. The location of that capsule in the experiment train, closest to the recording instruments, and the fact that the as-run reactor physics and thermal analysis temperature calculations are similar to the recorded values, suggests that these TC readings are relatively accurate. Initial modeling therefore consisted of application of several regression techniques to predict TC-2 temperatures in that capsule. Because ATR configuration and gas flow mixture were believed to be important controls, regression models included at least neon fraction and one ATR variable.

**Discussion of Method Details.** A first model explored model fit using a minimum of input parameters to predict temperature from ATR parameters. The  $R^2$  and root mean square error (RMSE) terms were computed for each model under consideration using the training data. Separate calculations were performed using the testing data. For the  $R^2$  estimates, a correlation coefficient for the correlation between the observed TC readings in the testing data set and the predicted TC readings for those data was obtained using the “CORR” SAS Procedure.

**Results and Their Interpretation .** The best simple linear model, using only the neon fraction and one ATR configuration parameter, was found using N1D2 (Table 3). The RMSE for the training period in that example was relatively low (21°C), and casual inspection suggests that the predictions provide a good representation of variability. The RMSE for the testing period, however, is significantly higher (37°C) demonstrating that a good fit to the training data does not necessarily imply a good fit to subsequent data that were not used to develop the model. Interestingly, a two-parameter model using S1D2 instead of N1D2 provides a similar fit to the training period but provides a better fit to the combined training and testing set. Examined at a scale of daily averages, this model (Figure 31. Ne fractions and control cylinder positions, with two models of Capsule 6 TC\_2 readings. Figure 31 C)

Table 3. Comparison of models of Capsule 6, TC\_2 readings using Ne fraction and control cylinders.

Control Cylinder Variable(s) used in Model	Corner of ATR	Training data		Test data	
		R <sup>2</sup>	RMSE	R <sup>2</sup>	RMSE
N1D2	NW	<b>0.89</b>	<b>21 °C</b>	<b>0.62</b>	37 °C
S1D2	<b>SE<sup>a</sup></b>	0.84	26 °C	0.74	29 °C
W1D2	SW	0.79	30 °C	0.72	29 °C
E1D2	<b>NE</b>	0.85	25 °C	<b>0.82</b>	23 °C
All control cylinders	—	0.93	17 °C	0.88	20 °C

a. The SE and NE corners are closest to the AGR-1 experiment, which is on the east side of the ATR.

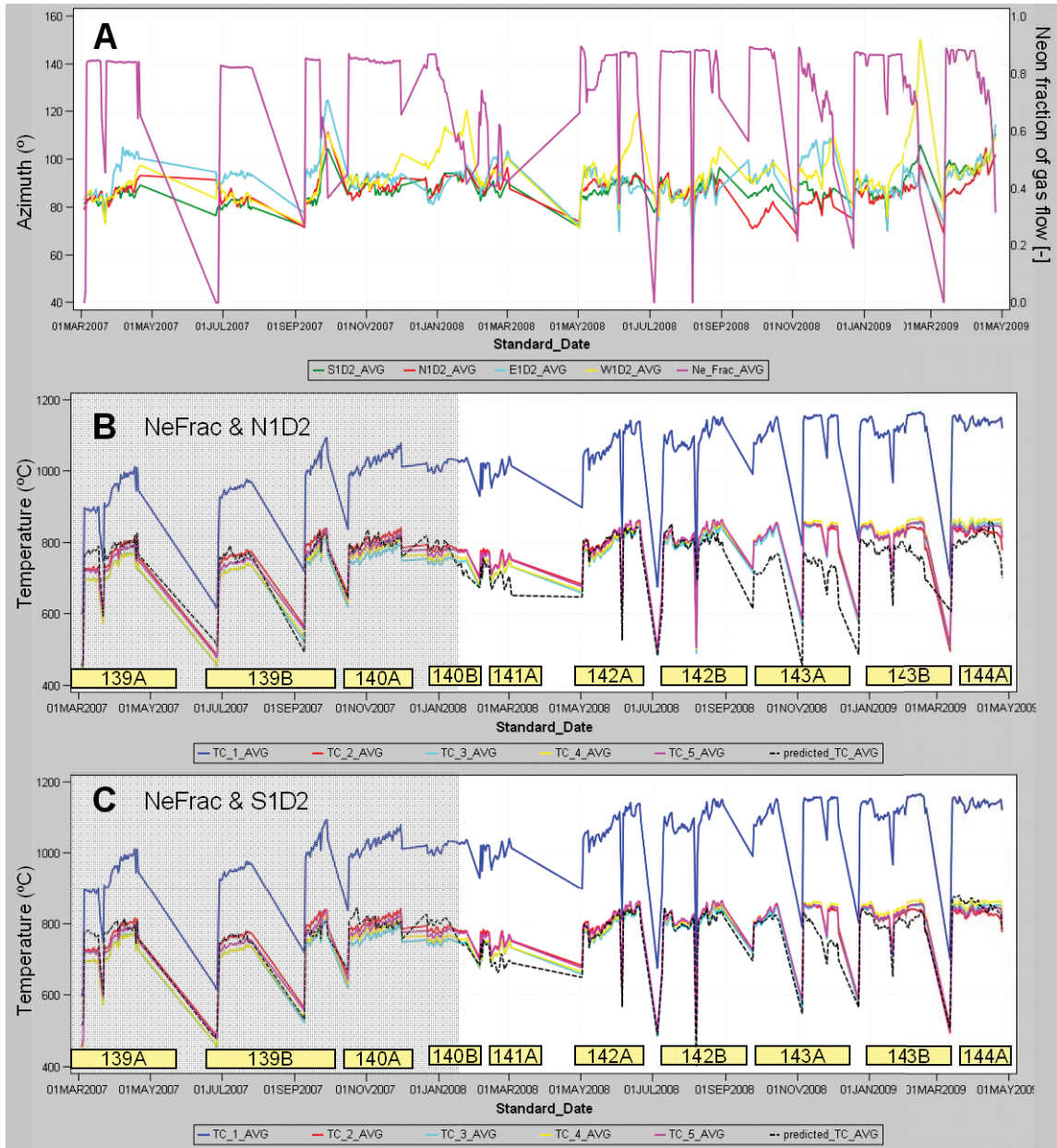


Figure 31. Ne fractions and control cylinder positions, with two models of Capsule 6 TC\_2 readings.

appears to provide the best fit of the all two-parameter models, and demonstrates the relative accuracy that can be obtained with an extremely simple model.

### 3.1.1.7 TC Temperature Readings from a Response Surface

**Purpose.** The regression models described here have separated most of the AGR-1 data into one training period and one, significantly longer, testing period. In practice, the testing period might represent some period for which an independent measure of TC temperature is sought, which might be a period as long as the testing period used in these examples but also might be restricted to just one to several cycles. As an example, simple regression models like this might be used to estimate TC temperature for an upcoming cycle based only on several first-order independent variables.

**Input Data.** The previous model was used.

**Data Preparation.** (Not applicable.)

**Modeling Method.** The previous model was converted to a different type of display for prediction.

**Discussion of Method Details.** (Not applicable.)

**Results and Their Interpretation .** Figure 32 illustrates how a simple linear regression model for TC-2 in Capsule 6 might be used to estimate, for an upcoming cycle, temperature range that gas mixture variations could provide based on knowledge of control cylinder position. In other cases, similar regression models might be applied to the larger dataset, to attempt to find influences on TC behavior that are not part of the reactor or experiment control. Decreasing TC temperature with a linear relationship to effective full power days, for example, might reflect increasing annular space between the fuel assembly and the capsule wall. By altering the relationship between reactor controls, experiment controls and TC temperature, such effects might identify in disparities between regression calculated temperatures and measured temperatures.

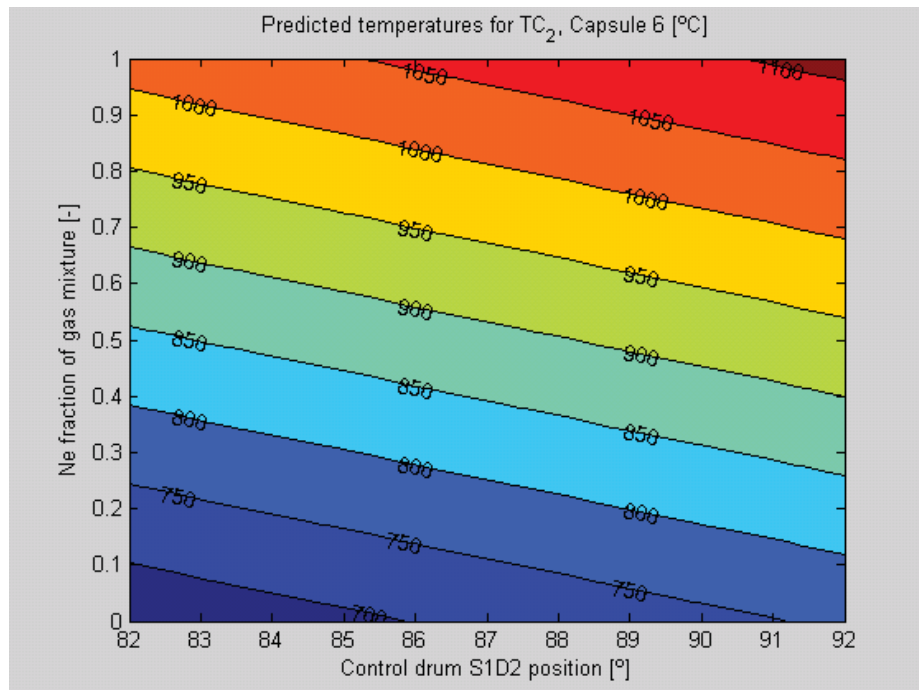


Figure 32. Contour plot of predicted temperature for TC<sub>2</sub> in Capsule 6 as a function of Ne fraction and the angular position of ATR SE control drum S1D2.

### **3.1.1.8 Fission Power as a Function of Irradiation and ATR Power Parameters, Leading to a Model for Temperature**

**Purpose.** To separate the problem of predicting TC temperature from ATR operating conditions into two fundamental relationships, one describing the reactor control on fission heating rates in the AGR-1 fuel, and a second describing the change in temperature in the capsule as a function of the fission heating rates. Examining these issues separately may suggest a means of developing an improved model for the overall relationship.

**Input Data.** Fission power in MW was calculated for two positions in each of the four fuel compacts in each of three stacks, for each capsule in the AGR irradiation experiment (Sterbentz, 2009). A total of 144 values were obtained. This analysis was performed in daily time steps for the days in Cycle 139B (the third ATR cycle in the experiment). Data are present for 55 days. Qualified temperature and gas flow data came from the NDMAS Vault.

**Data Preparation.** The fission power data were averaged for each day but not for each stack. The data were merged with the daily averaged ATR power parameter data, and filtered to observe behavior for TC\_2 in Capsule 6 for ATR Cycle 139B. The following were considered as possible predictors of fission power in Stack 1, the stack that is closest to the north side of the ATR: daily mean values for the four control cylinder positions, the “REGcombined” term, pressure, and Ne fraction.

**Modeling Method.** SAS Procedure REG was used to select an optimum set of variables for the regression. The ATR input variables included the five thermal power measurements, four control cylinder positions, and two regulator rod positions. For the regression model of temperature from fission power, only the fission power and neon fraction of gas flow variables were used.

**Discussion of Method Details.** All of the data were used for training. To compare the model with data from other cycles would require more fission power data.

**Results and Their Interpretation .** Listed in decreasing order of significance, the fission power model used the position of the E1D2 control cylinder, the two regulator rod insertion positions, and three lobe power variables (from the SE and NW and center lobes). Other variables were not significant in the model at the 10% level. The observed and predicted values are shown in Figure 33. The model provides an excellent fit for the fission power data.

The number of physical controls on temperature in the capsules should be considerably less complicated than that for fission heating. The thermal conductivity of the gas mixture flowing through the capsule, and the temperature gradients in the heat flow system are presumed to be the primary controls. Because the most important thermal gradient in the system is between the interior and exterior of the capsule, and that thermal gradient is generally large and relatively constant, a model involving only fission heating rate and thermal conductivity for capsule temperature at a single location could be reasonable. In Figure 34, Ne fraction is used as a proxy for thermal conductivity. The two-parameter model provides a good fit for the observed temperature data.

The temperature model in Section 3.1.1.3 is like the model of Figure 34, but it contains additional functions of the two independent predicting variables that are motivated by additional physics considerations. That model, in Figure 26, applies for TC\_3 in Capsule 4. With more terms, it fits the data even closer.

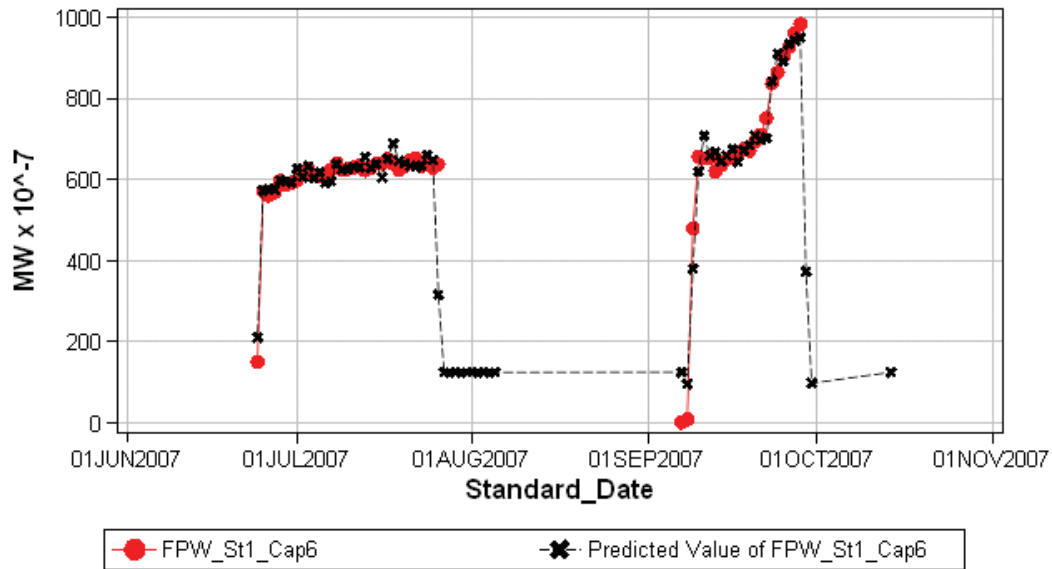


Figure 33. Predicted and observed fission power in Stack 1 for Capsule 6 in Cycle 139B.

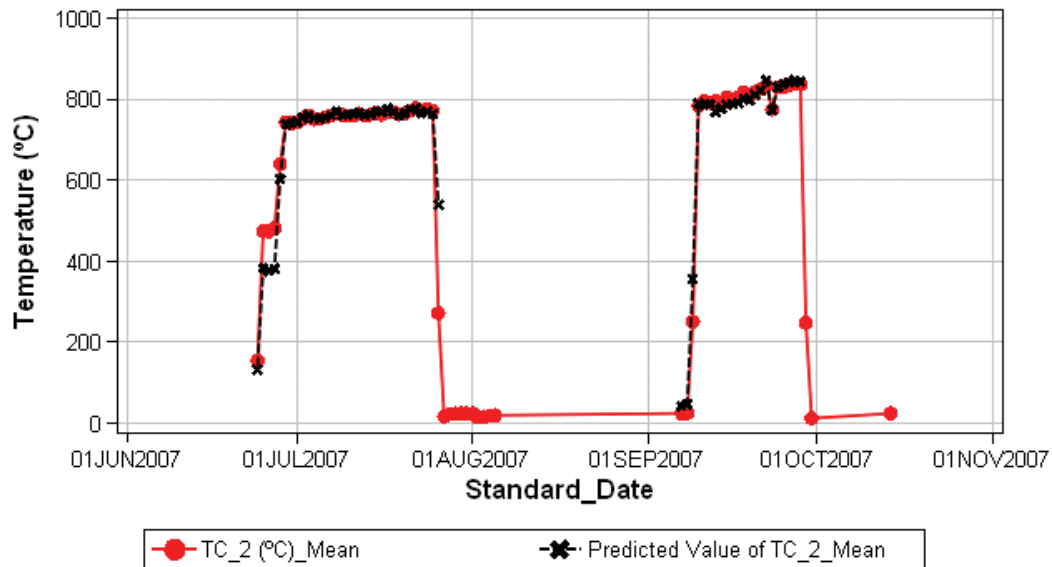


Figure 34. Predicted and observed temperatures for TC\_2 in Capsule 6 based on fission power and Ne fraction.

### 3.1.2 Capsule R/B Ratio Models

The relationship between R/B ratios for Kr-85m and temperature has been examined on an individual cycle basis, as shown in the webpages (see Section 2.2.1.4). One example of a more detailed model exists. The model considered data spanning several cycles and in groupings based on the EFPDs accruing during the AGR-1 experiment. This model is an example of modeling by outside users who access the data via the INL NDMAS web portal. The analysis was performed by Dr. J. M. Kendall, who kindly consented to



the use of his example for this report [Reference: e-mail from Dr. J. M. Kendall of Global Virtual, LLC, in Prescott, AZ, to David A. Petti at the INL, 6/9/2009].

**Purpose.** To observe how the Kr-85m R/B ratios respond as the EFPD in the experiment increases, while controlling for the effects of temperature.

**Input Data.** Dr. Kendall downloaded data for Capsule 4 using the SAS AGR-1 summary plots data table.

**Data Preparation.** Dr. Kendall used the effective power, TC\_1, TC\_2, and Kr85m R/B ratios for each day in the test period spanned by the data. He used 22 MW effective power to calculate an EFPD to associate with each day. He partitioned the data into five groupings, with EFPD varying from 1–250, and then in increments of approximately 55 days up to the maximum days at the time that he captured his data, which was 472 EFPD. He based the temperature information on TC\_2 in capsule 4, which is the TC in the center of the capsule. However, he first checked that TC\_2 and TC\_1 correlate well by performing linear regressions in each group on the TC\_1 readings as a function of the TC\_2 readings. He found fairly good fits in these regressions, and concluded that TC\_2 was probably not drifting (or, if it was, then both TC\_1 and TC\_2 would be drifting).

**Modeling Method.** Dr. Kendall performed a linear regression analysis of R/B as a function of TC\_2 readings within each grouping.

**Results and Their Interpretation.** The results appear in Figure 35. Dr. Kendall observed that the regression lines all have somewhat similar increasing slopes in R/B with temperature, but the position of the lines on the R/B scale tends to increase as the EFPD increases. He concluded that, since the TC data were apparently valid and not drifting, the results show a significant increase in R/B in the later cycles. He thinks that the increase is “probably due to the falloff in fission product production from depletion in the particles, in combination with a build-up of plutonium and/or U-233 from natural uranium and/or

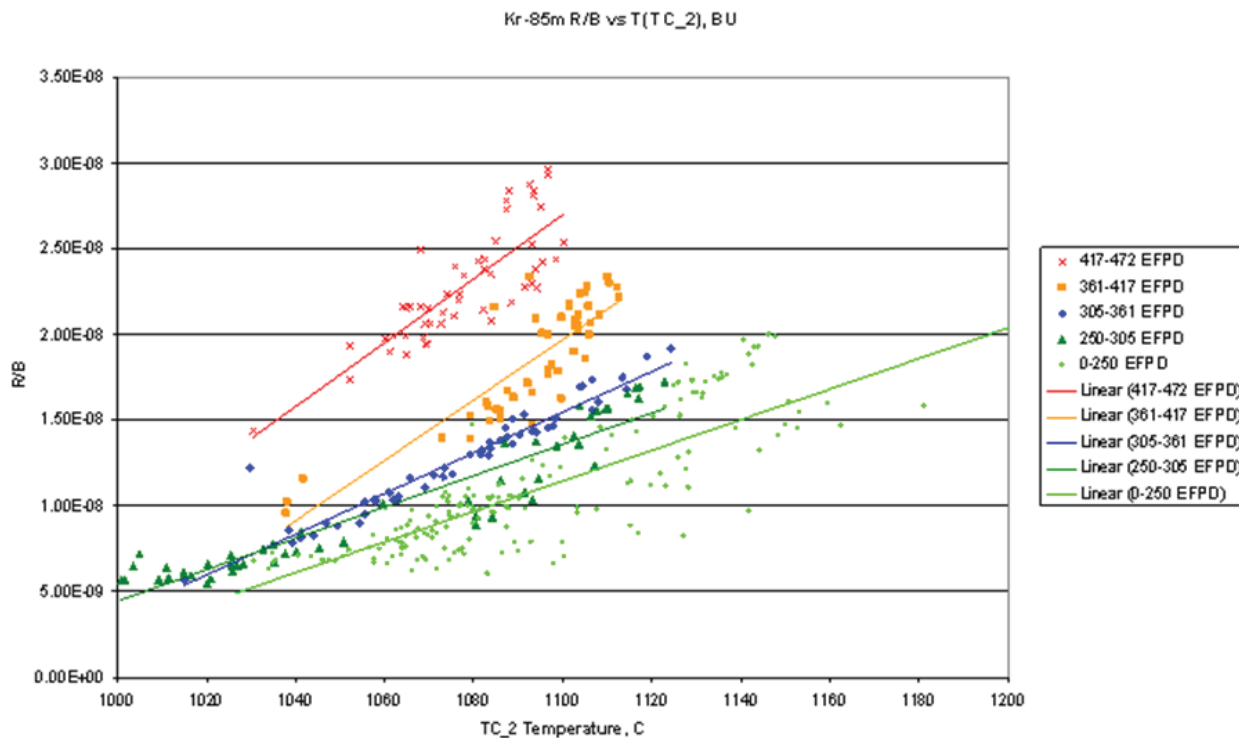


Figure 35. Model from Dr. J. Kendall, showing R/B increases as EFPD increases.

thorium contamination outside the particles.” He also notes that the increase is well below what might be expected from a particle failure.

### **3.2 Models related to Graphite**

The initial NGNP graphite experiments are to test the physical properties of various grades of graphite to identify which ones might be most likely to perform well as reactor core materials in the high-neutron flux, high-temperature environment of the VHTR. No particular models at this time need further discussion beyond the presentation of the displays in the webpages. More modeling is expected after PIE data are available for comparison with the initial characterization data.

## **4. ONGOING AND PROPOSED FUTURE MODELING**

Ongoing and future modeling capabilities can be viewed from two perspectives: the applications that may be developed and the new capabilities that come from enhancements in the set of modeling tools available to support those applications.

### **4.1 Applications**

The primary ongoing modeling effort for NDMAS is to add displays to the website that will show each new data stream as it is identified and added to the data base. The fuel irradiation project will be generating postirradiation examination data starting in the winter of FY 2010. Irradiation data from the graphite project will start coming in when that experiment is placed in the ATR. The High Temperature Materials project is also expected to be generating data before the end of FY 2010.

Another priority for ongoing work is to look into models and relationships that might exist based on requests received from the community of VHTR researchers.

Extensions to current work are also envisioned. For example, one goal is to obtain information about thermocouple performance from the AGR-1 experiment that will support the use of more reliable thermocouples in future irradiation experiments. A number of these extensions are discussed in this section. These models all relate to irradiation experiments.

#### **4.1.1 Capsule Temperature Models**

##### **4.1.1.1 Accuracy Tests Based on Departure from Means**

Reactor physics simulations of fission heating rates in the AGR-1 fuel stacks indicate that although heating rates are generally greater toward the middle of the capsule train than toward the ends, heating rates are generally proportional to one another throughout the capsule train. Where gas flows for each capsule are varied in a similar manner, capsule temperatures can be expected to generally behave quite similarly. Departures from mean temperatures for each cycle, for each capsule, could provide a graphical means of examining relative behavior between thermocouples, and between capsules.

##### **4.1.1.2 Identification of Stable Reactor Power Operation Periods**

Many of the models being considered for the fuel irradiation experiment data are expected to perform best when the reactor is up and operating. Short interruptions in periods of full power operation occur, but do not signal a transition to a shutdown state. Therefore, a simple filter that identifies the at-power data based on a simple range of temperatures or on a fixed cutoff for some ATR power parameter does not always give an optimal way to exclude transitional and shutdown data from operating data.

A data-driven method using clusters and a Markov chain will be implemented to identify reactor operational times. The method begins with a cluster analysis using temperature readings from one TC. Clusters will be sought for three states: shutdown, transition, and operating. The cluster procedure creates estimates for the probability that any particular temperature reading could come from each of the states. The Markov chain part of the process refines the probabilities to ensure that, for example, a transition period occurs between each change of state from shutdown to operating. The result of the process will be a flag for each TC reading showing whether it is regarded as being in operations, transition, or shutdown. Filtering for operating data will then be accomplished easily.



#### **4.1.1.3 Accuracy Tests for Temperature Based on Correlation Coefficients**

The correlations studies displayed on the website show high correlations between TC readings in a capsule. Lower values are typically associated with changes in the temperatures as reactor conditions change. If these effects could be separated out, dips in correlations might provide an early indication of TC drift or failure. Use of a filter based on the output from the identification of stable reactor power operation periods described above will be a first step. The goal is to develop cutoff values for the correlations such that correlations below the cutoff flag a need for additional data review for TC accuracy.

#### **4.1.1.4 Accuracy Tests for Temperature Based on TC Regression Models**

The TC prediction models described above need further refinement so they can provide reliable estimates of TC readings. The refinements include using fewer TCs in the models and including terms in the models for different capsules. Also, the filtering of the data will be improved, based on the Stable Periods task above, so that all TC reading streams are filtered consistently. In current models, a filter that removes values less than 100°C removes more data from those TCs in the cooler parts of the experiment. As the regression models are further refined, error bounds will be developed that describe the expected variation between the predicted values and the observed readings. This process will lead to the development of cutoff values. TC readings that differ from the predicted values by more than the cutoffs will be flagged for further checking.

#### **4.1.1.5 Accuracy Tests for Temperature Based on Regressions Using Other Variables**

As with the previous modeling enhancement, TC models based on other reactor parameters can be refined further with enhanced filtering and possible model development. Future work will extend the analysis to include the 22 neck shim variables in order to further explain differences in correlation with control cylinders over time. In addition, because non-linear relationships frequently do not produce high correlation coefficients, analyses that may better recognize such relationships, such as correlation ratio, will be tested. Plausible explanations will be investigated for the low correlation coefficients between temperature and lobe power, relative to that with control cylinders.

Error bounds and cutoffs can be developed that will allow the flagging of any TC readings differing from the predicted values by more than the cutoffs. Flagged readings could then be checked further.

#### **4.1.1.6 Accuracy Tests for Temperature Based on Fission Heat Rate Models**

Access to MCNP-calculated fission heating rates provides a means of dividing the problem of predicting temperature from ATR configuration into two parts, one that estimates fission heating in the fuel compacts from the configuration of the ATR, and a second that calculates TC and/or fuel temperatures from fission heating and other experiment-level parameters such as Ne fraction. The preliminary analysis suggests that relatively simple linear or non-linear regression models might provide a relatively reliable predictor of fission heating in the fuel. That possibility is supported by the rapid response time of fission heating to changes in reactor configuration, which is sufficiently short that as-run calculations of fission heating assume a steady-state response. Regression models developed from estimated fission heating rates and the Ne fraction might be used as with the regression models discussed above to develop error bounds and cutoffs for the flagging of possibly discrepant TC readings.

#### **4.1.1.7 Comparison of Qualified and Inaccurate Data**

Figure 36 shows green time lines for the nine failed AGR-1 TCs. Six of these TCs gave output readings for months after their failure dates. In the figure, these periods are labeled as “Inaccurate.” For TC\_2 and TC\_3 in Capsule 2, and for TC\_1 and TC\_2 in Capsule 3, the inaccurate periods are preceded by several months of qualified data. TC\_1 in Capsule 3 reported data during nearly the entire experiment,

although it failed in April of 2008, so it has a large quantity of both qualified and inaccurate readings. Modeling to identify a statistical difference between these readings would be worthwhile, because it might be applied to future data to provide an earlier warning of TC failure.

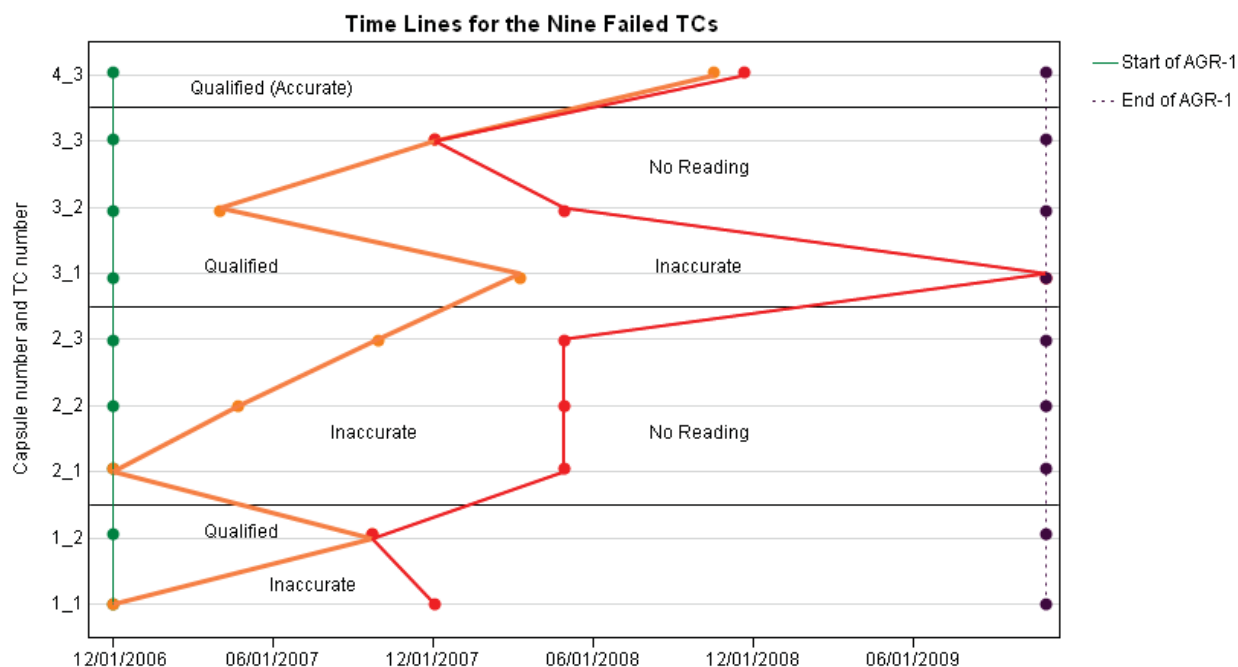


Figure 36. Time profiles for failed TCs, showing periods when they reported inaccurate data.

#### 4.1.2 Capsule R/B Ratio Models

The correlation models currently on the webpage will be enhanced by grouping the data differently so that the release data is more synchronized with the temperature data. More of the regression models are expected to show significant patterns after this change. Also, more of the type of modeling performed by Dr. Kendall (Section 3.1.2) may be developed.

### 4.2 Enhanced Capabilities

The acquisition of a faster server will increase the overall performance of the NDMAS for developers and INL users. The delay between requesting a report and seeing it on the screen is expected to be significantly reduced. Also the increased resources provided by this acquisition will improve throughput as the number of concurrent users increases. This increase in users is expected as more researchers realize the potential benefits of examining the data directly using NDMAS.

The NDMAS system is currently running on SAS Version 9.1.3. In the near future, the NDMAS system will be running on Version 9.2. In addition to improvements in the Base SAS software that provides the foundation of the analysis system, Version 9.2 provides enhancements for most of the statistical analysis procedures (see Appendix B) used to model the data. It also provides extensive improvements in the graphic capabilities. The ATR cycle shading in many of the graphs in the “Graphical Summary” webpage were produced using Version 9.2 graphic tools, which were available on one PC at the INL. The SAS version upgrade will distribute this advanced graphic generation tool to the rest of the development team.

SAS 9.2 also provides tools to automate the deployment of data and portal components (e.g. SAS Reports) from the NDMAS “Mart” to its mirror image on the INL NDMAS web server that resides

outside the INL's firewall. This automation can run on a schedule which will improve the current twice-weekly refreshing and updating of the webpages to a daily or even hourly promotion of changed data.

Another enhancement is the acquisition of the SAS "Data Integration Studio" software. Currently, the process of extracting data from the Vault and merging different data streams to get data sets for analysis can be intermixed with the analysis tasks themselves. The Data Integration Studio will create a more rigorous software engineering process with separate domains for integration and analysis. The integration processes will be linked directly to the data, so that certain types of data are always processed from source documents in the same way. It will increase the automation of these tasks.

SAS will be integrated during FY-2010 with the Phoenix Integration™ Model Center application described in the following website: [Phoenix Integration Model Center](#)

This capability will significantly enhance the ability to run dynamic linked models. Much successful integration of this product and JMP exists in the aerospace industry. This tool may provide a framework for studying detailed 3-D reactor physics and thermal analyses and NDMAS data together.

The project is also acquiring an enterprise license for the JMP data analysis and visualization tool. The license will make this powerful software available to all the NDMAS developers and INL VHTR researchers.

## 5. SUMMARY AND CONCLUSIONS

NDMAS provides many powerful modeling capabilities. For users accessing the INL NDMAS web portal, relationships between key attributes of the experiment and various experimental conditions can be studied using such features as:

- Scatter plots, line plots, and bar charts, and combinations of these
- Histograms and box plots that show distributions for the sample data
- Lattice plots that break the data into subsets such as data from different capsules, and show each in successive panels having a common time or other axis
- Matrix plots that show all the pairwise relationships within a set of variables
- “ActiveX” graphs that allow the user to manipulate many of the features of the graph to enhance understanding
- Plots and data displays based on hierarchical “cubes,” that allow users to drill down and display more detailed levels in the data
- Data exploration portals that allow users to perform their own variable selection, sorting, filtering, data display, and downloading
- Stored processes that, for example, allow users to view gross gamma counts for the time frame and capsule that they select

The report describes these website features as they are implemented as of August, 2009. Because the website is updated frequently, the content that can be studied using tools such as these is as current and complete as possible.

Even more modeling tools are available for developers creating content for the website. All of the statistical power of SAS, Inc.’s SAS/STAT statistical software is available, in addition to the SAS/QC software for control charts and complete access to SAS/GRAPH for data visualization. The SAS/STAT regression procedures, in particular, provide modeling frameworks that can be tailored to the nature of the data being analyzed. In the process of fitting a parametric model to data, the researcher makes assumptions about how the data set was generated, whether certain quantities are independent, etc. The SAS procedures allow many of these assumptions to be relaxed. Nonlinear regression is supported, so that functional relationships established from physical models can be accommodated. Different distributional forms can be considered, as well as a variety of variance structures. Ultimately, empirical data modeling is about separating process variation that can be understood and to some extent controlled from the random “noise” that is always a part of observed data. The flexibility and power of the SAS system for data analysis optimizes the possibility of deriving useful information from the data modeling efforts.

This report has provided examples of current applications of some of these technologies. Many of the applications deal with describing temperatures during the AGR-1 irradiation experiment currently underway. The applications are exploratory in nature, but show promise for use in future experiments for such applications as monitoring the behavior of the TCs.

Future enhancements to both the models and the SAS EBI platform on which they are implemented are planned. Some of these are highlighted in the report.

Since all VHTR researchers can request the NDMAS team to investigate particular relationships between variables, or download data and investigate these relationships themselves, the modeling capabilities of NDMAS are virtually unlimited.

## 6. REFERENCES

- Ambrosek, R. G., 2005a, *Thermal Analyses for Design of AGR-1*, EDF-5138, Idaho National Laboratory, October 3, 2005.
- Ambrosek, R. G., 2005b, *Evaluation of Thermocouples for Use in AGR Tests*, EDF-6257, Idaho National Laboratory, October 3, 2005.
- Ambrosek, R. G. ([Richard.Ambrosek@inl.gov](mailto:Richard.Ambrosek@inl.gov)), (2009), "Updated AGR-1 Data," John T. Maki ([John.Maki@inl.gov](mailto:John.Maki@inl.gov)), 4/15/2009.
- ASME, 2000, *Quality Assurance Requirements for Nuclear Facility Applications*, Nuclear Quality Assurance (NQA-1), ASME International, New York, NY.
- Chang, G. S., M. A. Lillo, 2003, *Confirmatory Neutronics Analysis of the AGR-1 Experiment Irradiated in ATR 8-10 Position*, EDF 7120, Rev 11 Idaho National Laboratory.
- Cox, J. R., 2009, *VHTR Technology Development Office Program Management Plan*, PLN-2494, Rev. 3, Idaho National Laboratory.
- Einerson, J. J., 2006, *Statistical Sampling Plan for AGR-3 and AGR-4 Fuel Materials*, EDF-6917, Revision 1, Idaho National Laboratory.
- INL, 2009, *Very High Temperature Gas Reactor Technology Development Office Quality Assurance Program Plan*, PLN-2690, Rev 2., Idaho National Laboratory.
- Krusch, S., 2009, *General Software Management Plan for the VHTR TDO*, PLN-2247, Rev 0, Idaho National Laboratory.
- Lillo, M. A., G. S. Chang, 2007, *Neutronics Projection Analysis to Support the End of Irradiation Determination for the AGR-1 Experiment*, ECAR-515, Idaho National Laboratory.
- Maki, J. T., 2007, *AGR-1 As-Run Analysis Status For FY-07*, INL/EXT-07-13630, Idaho National Laboratory, December, 2007.
- Maki, J. T., 2007, *AGR1 Irradiation Experiment Test Plan*, INL/EXT-05-00593, Idaho National Laboratory, Rev 2, March 2007.
- Petti, D., R. Hobbins and J. Kendall, 2008, *Technical Program Plan for the Next Generation Nuclear Plant/Advanced Gas Reactor Fuel Development and Qualification Program*, INL/EXT-05-00465, Idaho National Laboratory.
- PLN-2709, 2009, *VHTR Program Data Management and Analysis Plan*, PLN-2709, Rev. 1, Idaho National Laboratory.
- SAS, 2007, *SAS Enterprise Business Intelligence Server*, SAS Institute, Inc., Cary, NC.
- SAS, 2009, JMP 8.0.1, *JMP Statistical Discovery Software from SAS*, SAS Institute, Inc., Cary, NC.
- Sterbentz, J. W. ([James.Sterbentz@inl.gov](mailto:James.Sterbentz@inl.gov)), (2009), "AGR-1 Cycle 3 Compact Fission Powers," M. A. Plummer ([Mitchell.Plummer@inl.gov](mailto:Mitchell.Plummer@inl.gov)), June 11, 2009.
- Vargaftik, N.B., 1996, *Handbook of Physical Properties of Liquids and Gases: Pure Substances and Mixtures*, Third ed., New York: Begell House.

## **Appendix A**

### **VHTR Experiments and Associated Data Streams**

# Appendix A

## VHTR Experiments and Associated Data Streams

Data streams currently being processed or developed for the VHTR research are described briefly below, organized according to the data collection projects currently described in the NDMAS Program Plan (PLN-2709, Rev 1, 7/23/2009).

### A-1. Fuel Development and Qualification Project

A series of Advanced Gas Reactor (AGR) experiments are planned to study the performance of possible fuels for the VHTR. The two designs under consideration for the VHTR are a prismatic block design with low-enriched uranium oxycarbide (UCO) fuel particles and a pebble bed design with low-enriched uranium dioxide (UO<sub>2</sub>) fuel particles. Within these two major groupings, a variety of fabrication methods and coatings are possible for the fuel. The experiments are designed to identify fuel that can, among other things, endure the operating conditions of the VHTR, including high temperatures, without leaking or deforming. The experiments will provide data to justify Nuclear Regulatory Commission (NRC) licensing of the selected fuel design.

In the AGR-1 experiment, fuel particles were fabricated and loaded into compacts (approximately 4150 per compact), which are installed in capsules. The capsules were loaded in a test train that was installed in the Advanced Test Reactor (ATR) at the INL. There were twelve compacts per capsule and six capsules total. In the ATR, the capsules were irradiated over a period of 34 months to date, at a temperature of approximately 1250 °C. Conditions in the experiment were recorded frequently (e.g., every 5 minutes). After burn-up of the fuel, postirradiation examination (PIE) will reveal more information about the fuel performance. Additional experiments will test other fuels, and fuels at higher temperatures, and fuels sized at a scale comparable to the fuel planned for the demonstration VHTR.

The fuel experiments give rise to data sets such as the following:

- Fuel fabrication data (see Table A-4)
- Irradiation data (see Table A-5)
- Fission product monitoring system (FPMS) data (see Table A-6)
- ATR reactor operations data (see Table A-7))
- Neutronics and temperature analysis data (see Table A-8)
- PIE data (see Table A-9)

The tables below list attributes measured in the experiment by component, or experimental unit. Components are structured in a hierarchical fashion in the data base so that the data can be associated with the level of entity that is being monitored.

The last column of the table describes the data qualification category associated with each group of response variables. The *Qualified* designation means that the data has been reviewed and was collected under a QA program meeting the guidelines of ASME NQA-1. *Trend* data are also collected under these guidelines but have not been reviewed as thoroughly because either they were not regarded as being important enough for a full review, or they have known deficiencies that limit their applicability although they still might show general trends in the measured parameters. The *Archive* data are stored in the NDMAS backup records but are not entered formally into the data Vault. They thus may not be available for use in modeling. They could be upgraded to a higher status if a need were identified. These

designations are described further in the VHTR Program Data Management and Analysis Plan (PLN-2709).

Table A-4. Fuel fabrication data parameters and categories.

Component	Response Variables & Attributes	Qualification Category
Kernel batch, fabricated fuel kernels	Envelope density, diameter, and sphericity.	<i>Qualified</i>
Kernel composite	Enrichment, composition, impurity levels, diameter, density, sphericity	<i>Qualified</i>
Surrogate particle batch, kernels coated with buffer and IPyC layers.	Buffer and IPyC layer densities.	<i>Qualified</i>
Fully coated particle batches	Layer thicknesses, missing OPyC layer defect fraction	<i>Qualified</i>
Coated particle composite, kernels coated with buffer, IPyC, SiC, and OPyC layers.	Layer thickness, density, defect fraction, aspect ratio, pyrocarbon layer anisotropies, SiC layer microstructure.	<i>Qualified</i>
Individual compact, particles encapsulated into fuel compact.	Diameter, length.	<i>Qualified</i>
Compact composite <sup>a</sup>	Purity, strength, U loading, defects.	<i>Qualified</i>
Particle and compact	Manufacturing conditions—gas ratios during coating, temperatures during coating, compact molding pressure, compact carbonization and heat treatment conditions	<i>Qualified</i>
Compact	Irradiation position—stack, capsule	<i>Qualified</i>

a. A compact composite is a sample of compacts that is destructively tested for application to all compacts.

Table A-5. Reactor irradiation data parameters and attributes for the AGR (fuel) experiments.

Component	Response Variables and Attributes	Qualification Category
Capsule	Temperature from thermocouples, Helium, neon, and total gas flow	<i>Qualified</i>
Capsule and leadout	Gas pressure and moisture content	<i>Trend</i>

Table A-6. Fission product monitoring data parameters and attributes.

Component	Response Variables and Attributes	Qualification Category
Capsule	Fission product concentrations in sweep gas	<i>Qualified</i>
	Calculated release to birth ratios of fission products	<i>Qualified</i>
	Gross gamma monitoring data	<i>Archive</i>



Table A-7. ATR operating conditions data parameters and attributes.

Component	Response Variables and Attributes	Qualification Category
Reactor	ATR lobe power	<i>Qualified</i>
	ATR shim cylinder position	<i>Qualified</i>
	ATR core inlet temperature	<i>Qualified</i>

Table A-8. NGNP neutronics and temperature analysis parameters and attributes.

Component	Response Variables and Attributes	Qualification Category
Fuel compact or graphite specimen	Neutronics analysis data, calculated fluence	<i>Qualified</i>
	Thermal analysis data, prediction of specimen temperatures	<i>Qualified</i>

Table A-9. Fuel PIE data parameters and categories (preliminary data).

Component	Response Variables and Attributes	Qualification Category
Test train	Pictures, observation notes, gamma scans, metrology, graphite holder dimensions	<i>Archive</i>
Graphite holder, capsule components	Detailed gamma scan and radioisotope inventories	<i>Qualified</i>
Flux wire, melt wire, capsule liner	Estimated maximum temperature, neutron flux data, and emissivity values used in modeling	<i>Archive</i>
Thermocouples	Metallographic images and other data to examine chemical interactions and microstructure	<i>Archive</i>
Fuel compact	Physical dimensions, detailed gamma scan, radioisotope inventories, selected photos to support fuel qualification, fuel particle failure by leach-burn-leach, postirradiation safety testing	<i>Qualified</i>
	Photos, notes, irradiation	<i>Archive</i>
Fuel particles	Radioisotope inventory, metallography, inspection of layer integrity, photos, spatial distribution of fission products	<i>Qualified</i>

## A-2. Materials Testing and Qualification— Graphite Technology Development Project

The non-fuel components in the VHTR reactor core will be primarily graphite. As with test fuels, various graphite formulations will be irradiated in the ATR and examined to study performance in a high-temperature, high-neutron-flux environment. In a separate series of experiments, properties of the graphite materials will be studied for different graphite grades.

For the graphite that is tested in the ATR, many of the data streams are like the fuel data. In particular, the data streams will include the following:

- Irradiation data (see Table A-10)
- ATR reactor operations data (the data streams are the same as for the fuel; see Table A-7)
- Neutronics and temperature analysis data (same data streams as for the fuel; see Table A-8)

- PIE data (data to provide characterization and safety analysis of graphite after irradiation in the ATR will be stored, but a detailed list of response variables has not yet been developed)

The graphite characterization part of the project will generate the data described in

Table A-11.

Table A-10. Reactor irradiation monitoring parameters for the AGC (graphite) experiments.

<b>Component</b>	<b>Response Variables and Attributes.</b>	<b>Qualification Category</b>
Capsule, test train	Same parameters as for the fuel experiments, plus...	See Table A-5
Channel	Compressive stress applied to graphite specimens for analysis of radiation induced creep	<i>Qualified</i>
Capsule, leadout	O <sub>2</sub> concentration measured in the inflow gas; CO and CO <sub>2</sub> monitored in the effluent gas	<i>Trend</i>

Table A-11. Parameters and classification for graphite specimens (characterization).

<b>Component</b>	<b>Response Variables and Attributes.</b>	<b>Qualification Category</b>
Specimen	Physical properties. thickness, diameter, mass, volume, bulk density	<i>Qualified</i>
	Elastic modulus. modulus by time of flight, fundamental frequency, Poisson's ratio	<i>Qualified</i>
	Electrical properties. electrical resistivity	<i>Qualified</i>
	Thermal properties. instantaneous and mean coefficient of thermal expansion, thermal diffusivity, specific heat, thermal conductivity.	<i>Qualified</i>
	Mechanical properties. tensile strength, compressive strength	<i>Qualified</i>
	Grade, orientation, type, location within billet	<i>Qualified</i>
	Irradiation location information: position within capsule, channel	<i>Qualified</i>

### **A-3. Materials Testing and Qualification— High Temperature Materials Project**

The High Temperature Materials data project involves the performance of materials outside the reactor core. A particular focus will be on heat exchanger materials to be used in the design of the reactor-hydrogen interface. Guidelines for approving materials for high-temperature applications ask for tensile strength, yield strength, reduction of area, and elongation at 50°C-increments from room temperature to 50°C above the maximum intended use temperature and over a range of strain rates. Weld strength rupture factors will be determined for two welding processes as a function of time and temperature. Other properties to be measured at elevated temperatures (T up to 1,000°C) include elastic modulus, Poisson's Ratio, linear thermal expansion, thermal conductivity, thermal diffusivity, and density. Additional lab investigations will characterize weld creep-fatigue, effect of helium impurities, and aging effects on fracture toughness. Detailed development of the Materials data stream including identification and categorization of parameters will be performed in the fourth quarter of FY 2009.

## **A-4. Design Methods and Validation Project**

Data collection activities in support of code development and validation include measurement of nuclear interaction cross sections. Nuclear cross-section measurements relevant to the harder neutron spectrum of the VHTR will be made for selected isotopes, particularly  $^{240}\text{Pu}$ ,  $^{241}\text{Pu}$ , and  $^{242}\text{Pu}$ . These data will ultimately be incorporated into the Evaluated Nuclear Data Files, but may be retained in NDMAS if deemed appropriate. Other data to be collected include criticality, reactivity feedback coefficients, kinetics parameters, peak power, conversion ratio of sustainable cores, transmutation potential, maximum displacement per atom, decay heat, and radiation levels.

Thermal-hydraulic experiments are aimed at producing validation for computational fluid dynamics and systems analysis codes. The experiments will focus on core heat transfer, fluid behavior in core plenums, reactor cavity cooling, air ingress, and combined effects experiments. Two types of experiments are planned: isothermal fluid dynamics measurements, and heated flow studies. Approximately 20 to 50 new experiments will be required to validate software. Data to be collected include temperature, velocity, and pressure. Optical data collection techniques will also be employed. Very large data files will be created by these experiments to capture the spatial and temporal variation in fluid movement and temperature necessary to validate codes. Specific parameters and data categories will be defined for these data streams as the research continues.

## **A-5. Nuclear Hydrogen Initiative Project**

Hydrogen initiative activities focus on development of hydrogen production options to use the high temperature gases generated by the VHTR. High temperature electrolysis requires low-cost, efficient electricity and an energy source that can produce high temperature steam. The Hydrogen project focus is on design of nuclear hydrogen systems, optimization of solid-oxide electrolysis cells, and catalysis of hydrogen production using sulfur-based cycles. Response variable lists and data qualification categories for data streams associated with the nuclear hydrogen initiative project will be developed as further details of the research are defined.

## **Appendix B**

### **Use of SAS Tools for Modeling**

# Appendix B

## Use of SAS Tools for Modeling

Most of the data displays and statistical data modeling described in this document were created using the SAS product, Enterprise Guide (EG). This product provides an environment for accessing data, building queries that provide desired views of the data, including adding and removing fields and filtering the data, and performing a series of statistical analyses. The product also provides tools to graph the data and the model outputs.

Enterprise Guide comes with the SAS Business Intelligence software package. It is installed on the SASNGNP server. NDMAS team members access EG using a client interface on their PCs. EG also provides access to the underlying SAS Foundation, which includes an open-ended language for manipulating data and invoking SAS statistical procedures. The Base SAS product also includes a macro language that allows repetitive processes to be easily automated.

A second tool from SAS that provides modeling capabilities is the “JMP®” product. This tool is a stand-alone product that also interacts with the SAS EBI software. It is licensed and installed on individual PCs. It is designed to provide an interface for intuitive data exploration.

The use of each of these products in NDMAS is discussed further in sections below.

### B-1. Enterprise Guide

EG provides a workspace where data manipulation tasks, statistical analyses, and graphic display tasks are shown in a project view that gives the user an overview of the steps being performed to achieve results. Figure B-1 is an example of the EG “Project Designer” workspace. Here, an existing data set is referenced. Then a query selects particular fields (variables, columns) of interest. Tasks such as the query are each referenced in a box in the diagram. The query boxes have little funnel icons. The diagram also shows examples of Summary Statistics blocks that perform data aggregation, and Line Plot blocks that provide an interface for specifying details for output plots. Double clicking on these boxes brings up wizards that let the user specify how a particular analysis is to be done. Each type of task box invokes a particular SAS Procedure to perform the calculations.

The blocks with little red dots in the lower right-hand corner link to data sets. Most steps in EG projects either manipulate data or use it to produce output data, so it is not surprising that nearly every other block in the figure is a data block. Some tasks produce more than one data set, and some use more than one.

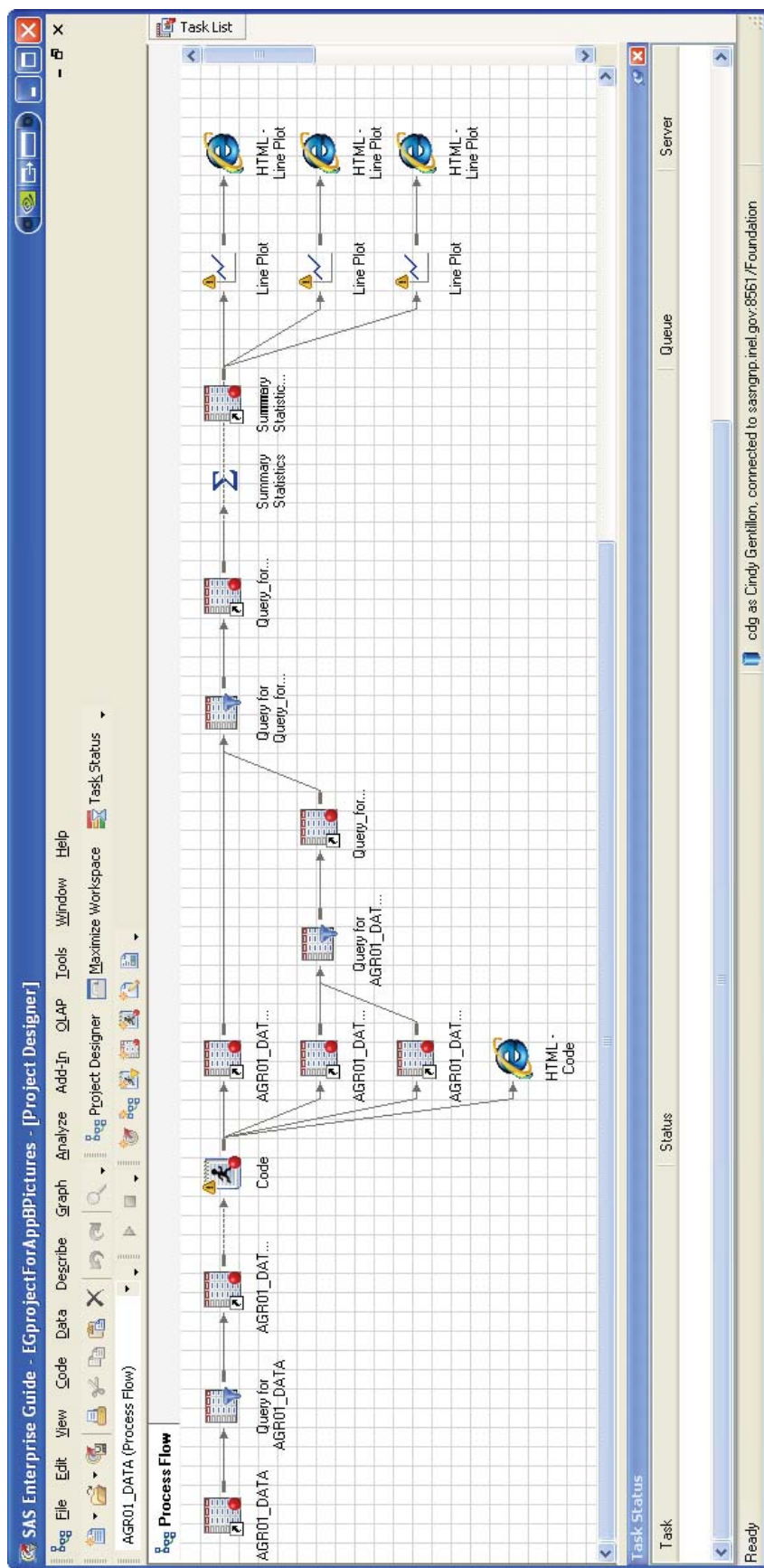
The fourth block in the figure is different from the others. It has an icon of a little person running. Such blocks are “code” blocks where data can be manipulated using the SAS language. Beginning users will not have these types of blocks, usually. However, each of the task blocks generates SAS code. Therefore one can modify the automatic code to achieve specified differences in the outputs, such as changing certain formats or labels. Eventually, one can observe the pattern and create SAS code directly if desired.

The other symbols in the flow diagram in Figure 1 are HTML outputs. These contain tables, graphs and any printed output that the procedures might generate.

A few more summary observations about the workspace, data manipulation tasks, analysis tasks, graphical tasks, and how the modeling efforts connect to the INL NDMAS webpages are in sections below. The last section provides references for further information.

## **B-1.1 Project Designer**

In one EG project file, one can have several “Process Flows” such as Figure B-1. Task boxes are created in a process flow using Menu items such as “Data,” “Describe,” “Graph,” and “Analyze.” A Task List, discussed further below, is also available. In addition to different icons on the blocks for different tasks, each block can be labeled to show its contents. The labels will show in the diagram if they are less than 20 characters long. The “Tools” menu at the top of the screen provides a set of options that allows a user to customize the interface. After a task is selected and the associated menus are completed, EG generates a SAS program that uses the SAS language and Procedures to perform the task. The user can execute the task by clicking, for example, the triangle icon button next to the process name box on the second toolbar. A Task Status window is available, if desired, to view notes about the task progress. The program runs and produces the desired output. If any problems occur, a “log” window will open with error messages. Another block that can be displayed with each task is a “Last Submitted Code” block. Customizing the results for items, if any, that are not directly supported by the wizard can be entered here and the task rerun.





## B-1.2 Data Manipulation Tasks

The “Filter and Query” task that was described in the introduction is the first item on the Data Menu. Figure B-2 shows the window that results, using one of the AGR-1 Fuel Irradiation data sets. The fields are listed in the panel on the left and there are tabs to describe the data desired for the output, any data filters, and how the data should be ordered on output.

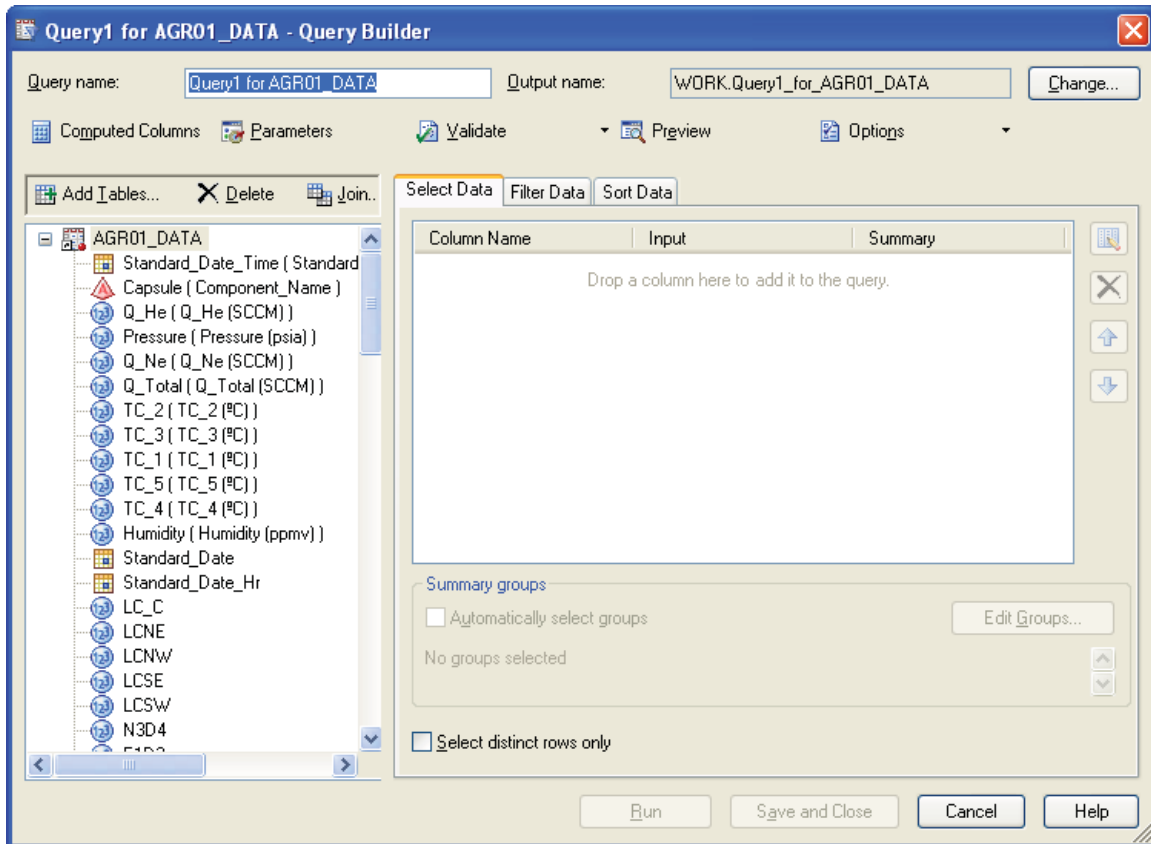


Figure B-2. Enterprise Guide Query Builder.

Several other data manipulation tasks are also available. Figure B-3 shows the Data tasks from the Task List window. These tasks are also listed in the Data Menu. For example, the Transpose task transforms a data set so that category labels in specified columns in the input set become columns in the output data set. This action can be performed in groups, as specified by the values of other column variables (that remain so in the output data). The operation is similar to making a “Pivot Table” in Structured Query Language (SQL) or in many spreadsheet or data base packages. The NDMAS team uses this capability extensively, because the data as stored in the SQL “Vault” has one data item per record, where its qualification status can be tracked. But for outputs, values in the associated “parameter” column become column headings and the various measurements collected at the same time become columns in wide, single records instead of multiple short records.

It is beyond the scope of this overview to discuss each of the Data tasks individually. Figure B-3 shows that EG provides tools to manipulate the data as needed to support modeling and data display.

The Data Menu also allows direct access to the rows and columns of a data table (if the table is not locked).

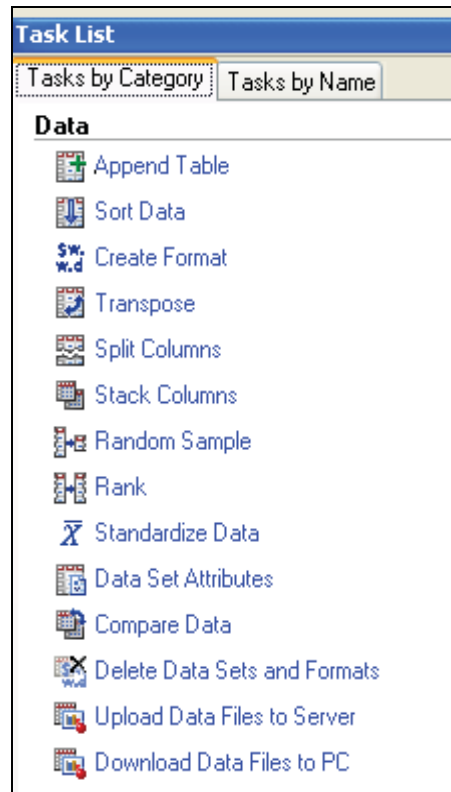


Figure B-3. Data Task List.

### B-1.3 Data Summary and Statistical Analysis Tasks

Figure B-4 shows various data summary and statistical analysis tasks that can be performed in EG. The “Describe” tasks provide summaries of different types of data. For example, the Frequency task deals with counts. The Table Analysis task also deals with counts. It will tally data and create tables based on categorical data, for example. It also provides statistical tests of the hypothesis that the pattern of counts in various columns is the same from one row to another in a table. The Summary Statistics task computes averages, standard deviations, coefficients of variation, minimums, maximums, percentiles, and several other measures for the numeric columns in a data set. The computations can always be performed in groups, based on other categorical or numerical variables.

The statistical tasks in the right-hand column of Figure B-4 are for various types of modeling. One can test hypotheses, look for linear or other relationships in the data, identify groupings of data, and so forth. Many of the tools work with categorical data as well as numerical data. The nonparametric methods deal with data that is not normally-distributed.

The Control Charts group is provided by the SAS/QC product. It allows one to establish control limits and monitor stationary processes to see if they continue to perform within established bounds.

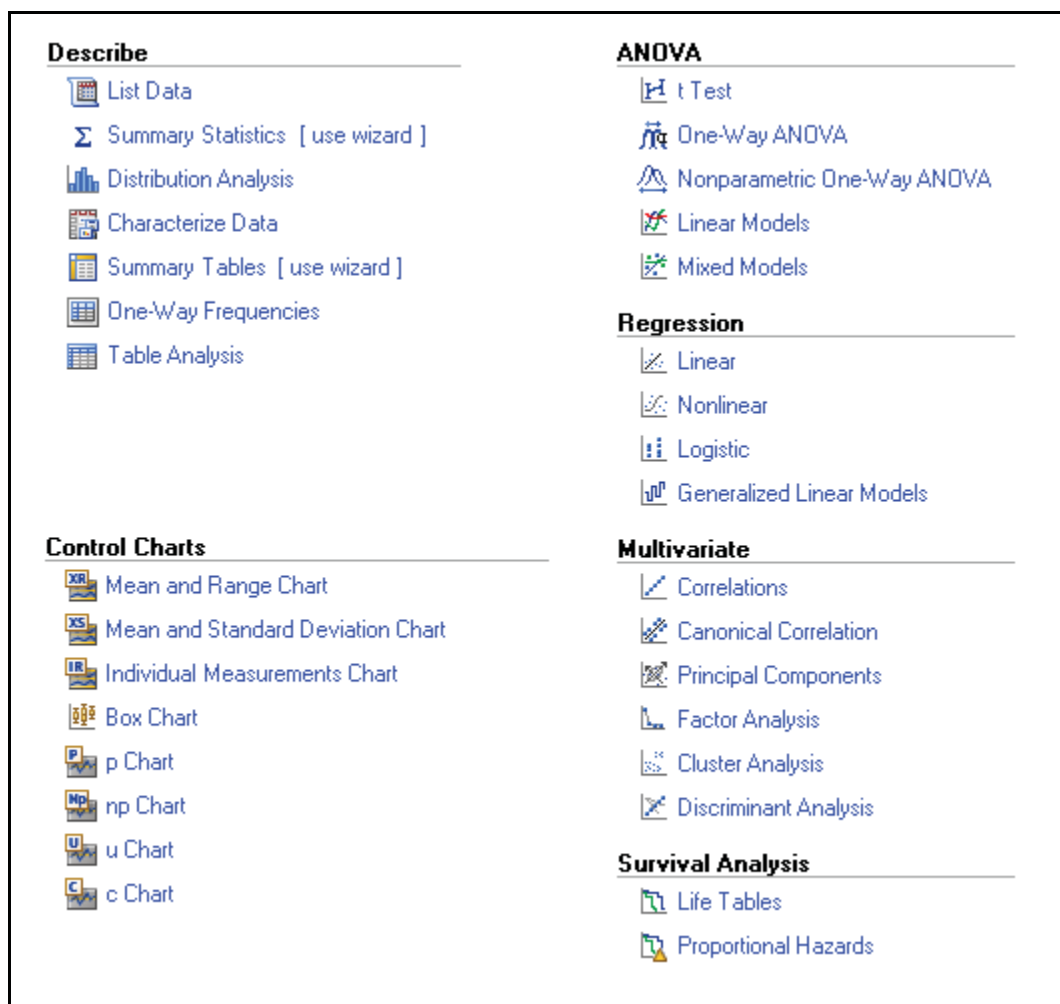


Figure B-4. Data Summary and Statistical Analysis tasks.

## B-1.4 Graphics Tasks

As shown in Figure B-5, several styles of graphs are available for displaying the results of the analyses. These are in addition to the output generated by many of the procedures discussed above, which themselves create graphical output. The graphs are provided by the SAS/GRAPH product.

The Capability graph tools listed in the figure generate graphs, but are also themselves statistical tools for exploring data and comparing probability distributions.























Graph	Capability
 Bar Chart [ use wizard ]	 Histograms
 Pie Chart [ use wizard ]	 Probability Plots
 Line Plot [ use wizard ]	 P-P Plots
 Scatter Plot	 Q-Q Plots
 Area Plot	 CDF Plots
 Bar-Line Chart	
 Bubble Plot	
 Donut Chart	
 Contour Plot	
 Box Plot	
 Map Graph	
 Create Map Feature Table	
 Radar Chart	
 Surface Plot	
 Interactive Graphics	

Figure B-5. Graphics tasks.

## B-2.5 Delivering Output to the Web

There are several ways to deliver output from EG to the INL NDMAS web portal. Three are mentioned here.

First, one can create a report that can be linked to a INL NDMAS web portal. From the menu bar, one can select New/Report. Or, the New Report dialog can be invoked from the rightmost button on the second toolbar . Within the dialog (Figure B-6), one can create text blocks and enter text explaining the data, and one can enter graphs and other displays. Then, using the SAS Portal software, one can display the report on the web.

A second method is to create a Stored Process. On the second tool bar, clicking the  symbol will invoke the Stored Process interface. A seven-step process follows, which is not shown here. In the process, one specifies SAS code, which can be extracted from previous EG steps using the “View Last Submitted” option. One also specifies prompts for particular conditions that might influence the process. For example, one could have a prompt that lets a person specify the name of the input data set. Later, when the process is run, the set specified at run time is accessed. A final input for the process is to specify where it will be stored on the INL NDMAS web server. After the process is created and runs successfully in EG, it can be delivered to the web by selecting the appropriate portal type and linking to the input instructions.

A third method comes from the “OLAP” option on the main menu bar. Here, wizards allow the EG user to create a “multidimensional data set,” or “cube,” that can later be displayed in an “OLAP Table Viewer” portlet on the SAS web. These portlets allow the web user to drill down into the data and view different levels of detail.

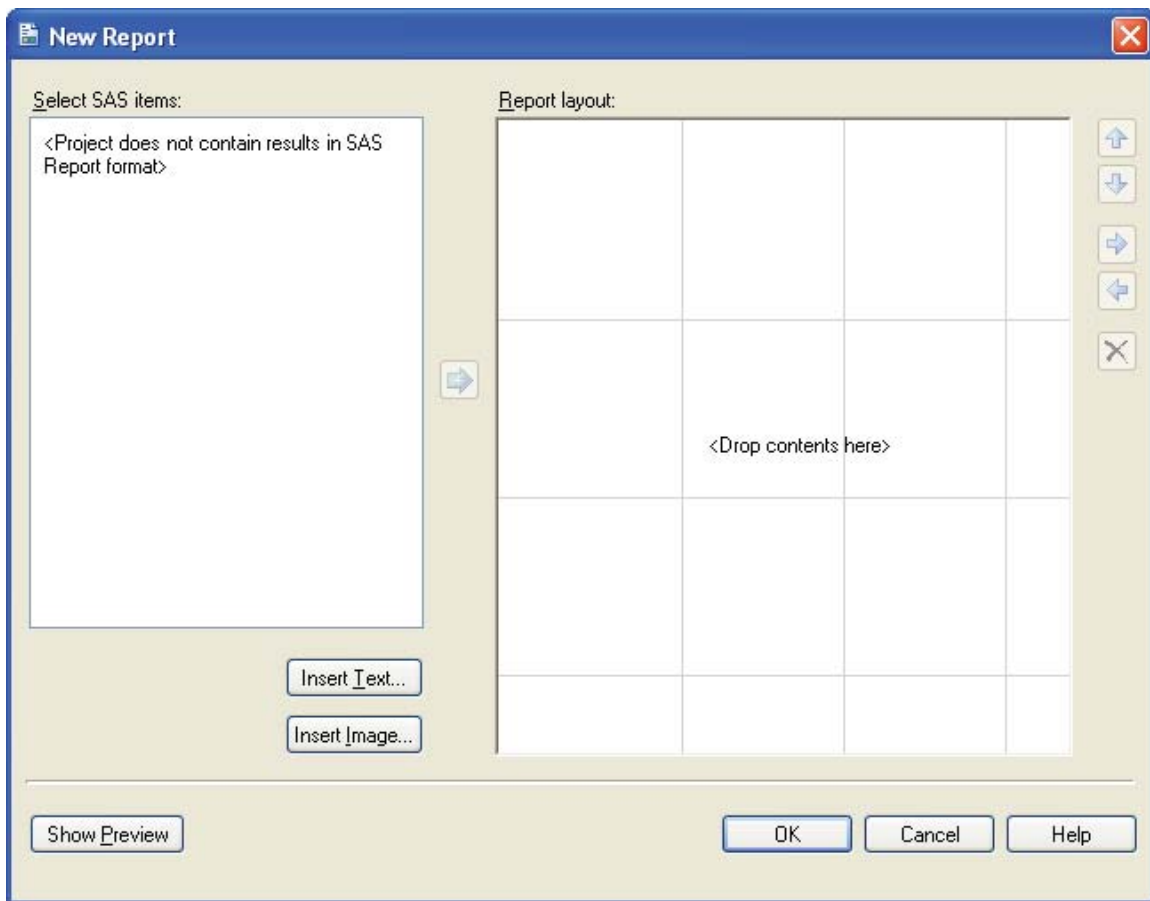


Figure B-6. New Report dialog.

## B-1.6 Use of Help Files

EG contains a help file that describes its use. SAS products are documented further at the following website:

<http://support.sas.com/onlinedoc/913/docMainpage.jsp>

Details about any particular SAS procedure can be found by clicking the SAS Procedures link near the top of the SAS OnlineDoc reference list. These procedures come from various SAS products. Just the procedures associated with products that are licensed for a particular site will execute. For NDMAS, the Base SAS, SAS/ACCESS, SAS/GRAPH, SAS/STAT, and SAS/QC products are licensed.

The list below shows links to follow in the SAS help page to learn about particular SAS features that might be used from EG.

- For details about Base SAS procedures that manipulate the data, pick  
Base SAS — Base SAS Procedures Guide — Procedures — Then select a procedure.
- For details about Statistical Procedures, pick  
SAS/STAT — SAS/STAT User's Guide — Then select the procedure of interest.

- For details about SAS Version 9.1.3 graphing procedures, pick  
SAS/GRAPH Reference — SAS/GRAPH Procedures — Then select a procedure.
- For details about the Base SAS language, pick  
Base SAS — SAS Language Reference: Dictionary — Dictionary of Language Elements —  
Statements — Then select a statement.

## **B-2. JMP**

JMP is a stand-alone product that is used in two primary ways by the NDMAS team. First, graphics from JMP appear in the INL NDMAS web portal. For the second application, users need to have local copies of JMP installed on their PCs. The applications are discussed briefly below.

### **B-2.1 JMP Plots**

First, JMP is a tool for producing graphs that then appear on some of the web pages. These graphs differ from the EG graphs (from “SAS/GRAPH”) because they show more than one set of axes and data in a single graph. The SAS NDMAS data tables can be imported directly into JMP after a link to the SAS metadata library is established using the SAS\Server Connections option from the JMP File menu.

For example, a single graph can contain a panel with data for each capsule. Such graphs can be produced using SAS/GRAPH, but the process involves several steps. The separate little graphs must be generated and stored, and then “replayed” into a template that defines the headings and positions of the individual graphs in the larger graph. Using JMP, the “Capsule” variable, for example, is dragged with the mouse into a region in the graphic user interface and the collection of small graphs inside a larger graph appears instantly. These graphs are called “lattice” plots or “trellis” plots because the classification variable(s) that characterize the individual little plots are like a framework for the little plots. The process of generating these types of graphs is often called “conditioning,” because they allow an examination of the data with regard to (or “conditioned on”) the different values of the lattice variable.

Another type of graph that JMP produces quickly and easily is a matrix graph. Here, scatterplots of pairs of variables in a multivariate data set are generated inside a larger “matrix” of plots. For example, if the user selects three numeric quantities, A, B, and C, in a data set, the matrix plot will have three rows and three columns. The variable names appear in the diagonal cells. The other cells have small scatterplots, with the X axis corresponding to the column variable for the matrix and the Y variable corresponding to the row.

These graphs can be saved as HTML files on the server. They can then be displayed in a “URL Display Portlet” on the INL NDMAS web portal.

### **B-2.2 Live JMP Reports**

Another way to deliver the JMP graphic output to users who have JMP installed on their local PCs is to create Stored Processes using JMP. The steps used by NDMAS developers to create such stored processes are beyond the scope of this report, but the results can be very useful for modeling. NDMAS team members use EG to create one or more SAS data sets. In JMP, they use the SAS interface options from the File menu to connect to the SAS metadata server and import the SAS data sets into JMP. Then they design a plot such as one of the views described in the previous section. They might also perform some analysis on the data using JMP and display the output of that process. Then they execute the process that makes this information available on the web.

Web users with JMP installed first open JMP and access the SAS menu options under the File menu to ensure that they have a connection to the SAS metadata server. Then they can close JMP.

From a “JMP Live” data portlet on the web page, web users execute the stored process for the desired data. After the process runs, they will find JMP open on their PCs, with the data loaded and the graph or other analysis output window present, showing the graphs or other results of the analysis. The JMP program will be in the same status at that point as it was in when the NDMAS developer started setting up the stored process.

Within JMP, many analysis options are available. As with EG, data can be manipulated, many statistical analyses can be performed, and many graphical output can be generated. Figure B- 7 is a list, from the JMP help file, of the statistical “platforms” that can be invoked from JMP. Most of them create graphs that illustrate the results. Thus, the modeling capability in JMP is virtually unlimited. JMP is described in more detail at the following website:

<http://www.jmp.com>.



Figure B- 7. JMP analysis tools.